



END-3900-1 M – ID Master Thesis

Floating Offshore Wind Turbine Operations in Arctic Conditions

Submitted by:
Hamza Asif



UiT The Arctic University of Norway

UiT – The Arctic University of Norway in Narvik, 8514 Narvik



Floating offshore wind turbine operations in Arctic conditions

University of Tromsø - The Arctic University of Norway
 IVT, Faculty of Engineering Science & Technology,
 Engineering Design.

Title: Floating Offshore Wind Turbine Operations in Arctic Conditions		Date: 15.5.2024
Subject code: END – 3900-1 M – ID	Subject name: Master’s thesis	Total number of pages: 105
Author: Hamza Asif		
Department: Department of Computer Science and Computational Engineering	Field of study: Master of science in Engineering Design	
Supervisors: Professor. Muhammad Shakeel Virk Dr. Guy Beeri Mauseth		
Keywords: Floating offshore wind turbine, Surface body, Hydrodynamic modelling, Analysis, MAC, Mooring lines, Time / Frequency based response, Numerical simulation		

Preface

This thesis study is a requirement of the END-3900 MASTER THESIS - M-ID - 30 ECTS, which serves as the last component of the Engineering Design master's programme at UiT Narvik. The course centres on completing an individual 30 ECTS master's thesis, thoroughly documented with a comprehensive report detailing the theoretical framework, computational aspects, and numerical simulations. The project aims to provide students with the opportunity to apply their knowledge and skills acquired from previous courses during the degree and to undertake an individual project relevant to the master's programme.

The project has been carried out under the supervision of Professor. Muhammad Shakeel Virk from the Department of Industrial Engineering at UiT – The Arctic University of Norway, Narvik.

Acknowledgement

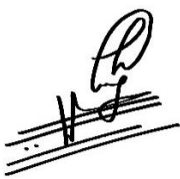
I would like to acknowledge all the people who have contributed to the work related to this Master Thesis. First of all, I would like to thank my supervisor Professor. Muhammad Shakeel Virk for providing me such a great opportunity to work on this project and providing all the necessary resources for completion of this master thesis. His prior knowledge and expertise within the field of Computational Fluid dynamics, icing and numerical simulation modelling helped me to develop a better understanding of the background and the relevant topics in detail.

Furthermore, I would also like to thank my co-supervisor Dr. Guy Beeri Mauseth who helped me to encourage working hard during this project through his weekly & special meetings for this master thesis. His contributions through valuable guidance during different courses of this master's study are significant which helped me to construct a base to work on different projects in the field of Engineering Design.

Additionally, I would like to thank Susmit Dhar – PhD fellow at the Department of Technology and Safety at UiT – The Arctic University of Norway to build python script to extract the meteorological data from NORA – 3 database for operating conditions at Utsira Nord – selected offshore site for FOWT dynamic response evaluation.

I am thankful to my supervisor Professor. Muhammad Shakeel Virk for his invaluable support and guidance throughout the project. His continuous support and guidance made me achieve this milestone.

Lastly, immense gratitude is expressed towards family, especially my wife, mother, and siblings for believing in me and their genuine support throughout the academic journey.



Hamza Asif

Narvik, May 2024

Abstract

Offshore wind energy is receiving increased attention as a promising renewable energy source day by day, and the research in the field of designing the floating platforms to support floating offshore wind turbine (FOWT) has become very important. The evaluation of the dynamic stability of a FOWT in a challenging marine environment is the platform's capacity to maintain its initial position. These are often assessed in terms of the floating platform's rigid body dynamic response, which supports the entire FOWT. This study uses Ansys AQWA to analyse the dynamic response of the NREL-5 MW reference wind turbine powered by a SPAR buoy platform at an offshore location well suited for production of offshore wind energy in Arctic region.

An offshore location in the Arctic region was selected systematically and meteorological data for past 7 years (2015 – 2021) was extracted to model operating conditions in Ansys AQWA. Firstly, best design configuration was chosen for Spar hull to support the basis of selection and designing the Spar buoy platform through numerical simulations and then full-scale model including the mooring system for FOWT was developed to evaluate the dynamic response in mean and extreme operating conditions. Time domain response was generated using Ansys AQWA in every Degree of freedom (Heave, Surge, Sway, Roll, Pitch and Yaw). The response was then analysed and concluded the effective dynamic stability of the FOWT. The results indicate that the design of the spar platform is reasonable and has good hydrodynamic performance.

The full report also emphasizes the importance of operating conditions, examining the structural dynamic behaviour, post-tensioned load on mooring lines, and motion of the whole structure. The conclusion of the thesis includes findings obtained from the study, implications for designed floating platform for FOWT and detailed resonant frequencies for each DOF. It also incorporates ideas for future research and guides employing hydrodynamic numerical modelling to design and construct more efficient, resilient, and durable floating platforms.

Table of Contents

Preface.....	3
Acknowledgement.....	4
Abstract	5
1 Introduction	12
1.1 Research Need and Importance	12
1.2 Thesis Objectives	12
1.3 Thesis Layout	13
2 Literature Review	14
2.1 History and Importance	14
2.1.1 Trend of Utilization of Wind Energy Resources	15
2.1.2 European Goals	15
2.2 Offshore Wind Energy.....	16
2.2.1 Types of Offshore Wind Turbines.....	16
2.2.2 Factors Effecting Offshore Wind Projects.....	16
2.2.3 Offshore Wind Turbine Design & Size.....	17
2.2.4 Wind Turbine Design & Size Relationship	18
2.2.5 Wind Turbine Rotor.....	20
2.2.6 Tower.....	21
2.2.7 Loads	22
2.3 Floating Base Design.....	22
2.3.1 Spar Buoy Platform	23
2.3.2 Semi-Submersible Platform.....	25
2.3.3 Tension Leg Platform	26
2.4 Floating Wind Turbine Mooring System.....	27
2.4.1 Spread Moorings	28
2.4.2 Taut Mooring.....	28
2.4.3 Single Point Mooring	29
2.4.4 Guideline for Mooring/Anchor Application.....	29
2.4.5 Material	29
2.5 Loads due to Wind and Wave Interaction.....	30
2.5.1 Aerodynamic Loads.....	31
2.6 Hydrodynamic Loads	32
2.6.2 Hydrostatic Loads.....	32

2.7	Site Selection.....	33
2.7.1	Environmental and Socio-Economic Considerations.....	33
2.8	Technical Suitability and Risk Assessment.....	33
2.9	Conflicts of Interest (case study from HAVVIND summary by NVE).....	33
2.9.1	Petroleum Interests.....	33
2.9.2	Shipping.....	33
2.9.3	Fisheries.....	33
2.9.4	Other interests.....	33
2.10	Review of Existing Studies.....	34
2.10.1	Structural Behavior.....	35
2.10.2	Geometric Design optimization and Operating Conditions.....	38
2.11	Floating Wind Turbine & Icing.....	40
2.11.1	Atmospheric Ice.....	40
2.11.2	Floating Sea Ice Chunks.....	41
2.12	Operations & Maintenance Strategies for FOWT.....	42
2.12.1	Offshore Maintenance Logistics Strategies.....	42
2.12.2	Maintenance Strategies for Bottom Fixed Offshore Wind Turbines.....	43
2.12.3	O&M Strategies.....	43
3	Design of Experiments.....	45
3.1	Floating Platform Selection for Numerical Study.....	45
3.1.1	Water Depth Suitability.....	45
3.1.2	Stability and Motion.....	45
3.1.3	Simplicity.....	45
3.2	Site Selection and Estimation of Operating Conditions.....	45
3.2.1	Estimation of Operating Conditions.....	46
3.2.2	Numerical Software Selection.....	48
3.2.3	Design Configuration for Spar Buoy Platform.....	48
3.2.4	Thesis Analysis Flow Chart.....	49
4	Numerical Setup.....	50
4.1	Hydrodynamic Analysis.....	50
4.1.1	Simulation Methodology.....	50
4.2	Units.....	51
5	Selection of Design Configuration.....	52
5.1	Operating Conditions.....	52
5.2	CAD Modelling.....	52
5.3	Numerical Modelling.....	54
5.3.1	Platform Properties.....	54

5.3.2	Mooring System	54
5.3.3	Mesh	55
5.3.4	Hydrodynamic Response.....	55
5.3.5	Results & Analysis	56
5.3.6	Optimal Geometric Shape	62
5.4	Pressure and Motions	62
6	Full Scale Study of Optimal Spar Buoy Design	64
6.1	Selection of Wind Turbine.....	64
6.1.1	Turbine Properties	64
6.2	Spar Buoy Hull Calculations	65
6.2.1	Important Formulas	66
6.3	Ballast Calculations	66
6.3.1	Material	67
6.4	CAD Modelling	68
6.5	Mooring System	68
6.5.1	Materials.....	69
6.5.2	Mooring Line Properties.....	69
6.5.3	Mooring Lines Connection Points.....	70
6.6	Numerical Setup	70
6.6.1	Defination of Point Masses	70
6.6.2	Modelling of Mooring Lines	71
6.6.3	Mesh	73
6.7	Operating Conditions	73
6.8	Hydrodynamic Solution	74
6.8.1	Solution During Mean and Extreme Operating Conditions	75
6.8.2	Pressure and motions.....	91
7	Conclusions and Future Work	93
7.1	Conclusions	93
7.2	Future Work.....	95
	References	96
	Appendix	99
	Python Script for NORA – 3	99
	Product catalogue for mooring lines.....	102
	Excel file	103
	Numerical setup in Ansys Aqwa.....	104

List of Figures

Figure 1. Evolution of wind turbine sizes [4].....	15
Figure 2. Power coefficient vs different wind speeds for different rotors[10]	19
Figure 3. Trend towards larger turbine heights and rotor diameter in offshore wind industry[12]	19
Figure 4. Flow chart of energy yield and rotor diameter & tower height.....	20
Figure 5. Offshore wind turbine - six DOF[15].....	23
Figure 6. Hywind spar buoy FOWT model[15]	24
Figure 7. Spar key components and characteristics[17]	24
Figure 8. Design space spar concept.	25
Figure 9. Semi-submersible type FOWT design & application [15].....	25
Figure 10. Key characteristics of semi-submersible platform[17]	26
Figure 11. TLP characteristics[17]	27
Figure 12. Spread mooring and taut mooring[12]	28
Figure 13. Different loads on FOWT due to wind and wave interaction[22].....	30
Figure 14. Major effects of Wind loads in two DOF[24]	32
Figure 15. NVE's identified offshore wind zones[25].....	34
Figure 16. 6 DoF for FOWT[28].....	35
Figure 17. RAO of Heave and pitch[20]	36
Figure 18. Time domain analysis for surge, pitch and heave motions[20].....	36
Figure 19. Heave, roll and pitch response in time domain[30]	37
Figure 20. 6 DOF time domain response[31]	38
Figure 21. Multi turbine platform concepts[32]	39
Figure 22. Natural periods in 6 DoF for DeepCWind platforms[32]	40
Figure 23. Atmospheric icing on wind turbine blades [42]	41
Figure 24. FOWT & floating sea ice chunks interaction.....	42
Figure 25. CSV file containing metrological data for 2015 at Utsira Nord.....	47
Figure 26. Mean, Maximum and Minimum operating conditions from 2015-2021 at Utsira Nord.....	47
Figure 27. Analysis workflow chart.	49
Figure 28. Circular CAD design.....	53
Figure 29. Square CAD design.....	53
Figure 30. Triangular CAD design	53
Figure 31. Mooring system	54
Figure 32. Mesh.....	55
Figure 33. wind and wave direction in Ansys Aqwa	56
Figure 34. Wave modelling	56
Figure 35. Heave motion in circular design configuration.....	57
Figure 36. Heave motion in square design configuration.....	57
Figure 37. Heave motion in triangular design configuration.....	58
Figure 38. Sway motion in circular design configuration.	59
Figure 39. Sway motion in square design configuration.	59
Figure 40. Sway motion in triangular design configuration.....	60
Figure 41. Pitch motion in circular design configuration.....	61
Figure 42. Pitch motion in square design configuration.....	61
Figure 43. Pitch motion triangular design configuration.....	62
Figure 44. Structural motion during mean operating conditions.....	62

Figure 45. structure interpolated pressure during mean operating conditions.....	63
Figure 46. CAD model	68
Figure 47. Mooring line.....	69
Figure 48. Defination of point masses in ansys aqwa	71
Figure 49. Fairleads	72
Figure 50. Mooring lines side view	72
Figure 51. Mesh.....	73
Figure 52. Range of wave frequencies / periods for numerical simulation in Ansys Aqwa	74
Figure 53. Wave modelling	75
Figure 54. Irregular wave model with Jonswap (Hs) for mean and extreme operating conditions.....	75
Figure 55. Heave time domain response during mean operating conditions.....	76
Figure 56. Heave time domain response during extreme operating conditions.	77
Figure 57. Surge time domain response during mean operating conditions.....	78
Figure 58. Surge time domain response in extreme operating conditions.....	79
Figure 59. Sway time domain response during mean operating conditions	80
Figure 60. Sway time domain response during extreme operating conditions.....	81
Figure 61. Roll time domain response during mean conditions.	82
Figure 62. Roll time domain response during extreme operating conditions.....	83
Figure 63. Pitch time domain response during mean operating conditions.....	84
Figure 64. Pitch time domain response during extreme operating conditions	85
Figure 65. Yaw time domain response during mean operating conditions.....	86
Figure 66. Yaw time domain response during extreme operating conditions.....	87
Figure 67. Frequency domain response for heave, surge and yaw RAO	88
Figure 68. Tension force along time domain response on Mooring line 1.	89
Figure 69. Tension force along time domain response on Mooring line 2.	90
Figure 70. Tension force along time domain response on Mooring line 3.	90
Figure 71. Structure motion amplitude in hydrodynamic diffraction during mean operating conditions.	91
Figure 72. Structure interpolated pressure during extreme operating conditions.....	91
Figure 73. Structure motion amplitude in hydrodynamic diffraction during extreme operating conditions.	92
Figure 74. Structure interpolated pressure during extreme operating conditions.....	92

List of Tables

Table 1. Development of wind turbines.....	14
Table 2. Trend of development in wind generation capacity between 1996 – 2000}[1].....	15
Table 3. Mooring/anchor selection combination[12]	29
Table 4. Mooring line material properties[12].....	30
Table 5. NVE's identified locations for offshore wind.	46
Table 6. Geographical co-ordinates for Utsira Nord in Norway	46
Table 7. Estimated operating conditions for analysis.	47
Table 8. Range of Wave frequency at Utsira Nord during 2015 – 2021.....	52
Table 9. Mean operating conditions at Utsira Nord during 2015 – 2021.	52
Table 10. Geometric properties	54
Table 11. Nacelle, Hub and Rotor properties combined.....	65
Table 12. Tower properties	65
Table 13. Spar Buoy hull design properties.....	65
Table 14. Fixed ballast properties.....	67
Table 15. Properties for stability	67
Table 16. Mooring system properties	69
Table 17. Chain properties.....	70
Table 18. Polyester properties	70
Table 19. Fairleads connection points location	70
Table 20. Anchor points location.....	70
Table 21. Mean operating conditions	74
Table 22. Extreme operating conditions	74
Table 23. Time domain response of FOWT in all DOF during extreme resonant frequency during first 500 s	89

CHAPTER 1

1 Introduction

The world's expanding energy demands have driven the investigation of innovative technologies in response to the intensifying effects of climate change and the urgent need to shift towards sustainable energy sources. The concept of floating offshore wind turbines, which represents a revolutionary advancement in renewable energy, is essential to this project. Solutions that are efficient and sustainable are desperately needed to optimally use the potential of clean wind energy especially in deep-sea environments and minimize the dependency on conventional fossils-based energy production methods to reduce the carbon footprint globally, since the world's energy demand keeps rising.[1]

1.1 Research Need and Importance

The limits of onshore wind turbines, which are characterized by land conflicts, visual impact difficulties, noise pollution, tourism problems and lower & non sustainable wind resources highlight the need for offshore wind energy research. Investigating the possibilities of greater offshore wind generating capacities is vital to get over these constraints. Norway offers a special chance for more effective use of offshore wind resources because of its vast deep coastal waters. This study supports larger Norwegian and European objectives for increasing floating offshore wind farms. This study intends to evaluate the technical and environmental aspects of migrating to floating offshore wind farms, given that Europe and Norway have set ambitious targets in EU 2030 goals for renewable energy, notably in offshore wind. The results will be crucial for strategic energy planning, fulfilling EU goals, and supporting a sustainable energy future. [2, 3]

1.2 Thesis Objectives

This thesis seeks to conduct exploratory review of existing floating offshore platform designs and multiphysics numerical simulations-based analysis of a Floating Offshore Wind Turbine (FOWT) design at a suitable location with the wind rich meteorological data. The primary objective is to study the type of loads identify potential challenges in areas such as structural integrity, dynamic response of floating platforms at different wave conditions & icing challenges in the Arctic region of Norway. Therefore, the aim of this research is to provide an insight in the effects of loading from wind-wave interaction on structural dynamics of FOWT. By comparing these findings with the dynamics in mean and peak values, it is aimed to enhance understanding of the implications these loading types can have for the applicability and design of FOWT in such environments.

As a tool in this study, a multiphysics numerical model is developed for simulating the dynamic motions and mooring loads of a FOWT. In the simulations performed with this model, the structure is subjected to aerodynamic and hydrodynamic loads both to compare the loading conditions in operating conditions and to study the structural response due to these load types. Given the interdependence of loads and the

movements of the floater and turbine system, they are coupled to capture effects of dynamic interaction. Where possible, the modelling approach and structure lay-out are based on the outcomes of existing studies. This is done to benchmark some of the findings with the outcomes of preceding studies and to enhance progress, given the limited scope of this master thesis of 30 credits.

1.3 Thesis Layout

First of all, an extensive literature on Floating Offshore Wind Turbines has been conducted in this master thesis to form the base for enough knowledge in this particular field of research.

In the next step a design of experiments was developed to form the methodology for numerical based simulations study and a suitable offshore wind location in Arctic region was identified out of various locations identified by Norwegian Water Resources and Energy Directorate's (NVE). The latitude and longitude coordinates of the selected location were identified and meteorological data for past seven year (2015 – 2021) was extracted and modelled using statistical analysis on MS Excel.

NREL 5 MW reference wind turbine was chosen to couple in the numerical simulations. Design properties for wind turbine were extracted from NREL report and several calculations regarding the design of Spar hull and ballast were made to design a floating platform which is massive & buoyant enough to support the loads from wind turbine at the desired height of the hull.

A mooring system consisting of three mooring lines with a combination of chains and polyester mooring line was designed for better station keeping of the FOWT.

A commercially used and available numerical software package, Ansys AQWA was chosen to model the numerical simulations and several numerical simulation models were created to mirror the possible realistic environmental conditions at the selected offshore site. Simulations were performed on mean and extreme operating conditions to evaluate the dynamic behavior of the FOWT in frequency and time domain response.

Natural frequency in each DOF was also calculated and a simulation was conducted to analyze the FOWT response during these extreme resonant frequencies.

At the end, a conclusion regarding the stability and survivability of designed FOWT and mooring system was made which was based on time response graphs generated through numerical simulations on Ansys AQWA

CHAPTER 2

2 Literature Review

2.1 History and Importance

In 1990, global wind energy capacity stood at approximately 2200 MW, with a significant portion located in California, USA. The landscape shifted in the late 1990s, as Europe embraced renewable energy and initiated substantial investments to reduce reliance on fossil fuels. By 1999, the world witnessed a remarkable growth in grid-connected wind power, reaching a total estimated capacity of 12 GW.[1] During the period from 1997 to 2000, Europe exhibited a proactive approach by installing new wind generating capacity at an impressive rate of 1600 MW per year. However, as the industry expanded, challenges related to land usage, visual impacts, and the need for consistent wind speeds prompted a shift in the focus. Wind turbine developers in Europe turned their attention to offshore locations, recognizing the vast expanse and higher wind velocities offered by the sea.

The strategic move towards offshore wind installations gained momentum due to the abundant space available at sea, mitigating concerns associated with land constraints. Additionally, the utilization of faster and more consistent wind speeds offshore presented a compelling solution to enhance the efficiency of wind energy generation. Building upon this historical trajectory, this thesis delves into the significance of offshore wind energy as a pivotal component in the global transition towards sustainable and renewable power sources. By exploring the motivations behind the shift to sea-based installations and the subsequent developments in offshore wind technology, the research aims to contribute valuable insights into the evolution of this critical aspect of the renewable energy landscape. Table – 1 highlights the development in the power generating capacity of wind turbine machines since previous years.

Year	Machine Capacity
Late 1980s	150 – 480 KW
Late 1990s	600 – 750 KW
Late 2000	1000 – 1600 KW
Late 2010	2 MW
Latest model	16 MW (Mingyang MySE 16-260 – Offshore wind turbine)

Table 1. Development of wind turbines

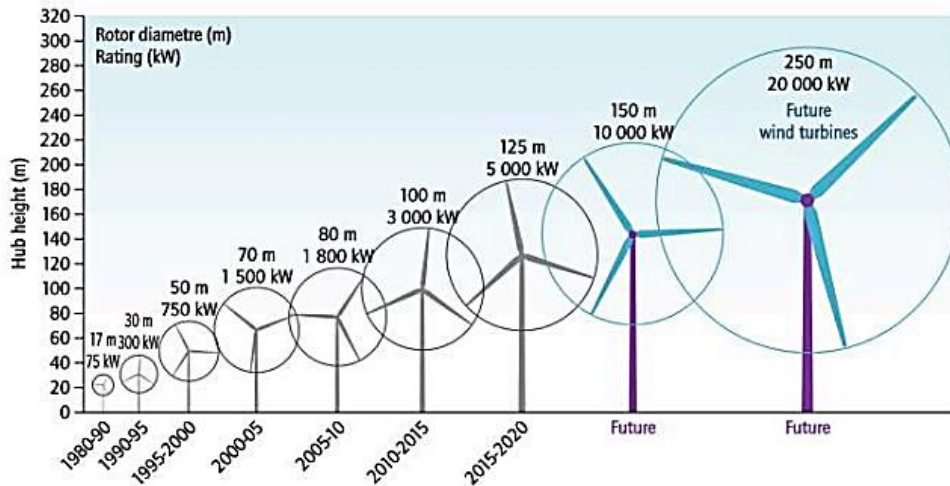


Figure 1. Evolution of wind turbine sizes [4]

2.1.1 Trend of Utilization of Wind Energy Resources

There is a noticeable upward trend in investments towards harnessing wind power resources and generating clean energy from wind. Most wind farm developments have occurred in Europe and North America.

Region	January 1996			January 1998			January 2000		
Europe	2518	52.0	46.1	4766	62.8	35.9	8349	67.0	29.1
North America	1676	34.6	-2.7	1615	21.3	0.2	2617	21.0	30.2
Asia and Pacific	626	12.9	157.6	1149	15.1	24.5	1363	10.9	8.4
Latin America	7	0.1	-30.0	34	0.4	21.4	87	0.7	67.3
Middle East	12	0.1	-50.0	21	0.3	0.0	36	0.3	38.5
Africa	0	0.0		3	0.0	0.0	3	0.0	0.0
Total	4839		20.0	7588		24.5	12455		26.9
	(MW)	(%)	(D%)	(MW)	(%)	(D%)	(MW)	(%)	(D%)
(D% --- percent change from previous year)									

Table 2. Trend of development in wind generation capacity between 1996 – 2000}[1]

2.1.2 European Goals

The European Wind Energy Association (EWEA) has predicted that by 2030, the European Union (EU) will have installed 320 gigawatts (GW) of wind energy capacity [5]. A major part of this target will likely be met by offshore wind farms, which have grown significantly since the first such turbine was set up in 1992. Offshore wind power, which was only 0.5% of global energy supply in year 2000, has seen a rapid increase over the years. The average cost to generate power from offshore wind, known as the Levelized Cost Of Energy (LCOE), has dropped and was expected to be around \$0.07 per kilowatt-hour in 2020 [6]. By the end of 2018, Europe had a total offshore wind capacity of 18.5 GW, distributed among 105 wind farms in 11 European countries, mainly in colder areas like the North Sea and Baltic Sea [7]. Wind Europe has forecasted that by 2030, there will be 70 GW of offshore wind capacity just in the North Sea [8].

Norway, a key player in this initiative, has committed to install 30 GW of offshore wind energy by 2040, with a specific focus on floating wind farms. In 2024, Norway is set to inaugurate a groundbreaking 1.5 GW floating wind farm, showcasing its dedication to innovation in offshore wind. As of today, Europe has 113 MW of floating wind turbines, with Norway leading with the 88 MW Hywind project. Looking ahead, the EU is expected to have 330 MW of floating wind in operation by 2024 and aims for over 10 GW by 2030. Apart from the environmental benefits, the development of floating wind capacities is set to generate 52,000 new jobs in Norway by 2050. Norway also aspires to claim a 5-14% share of the global offshore wind market, solidifying its position as a key player.[2, 3] In summary, the EU's offshore wind goals reflect a bold commitment to sustainability, innovation, and job creation. With strategic investments and technological advancements, the EU is set to lead the way in offshore wind development globally.

2.2 Offshore Wind Energy

Offshore wind energy, a clean renewable power source is gaining global scientific exploration due to its potential to reduce the carbon footprint of the global energy sector. In the 18th-century technology of wind turbines was first put forth in 1930. World wind installed the first offshore wind turbine in 1990. Many nations are now building offshore wind farms to produce sustainable energy.[9] Offshore wind energy is increasingly being utilized for large-scale projects due to its rich winds and potential for significant electricity production. Major electrical companies are increasingly interested in these wind farms.[10] Some other arguments other than utilization of faster and consistent wind speeds in open sea are land usage, visual effects & lack of tourism, avian interaction, noise problems and electromagnetic interference. These issues have been briefly explained in the reference, [1]

2.2.1 Types of Offshore Wind Turbines

Offshore wind turbines are classified in two major categories, defined as;

- a) Bottom fixed offshore wind turbine
- b) Floating offshore wind turbine

a) Bottom fixed offshore wind turbine

Offshore wind turbines are typically mounted on fixed support structures in shallow to intermediate depths of water (50 meters or less). These structures draw on design principles from the oil and gas industry to ensure stability and durability. The primary challenges for these supports come from the forces of wind and waves, necessitating comprehensive analysis to manage these loads effectively. The initiation of offshore wind energy took root in the North sea shallow waters, where plentiful locations and superior wind conditions offer advantages over land-based wind farms in Europe.[9]

b) Floating offshore wind turbine

The concept of floating offshore wind turbines is designed for deploying wind turbines in deep water areas. Currently, there are various floating foundation concepts for offshore wind turbines under development, with the key focus on exploring the potential of these turbines in deep water settings. The aim is to enhance the power generation capacity of each unit beyond what is possible with traditional fixed support structures.[9]

2.2.2 Factors Effecting Offshore Wind Projects

Important factors affecting decisions related offshore wind farm projects are,

- a) Depth of water
- b) Wind resources.
- c) Sea bottom

- d) Distance from shore.
- e) Turbulence intensity

2.2.2.1 Depth of Water

The depth of water at a proposed offshore wind farm site significantly influences the type of foundation that can be used for wind turbines. As the water depth increases, floating foundations become more feasible and sometimes necessary. Deeper water installations are generally more expensive due to the complexity of foundation structures and difficulties in installation and maintenance, as well as the cost of ships and equipment. Advanced technology is needed for deeper water sites to effectively utilize stronger wind resources and handle the harsh marine environment and dynamic loads on structures.

2.2.2.2 Wind Resources

Advanced technology is needed for deeper water sites to effectively utilize wind resources and handle the harsh marine environment and dynamic loads on structures. It is crucial to understand seasonal variations and the possibility of extreme weather when predicting the overall performance and resilience of the wind farm. Structure of the wind farm and the choice of turbine models are influenced by the wind resource's characteristics, such as direction and speed, to minimize wake effects and maximize energy absorption. Wake effects occur when turbines in front obstruct wind flow to those behind them.

2.2.2.3 Sea Bottom

The seabed composition particularly in the North Sea and Baltic Sea is crucial for the wind turbine construction. Soil strength and ocean currents affect vibration characteristics, requiring thorough soil analysis during planning for foundation stability.[10]

2.2.2.4 Distance from Shore

Wind resources are more abundant at higher distances from the shore, but further away from the shore can lead to higher costs and technical challenges, including longer cables and potential losses. This also affects maintenance and repair logistics, operational costs, and planning. To calculate project's profitability & feasibility it is important to analyze wind resources at greater distance on open sea or it's always better to find good wind resources nearby shore.

2.2.2.5 Turbulence Intensity

Turbulence intensity varies between environments, with land having 10-20% intensity and open sea having 8% at 60-70 meters' altitudes. This reduces fatigue loads for wind turbines but slows wake filling, necessitating greater sea spacing for optimal efficiency [10]. There are many methods available globally for wind resource assessment such as LIDAR, SODAR, anemometer, NWP models, CFD models, analysis of existing data & prediction with machine learning and wind maps from satellite data.

2.2.3 Offshore Wind Turbine Design & Size

In general, wind speeds over bodies of water are higher and more consistent than on land, which is why offshore wind turbines are designed to capture more wind energy. The efficiency, durability, and financial feasibility of these turbines are largely dependent on their size and design.

2.2.3.1 Swept Area and Energy Capture

The swept area A of an offshore wind turbine rotor, which determines the amount of wind energy it can capture is,

$$A = \pi R^2 \quad (\text{eq-1})$$

Where R is the radius of the rotor. For offshore turbines, larger diameters are common to maximize the energy capture as transporting and installing larger components at sea is feasible compared to land-based constraints.

2.2.3.2 Power output

The Power output of a wind turbine is calculated by,

$$P = \frac{1}{2} \times C_p \times \rho \times \pi R^2 \times V^3 \quad (\text{eq-2})$$

Where,

P = Output power generated by wind turbine.

C_p = Efficiency factor

ρ = Air Density

R = Blade length

V = Wind Speed

Offshore turbines benefit from higher average wind speeds at greater heights, but heights of wind turbine cannot be increased limitlessly as there are a lot of constraints of multiple loading conditions & cost implications. Therefore, we must be able to identify the optimal rotor diameter, tower & hub height to design best possible wind turbine.

2.2.3.3 Efficiency and Tip Speed Ratio

The tip speed ratio λ , crucial for the aerodynamic efficiency of the turbine, is defined as;

$$\lambda = \frac{\omega R}{V} \quad (\text{eq-3})$$

Where ω is the rotational speed of the blade. Optimizing λ is crucial for achieving maximum efficiency, as it affects the design of the blade profiles.

2.2.4 Wind Turbine Design & Size Relationship

Most offshore wind turbines have three blades and stand horizontally. Over the years, the average power of these turbines has grown from 2 megawatts in year 2000 to nearly 4 megawatts.[11] The economic value of a wind turbine primarily depends on the energy it produces, which is determined by the rotor-swept area, indicating the importance of rotor diameter overrated power for assessing turbine size and performance. While generator power impacts energy yield, it's less influential than rotor size. The design goal is to maximize power output across all wind speeds by optimizing the rotor's aerodynamic design, control systems, maximum generator power, and mechanical – electrical chain of conversion. The electric power output versus the wind speed, the so-called power curve, is the result not only of the technical characteristics of the turbine but to a certain extent also of the wind data forming the basis of the turbine design.[10]

Rotor diameter & rotational speed should be designed or optimized according to its design speed. Design Speed V_D is a speed on which the power coefficient of rotor is maximum. It can be less than the maximum wind speeds on site as well. The rotor speed must be selected in such a way that the highest power coefficients of the rotor are used within the wind speed range where the energy density of the wind frequency distribution has its maximum. It is only then that the energy yield will reach its highest value.

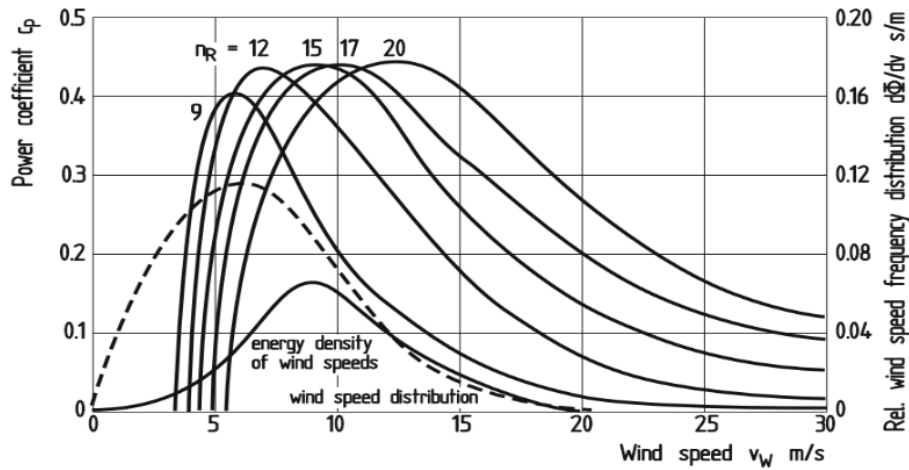


Figure 2. Power coefficient vs different wind speeds for different rotors[10]

Trends towards larger hub heights and rotor diameters is expected to continue in offshore wind industry.

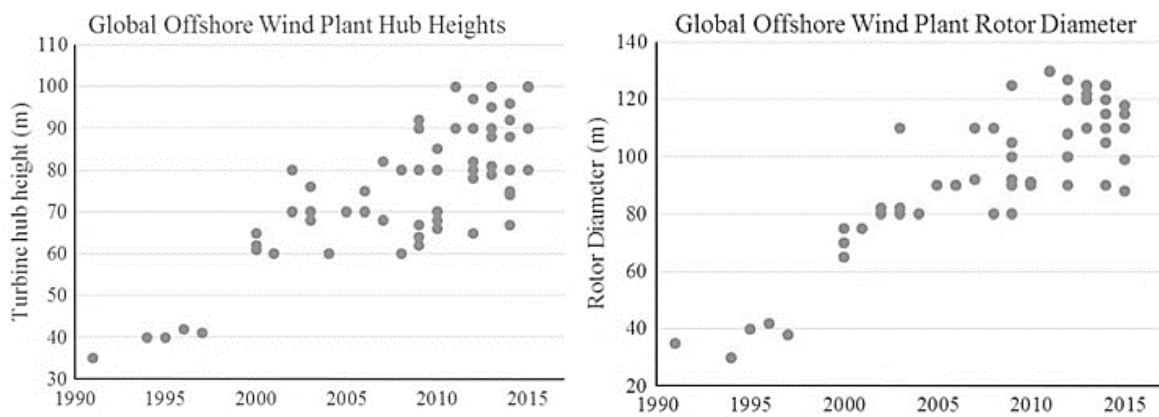


Figure 3. Trend towards larger turbine heights and rotor diameter in offshore wind industry[12]

Figure-4 provides an overview of the entire mathematical process with the required parameters and interconnections. The many interdependencies and variables influencing the energy yield of a wind turbine become clear. Naturally, these relationships are primarily of importance to the designer of a wind turbine who is involved in all the details of the design and calculation processes.[10]

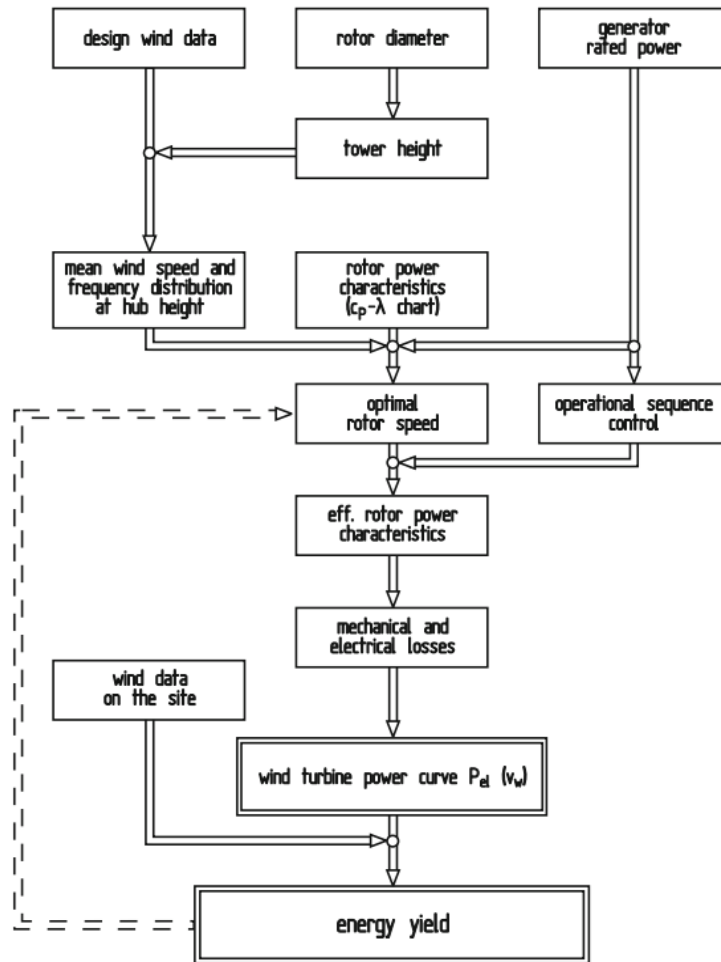


Figure 4. Flow chart of energy yield and rotor diameter & tower height.

2.2.5 Wind Turbine Rotor

The rotor of a wind turbine converts wind energy into mechanical energy, which is then converted into electricity by the generator. Its aerodynamic properties determine its efficiency, as it converts a maximum proportion of wind energy into mechanical energy. The design and technology of the rotor are tailored to optimize efficiency. Wind turbines are categorized based on their aerodynamic function and constructional design. Aerodynamically, they are distinguished by their method of power capture: "drag-type rotors" harness energy from the wind's force directly pushing against rotor surfaces, while "lift-type rotors" exploit aerodynamic lift from air flowing over specially shaped surfaces.[10] Classification according to constructional design aspects is more practicable for obvious reasons and thus more common. There are majorly two types of wind turbine rotors mentioned below.

2.2.5.1 Rotors with Vertical Axis of Rotation

Rotors with a vertical axis of rotation are a key component of Vertical Axis Wind Turbines (VAWTs), which are a type of wind turbine where the main rotor shaft is set transverse to the wind. The specific advantages of vertical axis turbine concepts are their simple design that includes the possibility of housing mechanical and electrical components, gearbox, and generator at ground level and that there is no yaw system. It has following different types of rotors,[10]

- Savonius rotor
- Darrieus rotor
- H – rotor

2.2.5.2 Rotors with Horizontal Axis of Rotation

Wind turbines that use a horizontal axis of rotation are predominantly based on concepts resembling propellers. This approach encompasses designs from traditional European windmills and American wind turbines to contemporary wind turbines, representing the prevailing design philosophy in wind energy technology today. The unparalleled dominance of this design is primarily attributed to the following characteristics:[10]

- In propeller designs, rotor speed and power output can be controlled by pitching the rotor blades about their longitudinal axis (blade pitch control). Moreover, rotor blade pitching is the most effective protection against overspeed and extreme wind speeds, especially in large wind turbines.
- The rotor blade shape can be aerodynamically optimized, and it has been proven that it will achieve its highest efficiency when aerodynamic lift is exploited to a maximum degree.

Together, these advantages are the reason why almost all wind turbines for generating electricity built to date have horizontal-axis rotors. Wind turbine rotor performance depends on the number of blades, with three-bladed rotors performing best at 7-8 tip-speed ratios, two-bladed at 10, and one-bladed at 15. Cost-effectiveness makes two or three-bladed rotors popular, but fewer blades can cause poorer dynamic behavior and increased noise.[10]

2.2.6 Tower

Towers are supports to raise the main part of the turbine up in the air. A tower is normally at least as high as the diameter of the rotor. For smaller turbines the tower may be much higher than that. Generally, tower height should not be less than 24m because the wind speed is lower and more turbulent so close to the ground.[13]

2.2.6.1 Lattice Tower

The simplest method of building high and stiff tower constructions is lattice, or truss tower. Lattice towers were, therefore, the preferred design of the first experimental turbines and in the early years also for smaller commercial turbines. Today, the lattice tower has again become an alternative to the tubular-steel tower in the case of the very high towers required for large turbines sited in inland regions.[10]

2.2.6.2 Concrete Tower

During the 1930s, "Aeromotors" in Denmark were known for their steel-reinforced concrete towers, a design feature that also marked the early large experimental turbines in the country. Steel towers dominated Danish commercial wind turbine sector, but concrete towers have re-emerged for structures over 100 meters, with prefabricated concrete designs becoming preferred.[10]

2.2.6.3 Free Standing Tubular Steel Tower

The free-standing steel tube tower is the most prevalent type of tower used today, due to advances in understanding its vibrational behavior. The advancement in technology has led to the development of "soft" designs, which significantly reduces the structural mass and consequently, the costs associated with these towers.[10]

2.2.6.4 Guyed Steel Tubular Tower

Down-wind rotors use slender tubular steel towers to reduce tower shadow, supported by steel cables or rigid trusses. However, these towers are not cost-effective due to extra anchoring foundations and obstacles in farming areas.[10] In addition to these types of towers, hybrid constructions can also be made for specific construction models specially when the tower height exceeds 100 meters.

2.2.7 Loads

Towers face two main types of loads: steady and dynamic. **Steady loads** come from the thrust and torque generated by the wind, along with the weight of the turbine itself. These loads are assessed under two conditions: when the turbine operates at rated power and when it's stationary in survival winds, using a 50-year extreme wind speed as recommended by IEC standards. These factors are crucial for evaluating the tower's resistance to bending and buckling.

Dynamic loads are particularly impactful on towers classified as soft or soft-soft, based on their natural frequencies in relation to the blade-passing and rotor frequencies. These types of towers are more susceptible to vibrations during turbine start-ups or shutdowns. To estimate a tower's natural frequency, especially for simpler models like a uniform cantilever with a top mass, the equation provided by Baumeister (1978) can be utilized.

$$f_n = \frac{1}{2\pi} \sqrt{\frac{3EI}{(0.23m_{tower} + m_{turbine}) L^3}} \quad (\text{eq-4})$$

where f_n is the fundamental natural frequency (Hz), E is the modulus of elasticity, I is the moment of inertia of the tower cross-section, m_{tower} is the mass of the tower, $m_{turbine}$ is the mass of the turbine, and L is the height of the tower. For non-uniform or guyed towers, the Rayleigh method may be quite useful. The method is described in general by Thomson (1981) and by Wright et al. (1981) for wind turbines.

To avoid resonance, a tower's design must ensure its natural frequency does not align with the turbine's excitation frequencies, such as the rotor and blade-passing frequencies. It's also crucial that these excitation frequencies remain outside a 5% range of the tower's natural frequency during extended operation.

$$\xi = \frac{\delta}{2\pi} \quad (\text{eq-5})$$

Damping of tower vibrations is due to both aerodynamic and structural factors. The damping decrement suggested by Germanischer Lloyd (1993) is 0.1 for reinforced concrete and between 0.05 and 0.15 for steel. [13]

2.3 Floating Base Design

The idea behind the floating offshore wind turbine platform design is the inspiration from the oil and gas industry. Currently, several platforms are already in place in discussions. The platform is majorly selected with respect to two major parameters; one is how it achieves the stability; the other is their resistance to loads and motions induced due to hydrodynamic and aerodynamic forces.[14] Due to absence of fixed bottom support, the motion of a floating support structure has six degrees of freedom described below,

Heave: linear movement up and down.

Sway: linear movement side-to-side.

Surge: linear movement forward–backward.

Pitch: angular movement forward–backward.

Yaw: angular movement around vertical axis.

Roll: angular movement side-to-side.[15]

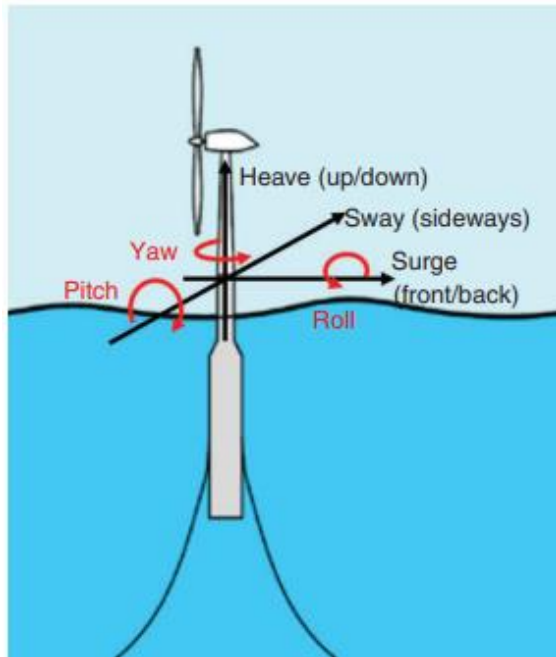
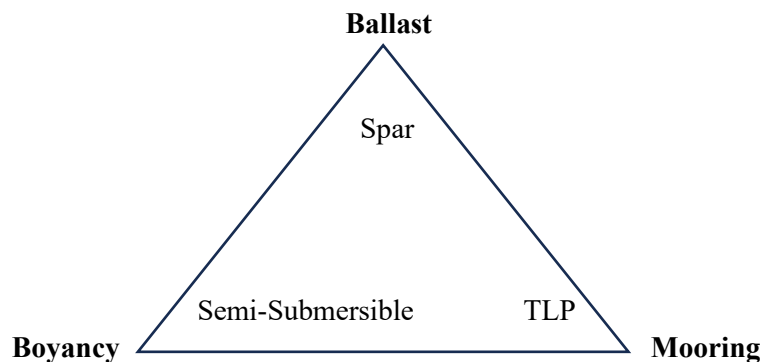


Figure 5. Offshore wind turbine - six DOF[15]

The categorization of offshore wind energy structures based on their sources of stability is often pictured as a stability triangle.



Three major types of floating platforms are,

- a) Spar buoy platform.
- b) Semi-submersible
- c) Tension leg platform

2.3.1 Spar Buoy Platform

The spar-type platform mainly achieves stability due to ballast. Spar-type floating foundation is a steel or concrete cylinder ballasted with water and gravel, ensuring the wind turbine remains afloat and upright due to a significant righting moment arm and high resistance to pitch and roll motions. It employs a permanent ballast of solid iron ore, concrete, or gravel for stability, with the foundation's draft typically matching or exceeding the hub's height above sea level to minimize heave motion. These turbines are anchored using taut or catenary spread mooring systems with anchor-chains, steel cables, or synthetic ropes. The Hywind demonstration project by Statoil off Norway's Karmoy Island marks the deployment

of the first full-scale spar floating turbine.[9] The design of a spar buoy necessitates a significant draft, roughly equivalent to the turbine's hub height above sea level. This is to ensure that the structure's center of gravity, including the turbine, is positioned below its center of buoyancy. Consequently, spar buoys are suited for deeper waters compared to other floating structures. Similarly, deep waters are essential for mounting the wind turbine onto the spar buoy. In addition to limiting movement in the forward-backward (surge) and side-to-side (sway) directions, the mooring system must also restrict rotational movement (yaw). This is accomplished through a yoke system, where each mooring line is divided into two shorter, equal-length link cables that attach to opposite sides of the spar buoy.[16]



Figure 6. Hywind spar buoy FOWT model[15]

Designing a floating offshore wind spar concept poses unique engineering challenges, especially when compared to traditional oil and gas platforms. The complexity arises from the need to balance several key design drivers: (1) maximizing pitch stiffness to minimize vessel heel, (2) extending the natural heave period to diminish wave-induced motion, and (3) reducing overall costs. These objectives often require compromises, particularly as larger wind turbines are considered. While bigger turbines enhance the design space by increasing the spar's natural periods in heave and roll/pitch, they also necessitate deeper water, potentially limiting wind farm locations.[17] Fig 7 shows key characteristics and components of spar concept.

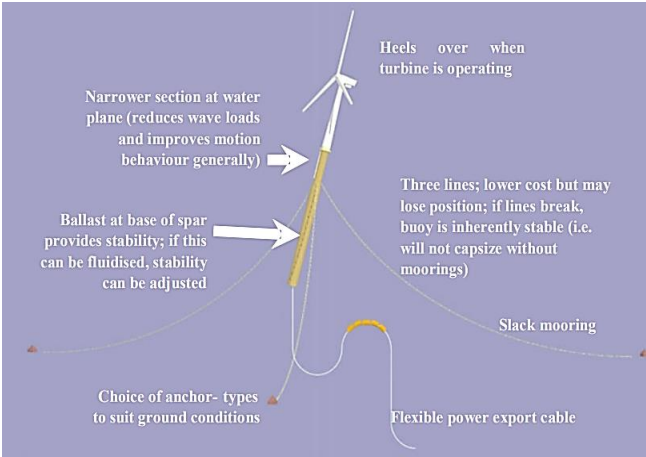


Figure 7. Spar key components and characteristics[17]

The successful development of a spar buoy for wind turbines hinges on several critical factors. Managing the spar's size is fundamental to accommodate the dynamic motions and the static limits of the wind turbine. Additionally, reinforcing the turbine tower is essential to withstand bending moments from operational heel and additional loads during transport, installation, and operation. The assembly process presents its own challenges; although vertical assembly is possible in the sheltered Norwegian fjords, most sites require a conventional horizontal tow and upending strategy. This method, coupled with the need to wait for suitable weather conditions, can significantly delay project timelines.[17] Figure. 8 provides a visual presentation of the viability of a matrix of conceptual designs, for increasing spar buoy diameter (left-to-right) and increasing spar buoy length (top-to-bottom). The diagram shows the viable design space and why other designs are not feasible, due to excessive motion, instability, fatigue, and cost.[17]

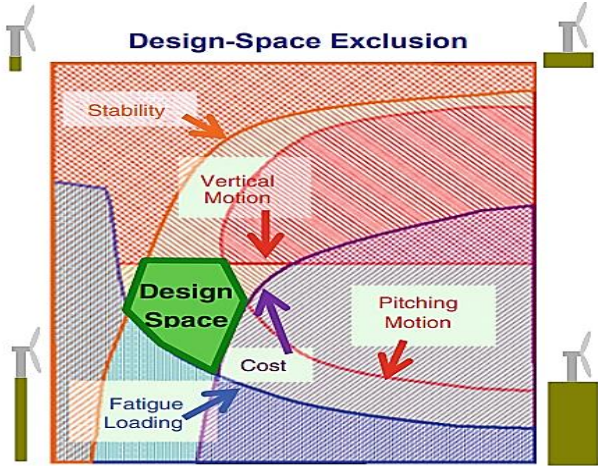


Figure 8. Design space spar concept.

2.3.2 Semi-Submersible Platform

The semi-submersible architecture integrates several prominent columns interconnected through tubular structures. Wind turbines can be mounted atop individual columns or distributed across all columns. An alternative configuration situates the wind turbine centrally among the columns, with support from lateral bracing elements. These columns serve a dual purpose: offering ballast while being partially inundated with water to maintain buoyancy. The stability of this design, especially when afloat, is primarily attributed to the water-plane area of the columns. This feature not only ensures stability for the wind turbine but also allows for operational flexibility due to the design's relatively shallow draft. To maintain its position, the semi-submersible floating wind turbine system employs mooring lines.[9]



Figure 9. Semi-submersible type FOWT design & application [15]

This concept exhibits various configurations, including:

- Three or four primary columns.
- Turbine placement at the center or atop one column.
- Construction using steel (specifically, the floating jacket or space-frame models, which are more prevalent) or concrete.
- Inclusion of heave suppression discs at the columns' base.
- Various numbers and arrangements of catenary mooring lines.

Such designs can be implemented in shallow waters, potentially as shallow as 25 meters for smaller turbines in calm wave conditions. However, designing catenary moorings in shallow waters is particularly challenging, as the moorings become taut with minimal horizontal displacement of the floater, complicating the design process. The structure's significant surface exposure leads to increased structural loads and motion amplitudes. The primary columns, providing buoyancy and counteracting wind turbine thrust, must be robust. The platform may also feature slender lattice members for bracing to mitigate wave loads.[17] Fig. 10 shows the key characteristics of semi submersible type platform.

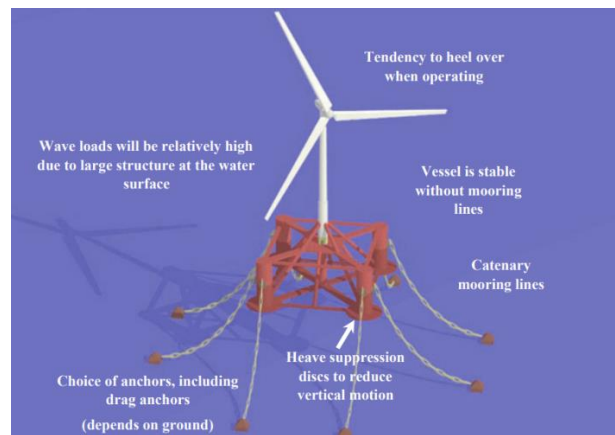


Figure 10. Key characteristics of semi-submersible platform[17]

Choosing a concrete structure alters the motion response significantly, necessitating a comprehensive redesign and optimization. To improve motion response on semi-submersible platforms, advanced design features may be employed, including:

- Strategic placement of major structural elements to offset wave loading from dominant waves, possibly requiring site-specific designs.
- Installation of heave-damping plates at primary columns' bases to align vessel movement with reduced wave amplitudes at depth.
- Incorporation of a moon-pool, an unconventional feature that alters natural frequencies and provides damping, demanding sophisticated CFD modeling and extensive testing.
- Designing structural geometry for additional damping, through specific shapes and sharp edges.[17]

2.3.3 Tension Leg Platform

Tension Leg Platforms (TLPs) are distinguished by their exceptional stability in their fully installed position, primarily due to their axially rigid mooring lines that effectively mitigate heave, roll, and pitch motions, though they allow for surge, sway, and yaw motions. The installation of wind turbines on TLPs at the quayside presents challenges, especially during on-site installation due to the potential for instability. This phase may necessitate buoyancy aids like collars, sacks, or chambers to prevent

capsizing, especially under wave conditions. Alternatively, vessel-assisted installations could offer stability but may be costly and reduce vessel availability for other projects.

TLPs exhibit low stiffness against surge and sway due to the inclination of mooring lines, leading to a set-down effect where the platform lowers into the water, dependent on water depth and mooring specifics. These platforms are fixed vertically by mooring tendons, rendering them unresponsive to sea-level changes, such as tides, which can vary significantly across locations. The design necessitates taut mooring lines to avoid snap loads that can cause catastrophic failure, especially in scenarios where tension loss occurs due to tidal variations or extreme waves. Thus, TLPs, while offering superior stability through mooring lines, face operational risks including potential total loss from mooring line failure, contrasting with the inherent stability of spar and semi-submersible platforms.[17] Fig. 11 shows the key characteristics of semi submersible type platform.

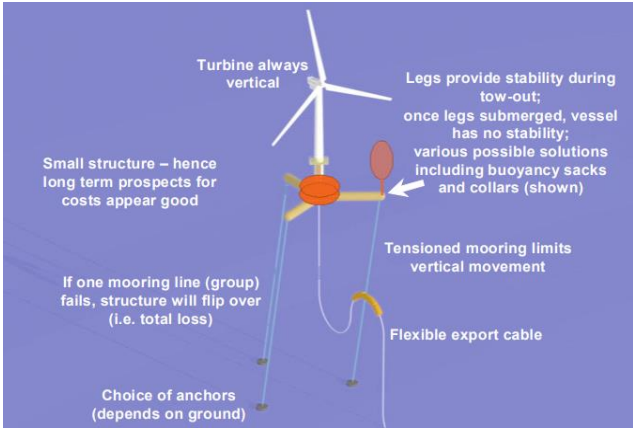


Figure 11. TLP characteristics[17]

TLP mooring lines exert vertical forces on their anchor points, necessitating specific anchoring methods such as gravity bases, suction caissons, and piles. These methods contrast with the horizontal or combined load capabilities of slack mooring systems used by spar and semi-submersible platforms, which can utilize simpler anchoring solutions like drag anchors. Gravity anchors are notably heavy and costly, both in fabrication and installation. Suction caisson and pile anchors, while effective, require precise design considerations, are limited by soil conditions, and have a less proven track record at the depths required for TLPs.

The development of TLPs for offshore wind turbines presents significant engineering and financial challenges when compared to spar and semi-submersible platforms. The requirement for specialized anchoring systems adds complexity and cost, raising doubts about the feasibility of achieving a cost-effective TLP design. However, if these challenges can be overcome, TLPs could offer a lightweight, cost-efficient solution for offshore wind foundations across a broad range of water depths, including shallower sites, providing a competitive alternative to bottom-mounted foundations.[17]

2.4 Floating Wind Turbine Mooring System

Floating offshore wind turbines must stay in place even during very strong storms. The systems that help these turbines stay anchored, called mooring and anchoring systems, are crucial. They directly influence how the turbines' platforms behave in the water. While anchoring ships and other structures at sea has been done for a long time, using these systems for floating wind turbines is new and comes with unique challenges. These systems must be carefully planned and evaluated at all stages of design to ensure they work correctly. The design of mooring and anchoring systems for floating wind turbines depends on factors such as cost, site conditions, expected environmental forces, and regulatory

constraints, with costs heavily influenced by water depth and distance from shore. [12] Following are the configurations of a mooring system.

- 1) Spread mooring system.
- 2) Taut mooring
- 3) Single point moorings

2.4.1 Spread Moorings

This system uses multiple lines connected to the floating structure to restrict horizontal movement and provide stability, preventing the structure from rotating to align with wind, waves, or currents, and is typically used in semi-submersible or spar platforms where directional response to external forces is minimal.[12] Spread moorings has following two different types written below,

- i. Catenary mooring
- ii. Multi catenary mooring

2.4.1.1 Catenary Mooring

Catenary mooring involves lines that hang in a natural curve from a structure to the seabed, anchoring horizontally to minimize vertical stress and using their own weight and length-to-depth ratio to stabilize the structure. In the past fifteen years, various design ideas for floating offshore wind turbines have emerged. Since 2009, multiple small-scale prototypes and three full-scale models, such as Hywind in Norway and WindFloat in Portugal, have been tested in real-world conditions.[12]

2.4.1.2 Multi catenary Mooring

This mooring system uses multiple lines with buoys or weights to create complex shapes, allowing the anchor point to handle vertical loads. Catenary moorings, characterized by lines that form a hanging curve and meet the seabed horizontally, mainly manage horizontal forces, making installation more cost-effective but allowing more motion in all directions. While these systems are cheaper and suitable for shallower waters, they provide less vertical tension, which can compromise stability, particularly in wind turbines where forces are exerted above the center of buoyancy.[18]

2.4.2 Taut Mooring

In this setup, mooring lines reach the seabed at about a 45-degree angle, managing both horizontal and vertical forces through their elasticity. For Tension Leg Platforms (TLP), the lines are almost vertical, and the restoring forces mainly arise from changes in the structure's buoyancy [19]. Taut leg mooring systems are more suitable than catenary systems in deeper waters due to their smaller area and shorter required mooring lines. When installed vertically, these systems require even less space and line length, but they also necessitate stronger, more complex anchors due to the high vertical forces involved.

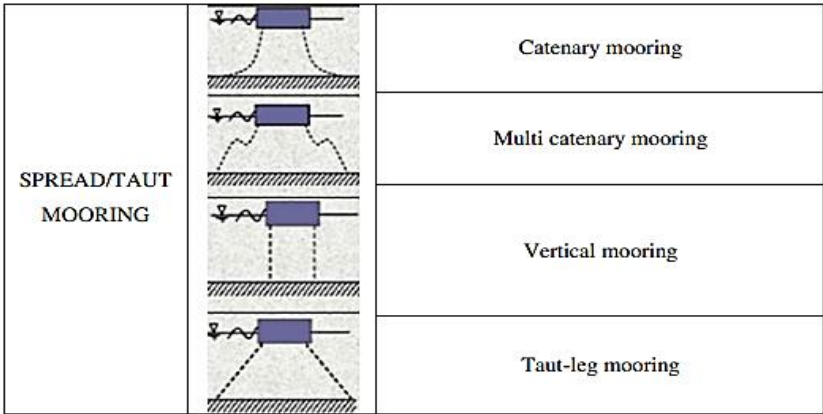


Figure 12. Spread mooring and taut mooring[12]

2.4.3 Single Point Mooring

Single point moorings enable floating structures to rotate freely, aligning with environmental conditions, and can connect directly to the structure or via an intermediary buoy, despite design variations all serving the same fundamental purpose.

2.4.3.1 Anchors

The anchoring system primarily consists of an anchor along with various supporting elements like shackles and swivels, which are crucial during installation, maintenance, and removal. Given the long history of their use, a diverse range of anchoring solutions is available, tailored to specific project needs, mooring setups, and seabed conditions. While a variety of anchor types exists, each has been extensively tested and applied in marine and oil and gas industries, and are also applicable to the floating offshore wind turbine industry.[12]

2.4.4 Guideline for Mooring/Anchor Application

A recommendation in [12] is given for selection of best anchoring system is given according to mooring application,

Type	Gravity anchors	Drag anchors	Piles	Suction piles	Plate anchors	Screw Piles
Catenary	Applicable but not the best choice	Recommended (1)	Applicable but not the best choice	Applicable but not the best choice	Applicable but not the best choice	Applicable but not the best choice
Taut-leg	Applicable but not the best choice	No Recommended (2)	Recommended (3)	Recommended (3)	Recommended (3)	Applicable but not the best choice
Vertical	Applicable but not the best choice	No Recommended (2)	Applicable but not the best choice (4)	Applicable but not the best choice (4)	Recommended	Applicable but not the best choice

Table 3. Mooring/anchor selection combination[12]

2.4.5 Material

Mooring lines are usually composed by a combination of metallic chains, metallic wires, or synthetic ropes. For anchors steel is the major material used in the manufacturing processes but other materials like aluminum and concrete are also used but in very less cases. In [12], mooring line properties with comments are also given so that mooring line selection could become easier according to the specific application. Numerical simulations were conducted in [20] to assess the dynamic behavior and hydrodynamic performance of the cell-spar-buoy. Spar-buoy support structure, designed for floating offshore wind turbines in deep waters like the South China Sea, uses a half-taut mooring system with nine mooring lines, each 720 meters long. This system is robust, with a breaking strength of 11,420,000 KN, far above the peak mooring line tension of 6,845 KN observed during severe storm simulations. Hydrodynamic analyses through numerical simulations show that the cell-spar-buoy performs well in harsh conditions, with its motion characteristics like a resonance frequency of about 0.23 rad/s ensuring minimal pitch, surge, and heave. The maximum pitch angle observed was only 4.5 degrees, and the heave and surge motions stayed under 1 m and 2 m, respectively, indicating a stable and safe operation.[20]

Material	Features	Comments
Chain	Broad use experience Readily Available	Unsuitable for water depths greater than 450 m Susceptible to corrosion Good abrasion resistance
Steel wire rope	Broad use experience Readily Available	Unsuitable for water depths greater than about 900 m Susceptible to corrosion
Polyester	High dry and wet strength Moderate stretch Frequent use in deep water taut moorings	Most durable of all fiber line materials Moderate cost
Nylon	High dry strength High stretch	Wet strength about 80% that of dry Low fatigue life Moderate cost
Polypropylene & polyethylene	Low weight High stretch	Low strength Low melting point Susceptible to creep Low cost
HMPE	Low stretch High strength to weight ratio	Replacing wire for towing-increased handling safety High cost
Aramid	Very low stretch High strength to weight ratio	Minimum bending radius similar to steel wire Roop Low abrasion resistance High cost
Elastomer	Low weight High elongation capacity High tear strength	Susceptible to cutting and breaking

Table 4. Mooring line material properties[12]

In [21] The OC3-Hywind SPAR-type floating offshore wind turbine used a mooring system with three slack catenary lines to stay stable in water. The study showed that these lines are crucial because they connect the turbine to anchors on the ocean floor and help control the turbine's movements caused by wind and waves. The study shows that these mooring lines are especially important for reducing side-to-side (sway) and forward-and-backward (surge) movements. They also help manage tilting movements (pitch and roll), ensuring the turbine stays upright and functions effectively in various weather conditions.

2.5 Loads due to Wind and Wave Interaction

FOWTs are subjected to various dynamic and static loads mainly due to waves and wind which influence their structural integrity and performance. The loads are,

- 1) Aerodynamic loads
- 2) Hydrodynamic loads
- 3) Hydrostatic loads
- 4) Mooring loads
- 5) Gravity loads

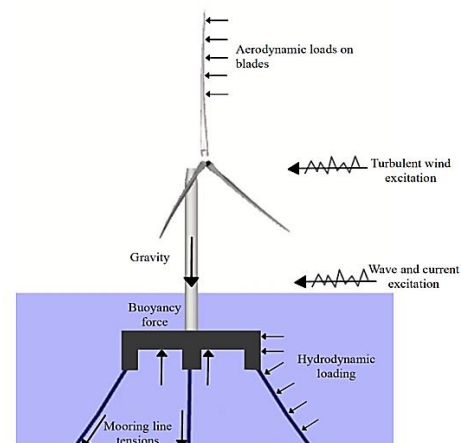


Figure 13. Different loads on FOWT due to wind and wave interaction[22]

These active elements together form the motion equation for the combined system of the platform and the wind turbine.

$$[M + A]\ddot{x} + [C]\dot{x} + [K]x = F_A + F_{HD} + F_B + F_M + F_W \quad (\text{eq-6})$$

M represents the generalized inertia matrix, which includes mass and moment of inertia. A is the added inertia matrix, C is the damping matrix, and K is the stiffness matrix. F_A stands for aerodynamic force, F_{HD} for hydrodynamic force, F_B for hydrostatic force or buoyancy, F_W for wind shear force, and F_M for mooring force. The next sections will briefly explain each of these external forces.

2.5.1 Aerodynamic Loads

Aerodynamic loads on the FOWT are mainly due to wind velocities are typically not constant but vary over time. It can be modelled as constant or varying wind velocity input in the selected numerical simulation software for hydrodynamics analysis such as Ansys Aqwa. Wind loads on the wind turbine rotor and tower can be predicted using CFD modelling but it takes CFD expertise and computational power to run. Aerodynamic loading is caused by the wind spinning the turbine blades and airflow through the rotor as it moves. Blade element momentum theory (BEM) treats wind turbine blades as individual segments, each acting like a two-dimensional airfoil. The total force on a blade is calculated by adding up the forces from each segment. [23]

$$F_{thrust} = \left(\frac{\rho_a}{2}\right) \times C_T \times A_{thrust} \times V_{hub}^2 \quad (\text{eq-7})$$

where F_{thrust} is the rotor thrust load, ρ_a is the mass density of air, C_T is the thrust coefficient, A_{thrust} is the swept area of the blades, and V_{hub} is the average wind speed at the hub height. . Integrating F_{thrust} along the whole length of the blade will result in the total thrust on that rotor blade and adding F_{thrust} from all 3 blades results in the total aerodynamic thrust for on the turbine. BEM is a popular method for estimating aerodynamic loads due to its simplicity and accuracy, but it requires additional corrections to address its basic assumptions and improve its accuracy in various conditions.[23]

The aerodynamic load along the turbine tower can be expressed by an approach based on Morison's equation, presented in equation below,

$$F_{aero}(z, t) = C_D, w \frac{1}{2} \rho_a [u(z, t)|u(z, t)|] D(z) \quad (\text{eq-8})$$

Here $u(z, t)$ is the wind velocity along the tower height and in time, C_D , is the dimensionless drag coefficient, which depends on tower dimensions and wind flow regime. ρ_a is the air density and $D(z)$ is the tower diameter at elevation z.[24]

2.5.1.1 Effects of Aerodynamic Loads

Aerodynamic loads cause movement in the platform of the FOWT, due to wind forces a platform can move in all six degrees of freedom but the DOFs with the most interest due to aerodynamic loading are Surge and Pitch motions as they both contributions towards the horizontal movements along the height of the wind turbine. Surge is denoted with X_1 and pitch is denoted with X_2 in figure below,

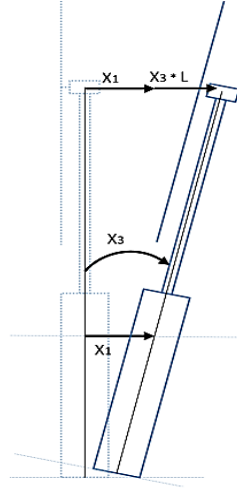


Figure 14. Major effects of Wind loads in two DOF[24]

2.6 Hydrodynamic Loads

When a body is placed in the water at an offshore location, it is subjected to different loads exerted by oscillation and wave excitation. There are various methods to model hydrodynamic forces, each varying in complexity depending on the chosen approach and wave theory like CFD, Navier stokes equation and Morsion's equation etc. Morison's Equation is least complex to model for prediction of hydrodynamic loads.

$$F_{HD} = \frac{\pi D^2}{4} \rho u + \frac{\pi D^2}{4} \rho C_A (\dot{u} - \dot{v}) + \frac{1}{2} \rho C_D D (u - v) |u - v \quad (\text{eq-9})$$

F_{HD} is the total hydrodynamic force, C_D and C_A are drag and added mass coefficients, u and \dot{u} are the water particle velocity and acceleration and v and \dot{v} are the floating platform velocity and acceleration, D is the diameter of the floating platform, and ρ is the density of water [23]. The coefficients C_D and C_A are dependent on the surface roughness and Reynold's Number.

2.6.1.1 Effects

Hydrodynamic loads can affect all translational and rotational DOF (Surge, Sway, Heave and Pitch, Roll and Yaw) of a wind turbine movement. These movements cause instability issues in the FOWT resulting the high response amplitude operator peaks and movements of wind turbines in any arbitrary direction thus reducing its power production efficiency.

2.6.2 Hydrostatic Loads

Hydrostatic loading on the submerged parts of a structure doesn't depend on wave activity, whether incoming or caused by the platform's movement. Instead, these loads are determined by how much of the structure is underwater and how the platform's movements affect this underwater volume. [24] The buoyancy force, or hydrostatic loading (F_B), is calculated simply using Archimedes' Principle based on how much of the floating offshore wind turbine (FOWT) platform is underwater. To accurately distribute this buoyancy force across the platform, software often calculates it by integrating the external water pressure on the submerged parts of the platform. This method accounts for the increase in water pressure with depth, causing deeper parts of the platform to experience more buoyancy force.

2.7 Site Selection

The selection of suitable sites for the deployment of floating offshore wind turbines involves comprehensive assessments focusing on environmental, geographical, technical, and socio-economic factors. The process ensures the optimization of renewable energy production while minimizing conflicts and adverse impacts on the environment and other maritime activities.

2.7.1 Environmental and Socio-Economic Considerations

Site selection for floating offshore wind farms begins with a strategic environmental assessment, which includes consultations and impact assessments. This process ensures that designated zones do not adversely affect critical habitats (such as birds, marine mammals, fish, and benthic organisms) maritime traffic, or other industries such as fishing and tourism. In Norway, the Offshore Energy Act governs the construction of offshore wind facilities, requiring a careful selection of zones that minimize environmental and socio-economic impacts. This act mandates the completion of a strategic environmental assessment before areas are opened for licensing applications.[25]

2.8 Technical Suitability and Risk Assessment

Technical evaluations focus on wind resource availability, water depth, distance from shore and seabed conditions, which influence the type of turbine technology—floating or bottom-fixed—that can be deployed. Areas are chosen based on their wind speed profiles, capacity for grid connections, and minimal interference with existing uses of the sea space, such as shipping lanes and oil platforms. For instance, in Norway, areas with minimal risk of interest conflicts, such as those between renewable energy production and petroleum extraction or fishing activities, are prioritized.[26]

2.9 Conflicts of Interest (case study from HAVVIND summary by NVE)

2.9.1 Petroleum Interests

Petroleum Interests and impacts are related to potential petroleum resource available within the selected zone for offshore wind farm. In detailed impact assessment in [25] highest petroleum potential is found in Sørlige Nordsjø 1 & Sørlige Nordsjø 2. These two zones are considered with highest wind resource availability within the Norway as well. Conflict of interest is also possible in other zones in Norway but in [25] it is mentioned that co – existence between these two conflicts is possible.

2.9.2 Shipping

Conflict of interest arises between shipping and offshore wind industries when an identified and selected offshore wind farm zone is located in between an existing shipping lane or route. Some zones like Frøyabanken, Olderveggen, Træna fjorden and Stadhavet are expected to cause the highest impact on the shipping. It is also mentioned in [25] that co-existence between these two conflicts is also possible by developing new routes or diverging from an existing route a little bit.

2.9.3 Fisheries

Co-existence between wind farm and fisheries activities is not possible within a zone that is why seven out of fifteen identified zones by NVE in Norway are not opened for license applications.[25]

2.9.4 Other interests

Some areas within the identified zones are used by Norwegian Navy and Airforce for different purposes and that is why one of the identified zones called as Gimsøy Nord is not recommended for any commercial offshore wind activities. It is also mentioned in [25] that none of the identified zones will impact meteorological and civil aviation radars.



Figure 15. NVE's identified offshore wind zones[25]

The selection of deployment sites for floating offshore wind turbines is a complex interplay of environmental, technical, and economic factors, all governed by regulatory frameworks. Thorough assessments and the application of advanced methodologies ensure the optimal selection of sites for sustainable and efficient wind energy production.

NVE has ranked the fifteen identified zones in three different categories of A, B and C with A ranked as highest and most feasible for offshore wind applications. Through detailed analysis of this summary by NVE it is concluded that four out of fifteen identified are most suitable and feasible for floating offshore wind production activities. They are mentioned as follow:

1. Utsira Nord
2. Sørilige Nordsjø 1
3. Sørilige Nordsjø 2
4. Frøyabanken

To analyze the technical suitability, accurate latitude and longitude coordinates are needed for the selected zone to find the meteorological data by NORA3 which I'll do in the later stages of this project.

2.10 Review of Existing Studies

FOWTs have emerged as a promising technology for harnessing wind energy in deep-water environments where conventional fixed-bottom turbines are not feasible. Extensive research efforts have been directed towards understanding the dynamic behavior and performance optimization of FOWTs through numerical simulations and experimental investigations.

2.10.1 Structural Behavior

Interaction between loads from wind & wave and floating offshore structures causes different types of movements of floating structures. These movements influence the efficiency and safety of a floating offshore wind turbine. These structural movements are categorized in six degrees of freedom for a floating offshore structure. Concept of offshore structural movement has been taken from already developed shipping and petroleum industries. The six degrees of freedom (6 DoF) for FOWTs represent the various ways in which these structures can move in response to environmental forces like wind and waves. These movements are categorized into three translational motions (heave (up/down), sway (left/right), surge (forward/backward)) and three rotational motions (roll, pitch, yaw) along the global x, y, z coordinates system. Understanding these motions is crucial for designing FOWT that can withstand marine conditions while maintaining efficiency and safety.[27] These movements are basically measured and analyzed in Time and Frequency based domains where structural movement amplitudes are studied during a set of loading conditions, time periods and wave frequencies. Translational movement amplitudes of a FOWT are measured in meters, and rotational movement amplitudes are measured in degrees against the time period in seconds.

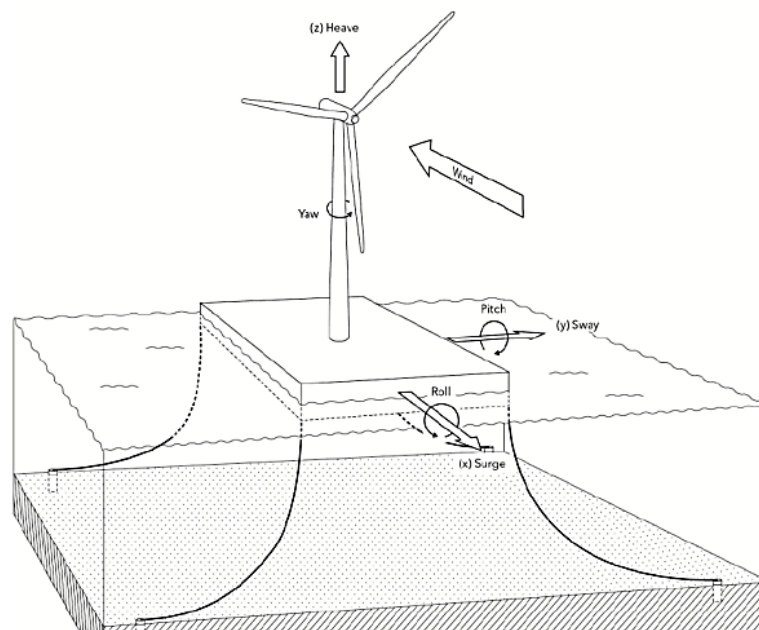


Figure 16. 6 DoF for FOWT[28]

To measure these six DoF in FOWTs, researchers often use a combination of sensors and simulation models. Sensors such as accelerometers and gyroscopes are installed on different parts of the turbine to record movements in oceans or wind tunnel tests. Additionally, computer simulations provide data on how the turbines would react under specific conditions, helping to predict and optimize their behavior in real environments.[29] Now a days, Numerical simulations based approach is used a lot in research fields as we are in the earlier stages of development of FOWT and not so many full scaled prototypes are available for testing. However, data analysis and accurate boundary conditions need to be applied for numerical modelling of such floating structures. Many commercially used software Packages are available for predicting full scale hydrodynamic behavior and response of the FOWT in different loading conditions such as Ansys AQWA, OpenFoam, FAST & Flow 3D.

In [20] numerical simulations of the cell-spar-buoy, designed to support a 5 MW offshore wind turbine, were performed to analyze its dynamic behavior and hydrodynamic efficiency. Through both frequency and time domain analyses, the response amplitude operators (RAOs) of wave-induced motions were

computed, which are crucial for its preliminary design validation. The frequency domain analysis utilized linear diffraction theory to calculate the inertia and diffraction forces on the buoy, while time domain simulations incorporated Fast Fourier Transform (FFT) generated excitation time series and direct numerical integration. This approach provided detailed insights into the 6-degree-of-freedom motion of the structure. Notably, the results demonstrated that the cell-spar-buoy exhibits long natural motion periods with a resonance frequency around 0.23 rad/s, which is outside of the prevailing wave frequency range of the South China Sea. Additionally, in time-domain analysis, under a 50-year return period storm condition, the tensions in the most loaded mooring line reached a maximum of 6845 kN, well below the breaking strength, thereby underscoring the mooring system's reliability. These outcomes collectively affirm that the cell-spar-buoy can be operated safely and effectively in offshore environments, promising significant contributions to wind energy exploitation. [20]

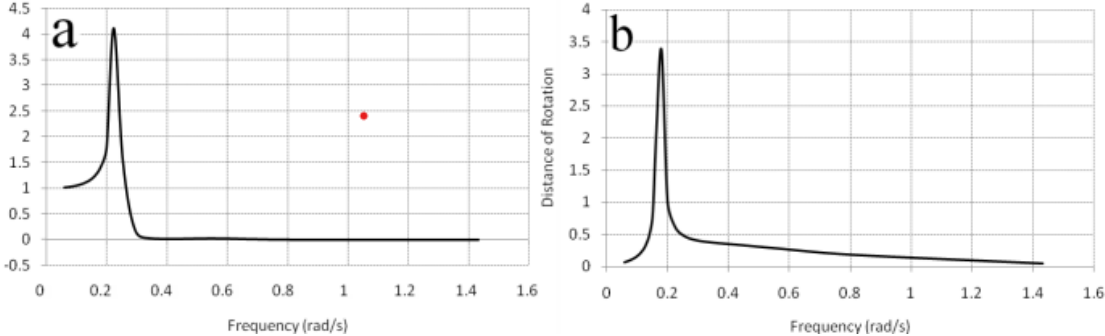


Figure 17. RAO of Heave and pitch[20]

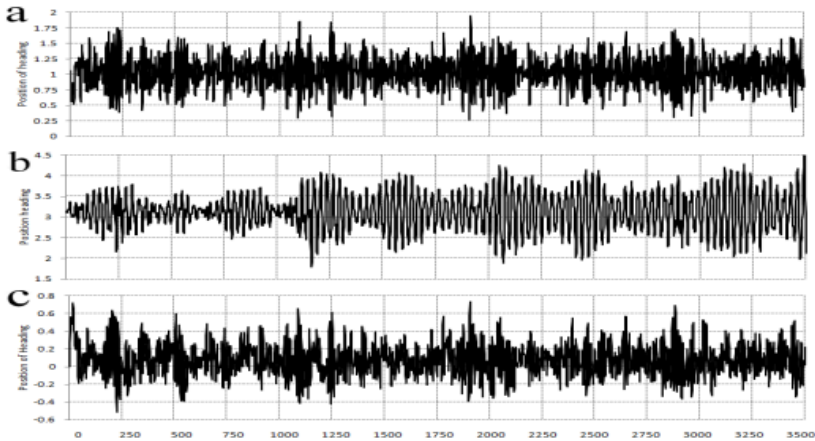


Figure 18. Time domain analysis for surge, pitch and heave motions[20]

In [30] the experimental and numerical analysis of a 1:300 scale model of a spar-type offshore wind turbine was conducted. It yielded critical insights into the dynamic behavior of floating structures under irregular wave conditions. Notably, the experimental results demonstrated a high degree of similarity with numerical predictions. Power spectrum density charts were obtained using numerical solution. The study revealed that the surge response exhibited a significant peak value at a frequency of approximately 4.4 rad/sec, closely aligning with the numerical predictions. Meanwhile, the sway, roll, and yaw responses were considerably lower, highlighting the model's directional stability under wave influence. The results indicated maximum surge motions between 6m to 8m, pitch motions ranging from 2° to 3°, and heave motions from 0.6m to 0.8m, providing a detailed spectrum of the model's response under simulated marine conditions. This comprehensive analysis not only underscores the effectiveness of numerical simulation tools like Ansys-Aqwa in predicting the complex dynamics of offshore wind turbines but also enhances our understanding of their performance in realistic sea states, thereby contributing to more robust designs and operational strategies for renewable energy technologies.[30]

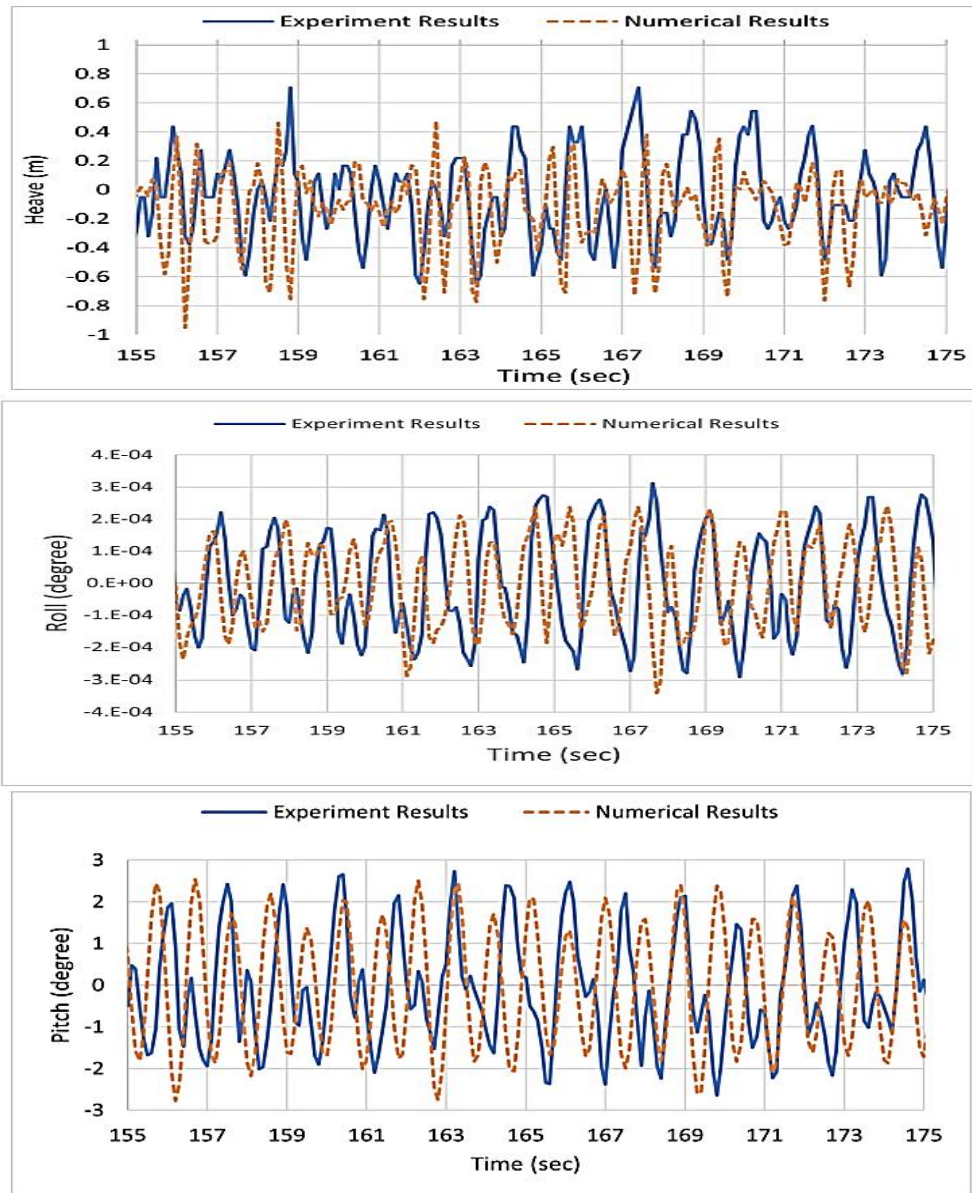


Figure 19. Heave, roll and pitch response in time domain[30]

In [31], the dynamics of a Spar-type floating offshore wind turbine were comprehensively analyzed using the ANSYS Aqwa software. This investigation focused on a three-column spar platform, distinct from conventional spar type studies. Simulations used the Jonswap model to represent irregular wave patterns, with significant wave heights reaching 9.01 meters and peak periods at 11.3 seconds. The platform experienced different amplitudes of motion across six degrees of freedom surge, sway, heave, roll, pitch, and yaw with notable peak and mean values. For instance, the surge peaked at 6.7 meters, with a mean of 1.5 meters, sway peaked at 4.2 meters with a mean of 1.3 meters, and heave peaked at 4.7 meters with a mean of 1.5 meters. Additionally, rotational movements were noted, with roll peaking at 2.6 degrees and averaging 0.5 degrees, pitch peaking at 10.6 degrees with an average of 3.6 degrees, and yaw peaking at 9.2 degrees and averaging 2.1 degrees. These values indicate considerable displacement and rotation but stayed within safe operational thresholds. Furthermore, the stresses on the connecting ropes were found to be half of the anticipated values, thereby satisfying classification requirements, and underscoring the robustness of the design under extreme conditions. Despite these promising results, the data preparation phase was described as time taking, highlighting a potential area for process optimization in future simulations. This study confirms the structural integrity and operational feasibility of the spar-type design under severe maritime condition.[31]

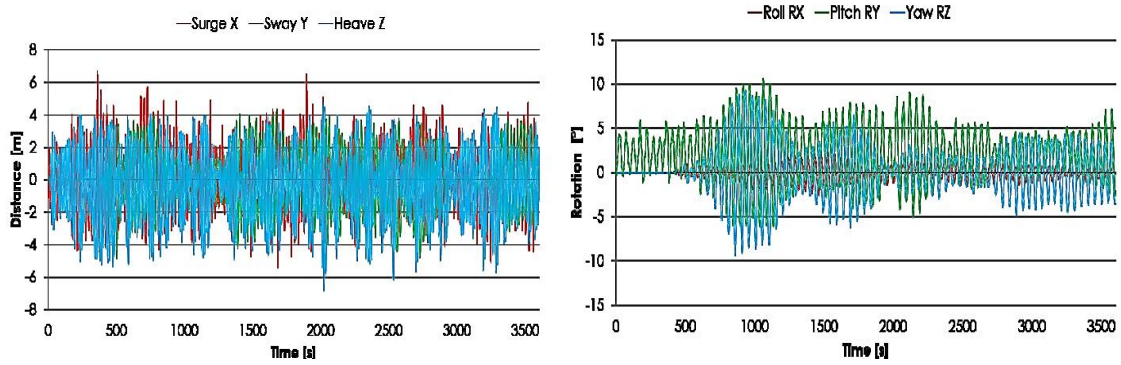


Figure 20. 6 DOF time domain response[31]

C.P.M Curfs in his study explored how offshore floating wind turbines behave differently when they are surrounded by level ice compared to open water. A MATLAB model was developed to simulate the turbine's structural response and the forces on its mooring system, considering mainly three types of movement: surge, heave, and pitch. The model, which assumed the turbine doesn't deform, includes complex calculations for how the water and mooring system affects the turbine's stability and used data from CFD software to predict how the structure interacts with water. Different scenarios were simulated, including those with wind and waves alone and others with added ice pressure. The findings show that ice pressure can significantly affect the turbine operation, especially if the ice crushes against it, causing high forces that could endanger the turbine's stability and longevity. In contrast, if the ice bends around the turbine, the effects are less severe. The study suggests designing turbines to encourage ice to bend rather than crush can reduce these risks, making it an important consideration for turbines in icy waters.[24]

2.10.2 Geometric Design optimization and Operating Conditions

2.10.2.1 Platform Concept Selection

Selection of floating platform for wind turbine majorly depends upon the operating conditions of the selected site for wind turbine deployment. Wind Float is one the examples for semi-submersible platform. Semi-submersible platforms often being deployed at rather more shallower waters and less water depth. It's also easy to manufacture and assemble this type of platform nearby shore as it doesn't have bigger draft underwater and can be assembled nearby shore and towed to selected location.

Spar buoy is a cylindrical structure stabilized by ballast weights, with its center of gravity lower in the water than its center of buoyancy. Usually, these buoys have enough depth in the water to offset vertical movements. They're relatively simple to build and offer good stability. However, their large draft requirement can make it tricky to assemble, transport, and install them, limiting their use to waters deeper than 100 meters. E.g Hywind by Statoil. As the platforms are intended for deployment in higher depths, the mooring length increases, and this may increase the cost. Spar buoys are often very stable, but their installation and assembly might not be feasible for so many locations around the world. Norway is one the most feasible sites for deployment of these kind of platforms due to availability of deep fjords very near to shores. Availability of deeper fjords makes the installation and logistics easier for deployment of spar buoy floating turbines.

Tension Leg Platform (TLP) is a type of offshore platform that is partially submerged and anchored to the seabed with mooring lines. These lines keep the structure stable by staying in tension. The design allows for a lighter and smaller structure due to its shallow draft and dependency online tension for stability. However, this setup puts a lot of stress on the tendons and anchors, making the installation process challenging and increasing the risks of survivability during operation. If a tendon breaks, it can significantly affect the platform's stability. E.g Pela star. Operating conditions such as wave periods and under water currents affect this type of platform a lot and it's not recommended to deploy TLP where

higher wave currents are expected and seabed conditions are not feasible for rigid connection with anchor.[32]

2.10.2.2 Design Optimization

In the field of offshore wind energy, engineers are constantly exploring alternative platform designs that better support turbines and towers. Some innovative designs combine features from different platforms to maximize their benefits, like the heave restrained TLP and SPAR, which control vertical motion to improve stability. Additionally, there's interest in integrating other energy sources, like wave energy, into these platforms. Another approach involves placing multiple turbines on a single platform, which offers efficiencies like shared mooring systems and grid connections but also presents challenges, such as managing the airflow between closely spaced turbines. For instance, Swedish company Hexicon and Shimizu Corporation with the University of Tokyo have developed multi-turbine platforms, aiming to optimize space and energy output while addressing the aerodynamic interactions between turbines.[32]



Figure 21. Multi turbine platform concepts[32]

The DeepCWind consortium in the USA conducted tests using three different floating platforms, each paired with a scaled model of the NREL 5 MW wind turbine. Among the platforms tested, there was a TLP, a semi-submersible, and a SPAR platform. These platforms were modeled on a 1/50th scale and subjected to controlled wind and wave environments to reflect real-life marine conditions. The experiment involved initial identification of each platform's natural frequencies through hammer tests, followed by static and dynamic assessments under separate and combined wind and wave impacts. Results indicated that the natural frequencies of these platforms are crucial for understanding their stability and response under environmental loads. Notably, the semi-submersible platform showed longer surge periods compared to the TLP and SPAR, affecting how it responded to wind and waves. The SPAR showed significant pitch and roll, which was less evident in the TLP due to its rigid mooring system. In scenarios without wave loads, the SPAR demonstrated advantages in resisting wind-induced movement. However, under combined wind and wave loading conditions, semi-submersible platform showed the highest motion responses.

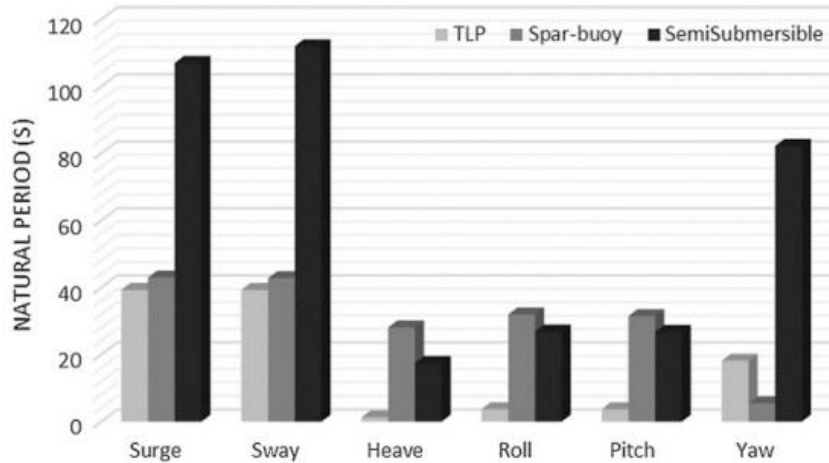


Figure 22. Natural periods in 6 DoF for DeepCWind platforms[32]

The type of platform used gives us some basic ideas about how it will perform when under loads. However, each design reacts differently due to its shape and water dynamics. Recent research has focused on finding the best designs through optimization, which involves adjusting various geometric aspects to improve performance according to established standards. This optimization process considers environmental factors and loads to determine the best shape for the platform. The possibilities for different designs are infinite, making this a very broad area of study. Despite the complexity of the issue, many researchers have made progress. For instance, some studies have focused on optimizing certain features like the size and depth of the platform by testing various shapes to see which ones work best. In some cases, simplifying the models by ignoring certain parts, like the connections in multi-body structures, has helped speed up this process.[32]

2.11 Floating Wind Turbine & Icing

The rapid expansion of offshore wind energy, with the European Wind Energy Association forecasting 320 GW of wind energy capacity in the EU by 2030, underscores the sector's pivotal role in meeting the EU's renewable energy targets.[33] Also, The ambitious goal set by Norwegian industry organizations to increase Norway's share of the global offshore wind market to 10% by 2030, alongside significant growth in sector turnover, underscores the pressing need for research in developing advanced offshore wind technologies suitable for Norway's unique environmental conditions.[34] The presence of both sea and atmospheric ice poses significant operational challenges for floating offshore wind turbines in cold regions of Northern Europe, necessitating innovative research to mitigate these effects and ensure optimal turbine performance and structural integrity.[35] Icing on FOWTs has two different types combined affecting the wind turbine operations in deep & ice prone offshore areas. Three types of icing are mentioned below,

- I. Atmospheric ice
- II. Floating sea ice chunks

2.11.1 Atmospheric Ice

Atmospheric icing significantly impacts the aerodynamics and structure of wind turbines, particularly those located in cold climates. The accretion of ice on turbine components, especially the blades, occurs when supercooled water droplets in the atmosphere freeze upon contact with the turbine surfaces. This accretion changes the blade profile and increases the surface roughness, thereby reducing aerodynamic efficiency and increasing structural load[36]. In the case of floating wind turbines, the rotor moves back and forth and that changes the flow behavior and related thermodynamic properties. In addition, the meteorological conditions in the sea such as wind speed, droplet size and Liquid Water Content (LWC)

are different from onshore and that leads to different types of atmospheric ice (mainly wet glaze) accretion on floating wind turbine rotor [37]. It was found that the wind turbine blade leading edge catching ice first gives a reduced torque, which changes the capability of the turbine to utilize wind energy. The shape of the accreted ice along the wind turbine blade depends upon many variables such as point of operation, the geometry of the wind turbine blade, relative wind velocity, atmospheric temperature, droplet diameter and the liquid water content [38]. Ice accretion on the wind turbine blade profiles has a range of shapes resulting from different temperatures and heat balance situations. Different types of icing have been identified as causing different levels of power losses [39]. Ice tends to accumulate unevenly across the turbine blades, increasing mostly near the tips while the base remains relatively clear. In extreme conditions, the added weight from the ice can be up to 50% of the blade's weight [40], posing a high risk of structural failure. This uneven ice distribution can cause vibrations and stress, leading to potential cracks and damage in the turbine components [41].



Figure 23. Atmospheric icing on wind turbine blades [42]

2.11.2 Floating Sea Ice Chunks

Sea sprays can reach just the lower levels of wind turbine structures, like the bottom of the tower and the blade tip while it is azimuthally downward pointing. The World Meteorological Organization in 1962 indicated an upper limit of 16 meters above the sea surface for the sea sprays, unless the sea surface roughness changes, when it is expected that waves can carry sprays up to levels above that limit. For current offshore turbines size, it is expected that sea icing will not cause additional problems for rotor parts[35]. Ice pack or floating blocks on the sea surface can cause additional static and dynamic forces on the turbine structure particularly along tower and foundations / platforms. The effects of sea ice occur as mechanical shocks and increased vibrations that may result in additional operational loads. This phenomenon becomes more complicated in the case of floating wind turbines where stability of the floating platform is the biggest issue. The additional loads caused by interaction between ice chunks and FOWT can increase the motion response amplitude of the wind turbine that could become a potential risk to power production, damage to the structure and mooring system infrastructure of the FOWT.

The interactions between sea ice and structures, such as ships and offshore platforms, are influenced by the structural design, which determines the mode of ice failure. For sloped surfaces like ship hulls, ice typically slides and breaks, which is mechanically favorable but costly to mitigate with protective measures for floating wind turbines in deeper waters[43]. In contrast, ice interacts differently with vertical structures, exhibiting crushing behaviors at various speeds that are divided into three regimes: intermittent crushing, frequency lock-in, and continuous brittle crushing. These interactions can induce significant structural vibrations and potentially reduce the lifetime of structures like offshore wind turbines, as outlined in current design guidelines[44].

Ice-structure interaction models have been advanced to better simulate these dynamic ice loads. One such model, developed at the Norwegian Sustainable Arctic Marine and Coastal Technology center

(SAMCoT SFI) by Hendrikse & Metrikine, offers a sophisticated representation of ice loads through a stochastic model involving multiple independent ice stripes interacting with a structure. This model, known as the VANILLA model, is now being adopted by the wind energy industry for its realistic portrayal of ice dynamics and has significant implications for the design of ice-resistant structures[45, 46]. However, understanding is limited for floating wind turbines, especially on how ice-induced vibrations combined with wind can impact the structures. New tests suggest that controlling the turbine's settings might help manage these vibrations. For floating turbines, the challenge is greater because they involve multiple closely spaced bodies, unlike the single cylindrical shape used in fixed turbines. The design of their anchoring systems also needs reconsideration since ice can cause higher loads, leading to more wear and tear. Additionally, the interaction between the ice and these floating systems could lead to different kinds of damage than seen with fixed structures. This complex scenario should be studied using a probabilistic approach to account for the uncertain nature of ice properties and their interactions [47].

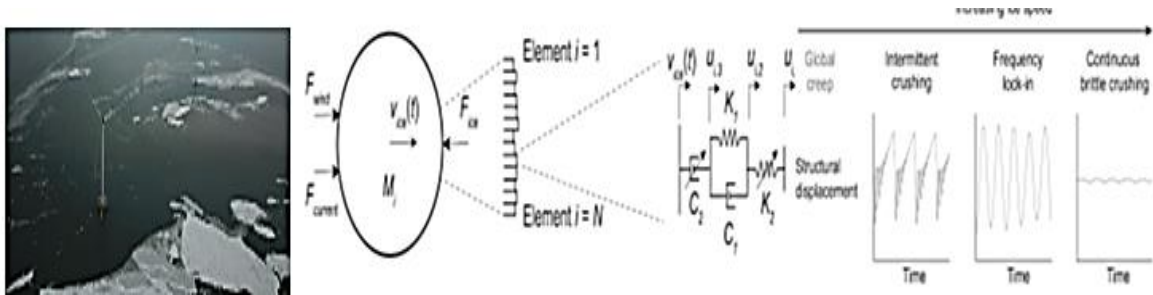


Figure 24. FOWT & floating sea ice chunks interaction

2.12 Operations & Maintenance Strategies for FOWT

Maintaining and operating offshore wind farms is tougher and more expensive than onshore ones because it's harder to get to the turbines out at sea. Even when the weather is good, it still costs more. This is because the wind farms are far out in the ocean, exposed to saltwater that can damage equipment, and require big ships with special gear to fix or replace large parts, which aren't always quickly available. As a result, producing energy at some offshore wind farms in Europe can be about 33% more expensive than at onshore ones.[48] As offshore wind farms get bigger and farther from shore, the need for better logistics and access technology grows. This is because safely and efficiently transporting technical staff to turbines, especially in bad weather, is crucial for reducing maintenance costs, which can make up about a quarter of the farm's total lifetime costs and up to 30% of energy costs.[49]

2.12.1 Offshore Maintenance Logistics Strategies

Different offshore wind farm projects have unique features that affect their maintenance strategies, mainly influenced by factors like distance to shore, nearby service hubs, layout, sea conditions, and the size and number of turbines, leading to three main logistical approaches.[50]

- i. Workboat based
- ii. Heli support
- iii. Offshore based

2.12.1.1 Work boat Based

In the Work boat-based approach, boats called crew transfer vessels (CTVs) carry maintenance workers from a nearby service hub to the wind farm and back, ideal for locations close to shore. As the distance to the wind farm increases, travel time goes up, reducing effective work time per shift and increasing the average repair time, which impacts production and availability.[49]

2.12.1.2 Heli Support

The Heli Support strategy uses helicopters for urgent repairs, complementing the workboats that handle regular maintenance. Helicopters cut down travel time, can operate in winds up to 20m/s, and are useful for far-off sites, though they are costlier and less effective in heavy rain or low visibility.[49]

2.12.1.3 Offshore Based

For offshore wind farms over 40 nautical miles from shore, where travel makes onshore support uneconomic, technicians go directly at the wind farm in either fixed or floating accommodations. They are transferred to turbines using combination of boats, helicopters, and advanced gangways, with additional support vessels like OSVs used for larger maintenance tasks.[50] Norway's unique geographical features provide specific advantages for the installation of floating offshore wind turbines (FOWTs) using deep draft spar buoys. The deep, sheltered Norwegian fjords allow for the assembly and ballasting of these turbines close to shore. This proximity simplifies logistics and reduces installation costs compared to other regions where similar installations are more challenging due to the required depth and other types of floating platforms such as semi-submersible floating platform are preferred. In Norway, once assembled, the FOWTs can be towed from the fjords to their designated offshore locations efficiently. This method leverages Norway's natural landscape to overcome common challenges faced in offshore wind turbine installations, demonstrating a significant strategic advantage in the deployment of renewable energy technologies [51]. The maintenance and operation of floating wind turbines are less explored and often rely on adapting models from fixed turbines. Recent approaches have used various simulation tools and mathematical models to better understand and optimize these operations under the challenging conditions of the sea, which leads to higher failure rates for offshore turbines compared to onshore [52, 53].

2.12.2 Maintenance Strategies for Bottom Fixed Offshore Wind Turbines

2.12.2.1 Structural Failure

So far no major offshore structural failures have been observed but a study report in [32] revealed structural failure data for onshore wind turbines. The study shows that tower failure is the most common type of structural failure, accounting for 67% of such incidents. This is significantly higher than failures involving blades, nacelle-housing, or the rotor. The primary reasons for tower failure include storms (28%), strong winds (21%), typhoons (10.5%), and failures in the braking system (7%), among others. The most frequent result of tower failure is the complete collapse of the tower, which happens 88% of the time.[32]

2.12.2.2 Wind Turbine Failure

Another study report in [32] shows that minor issues with the electrical and electronic systems of wind turbines are a major contributor to their downtime, despite being more frequent but less severe compared to other components. These minor problems, accounting for 75% of failures, lead to only 5% of the downtime, whereas the more critical 25% of failures cause almost all the downtime. Therefore, maintenance should primarily address these significant failures, especially in key parts like the rotor, gearbox, generator, and yaw system, to enhance turbine availability. Improving the reliability of the electrical and electronic parts is also crucial, particularly as challenges increase in offshore environments where accessing turbines is difficult.[32]

2.12.3 O&M Strategies

Reliability-centered maintenance (RCM) is a modern method used in the wind turbine industry to decide the best maintenance approach. It involves preventive maintenance that relies on monitoring performance and various parameters to take appropriate actions. This method uses condition monitoring systems (CMS) to strike a balance between immediate repairs and regular scheduled maintenance. By implementing effective CMS and fault detection systems, the reliability and functioning of turbines can be significantly enhanced. These systems utilize sensors to gather data periodically, which is then analyzed to assess the condition of critical turbine components, detect existing faults, or predict future

issues. This analysis helps in choosing the most suitable maintenance strategy, applying specific condition monitoring techniques either to certain parts of the turbine or the entire system. Some of the maintenance strategies that can be used to reduce the risk of failure are mentioned below,[32]

Vibration Analysis: This technique uses sensors to analyze vibrations in wind turbine parts like shafts and bearings to predict failures early, but it can be expensive due to the additional equipment required.

Oil Analysis: By examining the metal debris in oil, this method assesses the condition of gearbox components in wind turbines to monitor their health.

Temperature Measurement: This method tracks changes in temperature of turbine parts to identify potential failures, often used alongside other techniques as it detects issues slowly.

Strain Measurement: Utilizes strain gauges on turbine blades and towers to measure stress, helping in the structural health monitoring of these components.

Optical Fiber Monitoring: Involves using optical fibers either on the surface or inside turbine components like blades to monitor critical conditions.

Visual Inspections: Regularly checks visible parts of the turbine such as blades and nacelles for any signs of damage or wear.

Acoustic Emission: This expensive method detects faults in turbine parts like gearboxes by capturing the sound of the emitted waves, which is effective over a wide range of frequencies.

Ultrasonic Testing Technique: Uses sound waves to detect internal flaws in materials through methods like pulse-echo, which helps identify structural integrity.

Thermography Analysis: Applies infrared technology to spot heat-related issues in both electrical and mechanical components of wind turbines.

Signature Analysis: Analyzes the patterns from electrical or mechanical signals to identify potential faults in turbines.

SCADA Data Analysis: Analyzes existing sensor data from turbine control systems to assess overall turbine condition, which is cost-effective and reliable.

CHAPTER 3

3 Design of Experiments

3.1 Floating Platform Selection for Numerical Study

Selection of floating platform for wind turbine majorly depends upon the operating conditions of the selected site for wind turbine deployment and specific project goals. I have chosen *Spar Buoy Platform* for structural response evaluation due to following reasons.,

3.1.1 Water Depth Suitability

One of the reasons, why world is moving towards floating offshore wind energy is availability of greater and consistent wind resources. Wind resources are available often at locations far from shore where water depth is generally more than 60-80 meters. Spar buoys are designed for deep waters, typically over 100 meters, and are known for their stability in these environments due to deep draft design. On the other hand, semi-submersible and TLP platforms are more suitable for the shallow waters though they may not be as stable in deep water conditions due to their design and requirements for stability.

3.1.2 Stability and Motion

Spar buoys have a long cylindrical hull that extends deep into the water, resulting in very low movement in terms of heave, pitch, and roll, which is important for the efficiency and longevity of turbines. Semi-submersible platforms, in contrast, experience more movement, which could affect turbine performance in rough weather. Tension Leg Platforms (TLPs) are generally stable but can be sensitive to certain types of movement like pitch and roll. They also require rigid moorings to stay in place, which can be costly and complex in deep waters.

3.1.3 Simplicity

The Spar buoy features a simple design with a single large column that supports the turbine, making it robust and requiring less maintenance, which is crucial for installations at locations far offshore. In contrast, semi-submersible and TLP have more complex structures and systems for maintaining stability, leading to higher maintenance needs and more operational oversight. The simplicity of spar buoy design makes it easier for researchers as well to study hydrodynamics response of floating offshore wind turbines in these earlier stages of development and research.

3.2 Site Selection and Estimation of Operating Conditions

Norway being located at the heart of Arctic and its active role in policy making for development of renewable energy sources make it the best location to choose for the study of FOWT in Arctic conditions. Norwegian Water Resources and Energy Directorate (NVE) has identified and categorized 15 zones for development of offshore wind farms in its HAVVIND project summary. These zones have been ranked in three different categories from A-C as A being the most suitable & feasible and C being the least suitable & feasible. This ranking is a result of several impact studies conducted by NVE. NVE has not opened seven out of these fifteen zones for license applications because of their conflicts and impossible co-existence with fishing industries / fish farms. Zones that are feasible for floating wind generation are mentioned below in table 5.

S.Nr	Zone Name	Category	Licensing
1	Sørlige Nordsjø 1	A	Open
2	Sørlige Nordsjø 2	A	Open
3	Vanøya Nordøst	B	Open
4	Nordmela	C	Not open
5	Træna fjorden	B	Not open
6	Træna Vest	B	Not open
7	Frøya Banken	B	Open
8	Stadhavet	B	Open
9	Utsira Nord	A	Open

Table 5. NVE's identified locations for offshore wind.

NVE's identifies offshore wind farm locations. Three out of nine mentioned zones are not open for licensing. Stadhavet, Utsira Nord and Frøya Banken are considered as the most suitable specifically for Spar Buoy FOWT as the water depth within these zones are feasible for the deployment of FOWT with spar buoy platform. All other zones have water depths less than 80 meters. Out of three considered zones, I selected *Utsira Nord* to as an identified geographical location that is most suitable for this study because it is categorized as A and it doesn't have any major impacts and conflicts with other interests such as petroleum, tourism, and shipping.[25]

To get the much-needed metrological data related to wind and wave, first of all geographical coordinates of Utsira Nord were identified using a report from Royal Norwegian Ministry of Petroleum and Energy. Coordinates of identified zone are,[54]

Latitude	Longitude
59.2 °	4.5 °

Table 6. Geographical co-ordinates for Utsira Nord in Norway

3.2.1 Estimation of Operating Conditions

I used the NORA 3 database which is managed by the Norwegian Meteorological Institute for extracting the metrological data of this site. This database provides detailed forecasts of the ocean and atmosphere, which are crucial for understanding the operating conditions at potential turbine sites in Norway. Using customized Python code, I was able to access specific data from this database, such as *wave height*, *wave period*, *wave direction*, and *wind speed*, for exact coordinates of Utsira Nord from 2015 till 2021. This information is vital for FOWT platform design because it helps to evaluate that what will be operating conditions at the site and what will be turbine's response in these conditions. Wind and Wave data informs us about the sea conditions that can affect the structure and performance of the turbines. By integrating this data into analysis, I could provide a strong scientific basis for designing of my experiments.

3.2.1.1 Python Code

This customized Python code will give the hourly metrological data for each year mentioned in the code. This code can be used to extract data from last fifty years. I ran the code from 2015 – 2022 but in NORA – 3, data till 2021 is available only. For this project i extracted data from 2015 – 2021. This script ensured efficient handling of the large datasets, allowing for quick iterations and updates when required. The code is attached as appendix.

3.2.1.2 Data Estimation

After successful completion of the Python code, separate CSV files containing hourly metrological data were generated for each year (2015 – 2021). The CSV file example is attached as a figure 26,

	A	B	C	D	E	F	G	H	I
1	Date	Time	Total significant wave height (m)	Total mean period (s)	Total peak period (s)	Total mean wave direction (deg)	Wind speed (m/s)	Water depth (m)	
2	1/1/2015	0:00:00	2.44	7.05	7.63	58.03	10.82	259.93	
3	1/1/2015	1:00:00	2.47	7.05	7.63	56.93	10.88	259.93	
4	1/1/2015	2:00:00	2.49	7.06	7.63	55.76	10.86	259.93	
5	1/1/2015	3:00:00	2.57	6.99	7.63	54.11	12.06	259.93	
6	1/1/2015	4:00:00	2.68	6.97	7.63	52.41	11.76	259.93	
7	1/1/2015	5:00:00	2.69	7.04	7.63	52.46	11.05	259.93	
8	1/1/2015	6:00:00	2.71	7.07	7.63	53.24	11.76	259.93	
9	1/1/2015	7:00:00	2.73	7.09	8.39	54.23	10.98	259.93	
10	1/1/2015	8:00:00	2.74	7.13	8.39	54.7	10.47	259.93	
11	1/1/2015	9:00:00	2.76	7.18	8.39	54.15	10.89	259.93	
12	1/1/2015	10:00:00	2.75	7.27	8.39	53.3	9.67	259.93	
13	1/1/2015	11:00:00	2.72	7.3	8.39	52.25	10.17	259.93	
14	1/1/2015	12:00:00	2.71	7.28	8.39	51.34	10.55	259.93	
15	1/1/2015	13:00:00	2.71	7.27	8.39	51.04	9.83	259.93	
16	1/1/2015	14:00:00	2.72	7.3	8.39	50.98	9.64	259.93	
17	1/1/2015	15:00:00	2.74	7.33	8.39	49.74	10.33	259.93	
18	1/1/2015	16:00:00	2.8	7.29	8.39	46.58	11.79	259.93	
19	1/1/2015	17:00:00	3.02	7.17	8.39	42.27	14.4	259.93	
20	1/1/2015	18:00:00	3.36	7.2	8.39	39.92	14.99	259.93	
21	1/1/2015	19:00:00	3.65	7.38	8.39	40.37	15.12	259.93	
22	1/1/2015	20:00:00	3.89	7.57	8.39	41.8	15.71	259.93	
23	1/1/2015	21:00:00	4.04	7.83	9.23	42.43	14.68	259.93	
24	1/1/2015	22:00:00	4.11	8	9.23	42.16	15.12	259.93	

Figure 25. CSV file containing metrological data for 2015 at Utsira Nord

The CSV files for all the years were used to estimate the mean, maximum and minimum values using statistical methods. Mean values were calculated to determine typical operating conditions, while extreme values were calculated to understand the maximum loads and conditions the turbine structure might encounter. This assessment is crucial for designing a FOWT structure that can withstand rare but potentially catastrophic conditions.

	A	B	C	D	E	F	G	H	I	J	K	L	M	N	O
1															
2	Location	Utsira Nord	Latitude	59.2	Water Depth = 259.93										
3			Longitude	4.5											
4	Mean	Wave height	Wave period	Wind speed	mean wave direction	Maximum	Wave height	Wave period	Wind speed	Minimum	Wave height	Wave period	Wind speed		
5	2015	2.290216895	7.372650685	8.832868721	130.6424852	2015	14.74	19.78	29	2015	0.32	3.61	2		
6	2016	1.988616438	7.11410274	8.08836758	132.2456073	2016	13.74	17.99	25.8	2016	0.25	3.4	2		
7	2017	2.159592466	7.095214612	8.521638128	138.3837432	2017	11.57	17.99	25.42	2017	0.27	3.23	2		
8	2018	1.957267123	7.07231621	8.295689498	148.5025183	2018	8.63	17.99	26.59	2018	0.25	3.45	2		
9	2019	1.953829909	6.995212329	8.094457763	149.2840468	2019	11.21	21.76	23.32	2019	0.25	3.49	2		
10	2020	2.243360731	7.421751142	8.666753425	128.4388436	2020	9.25	17.99	24.72	2020	0.21	3.82	2		
11	2021	1.960591324	7.207518265	8.088876712	147.0331461	2021	8.37	19.78	23.67	2021	0.27	3.48	2		
12	Total mean	2.079067841	7.182680855	8.369807404	139.2186272	Total Max	14.74	21.76	29	Total min	0.21	3.23	2		
13															
14															
15	Parameter	Units			Wave Frequency	Mean	Minimum	Maximum							
16	Wave height	meters (m)				0.1392238	0.045955882	0.309597523							
17	Wave Period	seconds (s)													
18	Wind Speed	meters per second (m/s)													
19	Wave Frequency	Hertz (Hz)													
20	Wave direction	Degrees													
21															

Figure 26. Mean, Maximum and Minimum operating conditions from 2015-2021 at Utsira Nord

	Wave height	Wave period	Wind speed
Mean	2.08	7.18	8.37
Maximum	14.74	21.76	29
Minimum	0.21	3.23	2

Table 7. Estimated operating conditions for analysis.

3.2.2 Numerical Software Selection

For this project I chose ANSYS AQWA as the primary numerical simulation software due to full scale research license availability at UiT, robust capabilities and industry-wide recognition. ANSYS AQWA can be coupled with other Ansys suites such as static structural for structural analysis and Ansys Fluent for CFD study to use in comprehensive analysis. AQWA is particularly effective for modeling the dynamic interactions between waves, wind, and floating structures, which is essential for my research. It provides accurate hydrodynamic modeling and dynamic mooring analysis, essential for evaluating floating wind turbines under various sea conditions. Its extensive user support and detailed documentation simplify troubleshooting and optimize the simulation process. The choice of ANSYS AQWA was supported by its successful use in similar studies and preliminary tests that confirmed its suitability for my project's specific needs. It was also easy for me to adapt this software as I had previously worked with other Ansys packages during my Master studies at UiT. The software's ability to run multiple scenarios efficiently and its powerful visualization tools make it an invaluable resource for conducting detailed design iterations and presenting complex simulation results clearly.

3.2.3 Design Configuration for Spar Buoy Platform

ANSYS AQWA has been used in this thesis to study the hydrodynamic response of three simple and different geometric shapes for spar buoys: *circular, square, and triangular*. This will form the basis for selection of any design configuration for spar buoy platform and deliver a reason that why I chose certain geometric design shape for spar buoy. To evaluate a comparative analysis between these three different geometric shapes, all the input parameters are kept same. These include mooring lines, materials, wind and wave operating conditions, water depth, mooring fairleads and anchor points and water level (submergence height). Through this comparative analysis using same variables best geometric design configuration is chosen for full scale study of FOWT.

3.2.4 Thesis Analysis Flow Chart

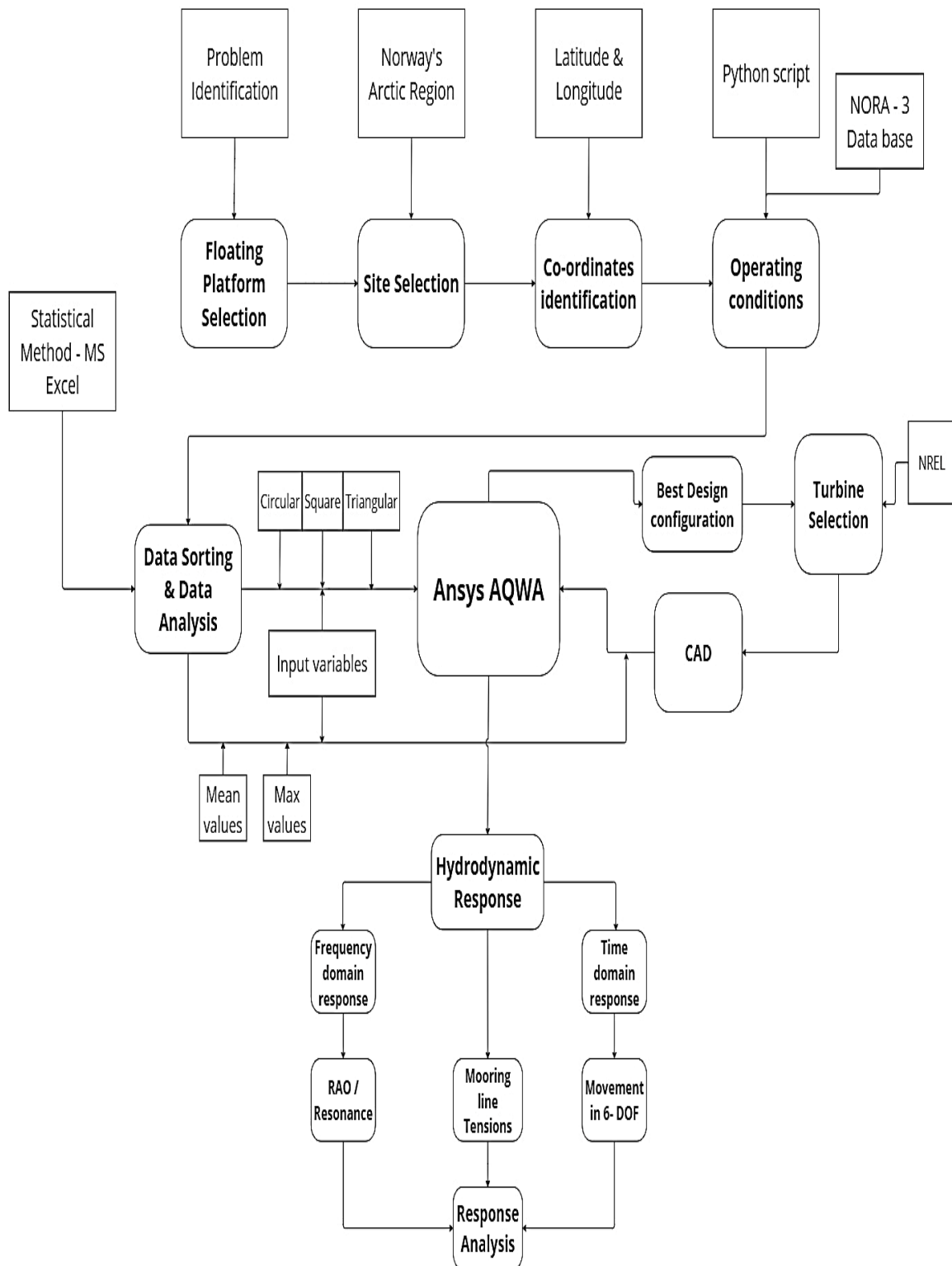


Figure 27. Analysis workflow chart.

CHAPTER 4

4 Numerical Setup

The choice of analysis method in numerical setup is crucial since it has an impact on the accuracy of the results. The structural response in operating conditions is an essential part of this study, and the techniques applied in these situations is:

4.1 Hydrodynamic Analysis

Hydrodynamic analysis is a method used to study the interactions between water and structures that are either submerged in or floating on the water. This type of analysis is crucial for designing structures like ships, offshore platforms, and other marine installations, ensuring they can withstand the forces of waves, currents, and wind.

ANSYS AQWA is a specialized software tool used for this purpose. It helps simulate and predict how water will interact with marine structures. Using ANSYS AQWA, we can create a virtual model of a structure and then expose it to various marine operating conditions. The software calculates how the water's and wind's movement affects the structure, helping to test the structure's stability, durability, and performance under different sea conditions. Simulation methodology in Ansys Aqwa

4.1.1 Simulation Methodology

Conducting a hydrodynamic analysis using ANSYS AQWA involves several steps to ensure accurate and reliable predictions about how marine structures interact with water. Here's a simplified explanation of the process:

4.1.1.1 *Idealization*

This first step is about simplifying the real-world structure into a model that can be analyzed. This means reducing complex elements into basic parts that still accurately represent the structure's behavior in water.

4.1.1.2 *Gathering Data*

Before simulation, it's important to collect accurate data about the marine environment where the structure will operate. This includes information about wave heights, wind speeds, wave direction to ensure simulations reflect real-life conditions.

4.1.1.3 *Calculations for Model Input Variables*

This involves determining key characteristics of the model like mass, volume, and center of gravity (COG) and center of buoyancy (COB). These calculations also include figuring out the right distribution of weight and buoyancy across the structure.

4.1.1.4 *Mooring System Design*

If the structure needs to be anchored or fixed in place, a mooring system is designed. This system must be able to securely hold the structure against marine forces.

4.1.1.5 CAD Modeling

A Computer-Aided Design (CAD) software is used to create a detailed 3D model of the structure. This model is then integrated with ANSYS AQWA for further analysis.

4.1.1.6 Applying Mass and Mooring Properties

In ANSYS AQWA, you input the mass properties you calculated earlier, along with the specifics of the mooring system and any boundary conditions that affect how the model interacts with water.

4.1.1.7 Mesh

This step involves creating a mesh network over the model. The mesh is a collection of interconnected points that cover the model's surface, which helps in accurately calculating wave – wind forces on each part of the structure.

4.1.1.8 Analysis Settings

Setting up the analysis involves choosing the methods and criteria for the simulation. This includes setting damping factors, frequency ranges, and other parameters that influence how the analysis is conducted.

4.1.1.9 Applying Operating Conditions

Here, you apply the gathered data on marine conditions to simulate different scenarios. This helps in obtaining Response Amplitude Operators (RAOs), which describe how the structure reacts to waves and other forces and it also helps to identify the natural frequencies or periods to avoid resonance in the structural movement.

4.1.1.10 Transferring Hydrodynamic Diffraction Solution to Response

The results from the wave interaction study (hydrodynamic diffraction) are used to predict the overall hydrodynamic response of the structure.

4.1.1.11 Hydrodynamic Response Modeling

This phase models the structure's behavior under the influence of calculated forces, simulating its response in various marine conditions.

4.1.1.12 Solution in Terms of Time Domain Response

Finally, the model's movements are analyzed in six degrees of freedom over time to understand how it behaves in realistic conditions.

4.2 Units

The numerical analysis has been performed using SI units, the governing parameters to be studied in the hydrodynamic analysis are movements in translational degrees of freedom (m) & rotational degrees of freedom (degrees), RAO (m/m) or ($m/degrees$), wave frequencies (Hz), wave periods (s), mass (kg), Force (N) and volume (m^3).

CHAPTER 5

5 Selection of Design Configuration

To investigate the hydrodynamic response of three basic and distinct geometric configurations—square, triangle, and circular—for spar buoys. This will serve as the foundation for choosing the right design configuration for the spar buoy platform and provide an explanation for my decision to use a certain geometric design shape for the spar buoy. All of the input parameters are left unchanged in order to assess a comparison analysis between these three distinct geometric shapes.

5.1 Operating Conditions

As I have mentioned above that, Utsira Nord has been selected to study the response of FOWT in various operating conditions at that particular site and five years data has been received using python code and NORA – 3 database. The operating conditions that I will use during my numerical simulations to evaluate the response are wave height, wave period / frequency, mean wave direction and wind speed.

During the statistical analysis mean, maximum and minimum values has been achieved during last seven years (2015 – 2021). For this comparative study for selection of the best design configuration, I will use the mean values of the operating conditions at the selected site and will select the design configuration which will perform best during the wind – wave interaction with structure on mean values.

For wave frequencies a range of lowest to highest wave frequency was received during the statistical analysis on operating conditions at Utsira Nord. A mean wave frequency was also estimated during the statistical analysis in past seven years (2015 – 2021).

Mean wave frequency (Hz)	Lowest wave frequency (Hz)	Highest wave frequency (Hz)
0.139223783	0.045955882	0.309597523

Table 8. Range of Wave frequency at Utsira Nord during 2015 – 2021

Lowest wave frequency depicts the longest wave period and highest wave frequency depicts the shortest wave period. Wave period describes that in how much time (s) a wave completes its full cycle.

Mean operating values are mentioned below,

Significant wave height (m)	Mean wave direction (degrees)	Mean wind speed (m/s)
2.079067841	139.2186272	8.369807404

Table 9. Mean operating conditions at Utsira Nord during 2015 – 2021.

5.2 CAD Modelling

Design parameters for each spar buoy design configuration parameters were kept almost the same for all three design configurations to form a basis of comparative analysis. CAD models were designed using Ansys design modeler which is a built in CAD design software inside Ansys package. Ansys Aqwa only supports the surface bodies for hydrodynamic analysis. So, the CAD model was designed using no

solid bodies and point masses were described inside the numerical modelling in Ansys Aqwa using global coordinate system.

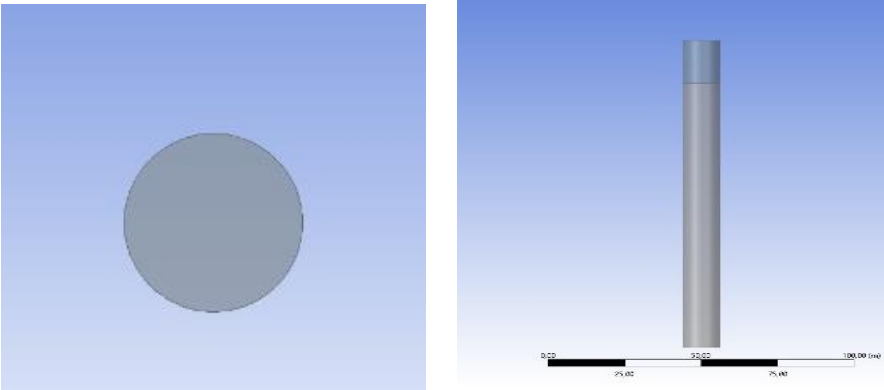


Figure 28. Circular CAD design

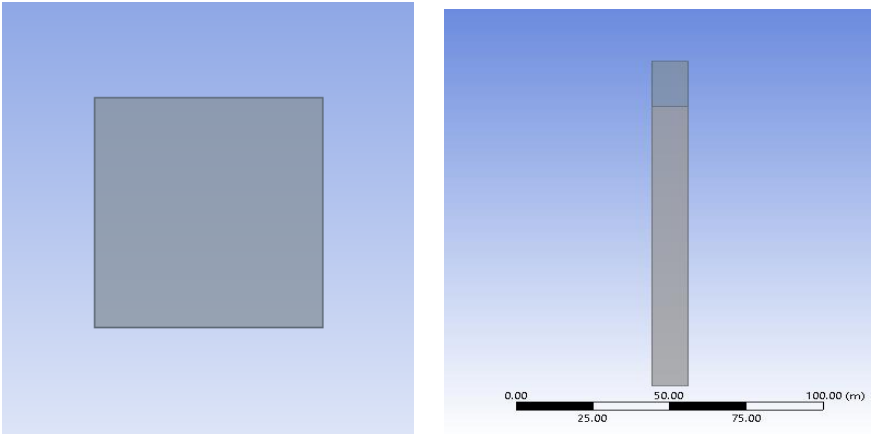


Figure 29. Square CAD design

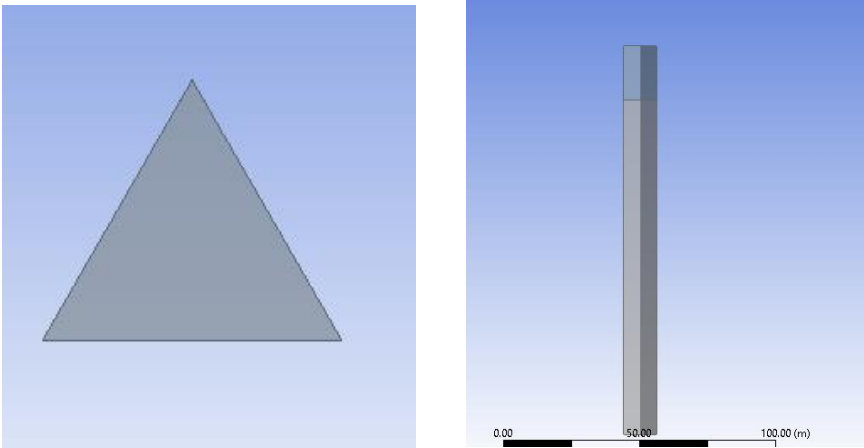


Figure 30. Triangular CAD design

5.3 Numerical Modelling

5.3.1 Platform Properties

Platform properties for all the design configurations were kept same and mentioned in a table below,

Global property	Value
Mass	13522254.577 kg
Center of gravity in z -direction	-93.6081218675284 m
Center of buoyancy in z -direction	-61 m
Moment of Inertia Ixx	20342450540.3786 kg.m ²
Moment of Inertia Iyy	20342450540.3786 kg.m ²
Moment of Inertia Izz	246334501.3968 kg.m ²
Water depth	259.93 m
Water density	1025 kg/m ³
Gravity	9.80665 m/s ²
Material Density	7850 kg/m ³

Table 10. Geometric properties

5.3.2 Mooring System

Mooring systems provide resistance to environmental loading by deforming and activating reaction forces. Due to the design water depth (259.93 m), the most suitable mooring system is the half taut mooring system. Three mooring lines with a material combination of chains and polyester mooring line has been designed to resist the movement of the structure and make it stable. Same mooring system will be used in the full-scale study of 5 MW NREL FOWT, that is why this section, and mooring properties and length will be extensively described in the next chapter. For selection of right design configuration, a mooring system must be coupled in the Ansys Aqwa for hydrodynamic analysis. Brief overview of the mooring system can be seen from the figures below, these figures were taken during the hydrodynamic analysis for selection of best design configuration.

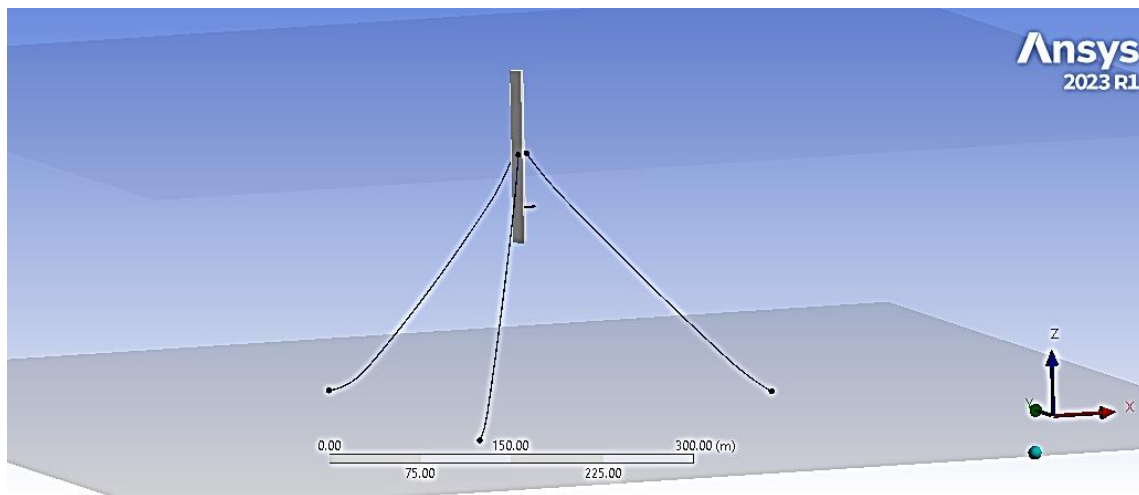


Figure 31. Mooring system

From the figures the location of the fairleads (connection points on the structure) and anchor points (connection points on the sea floor) can be seen. The exact locations of fairleads and anchor points will be mentioned in the next chapter of full-scale study of 5 MW NREL FOWT.

5.3.3 Mesh

In the simulation setup for the Spar buoy designs, I used a mesh size of 0.5 meters along with a connection tolerance of 0.05 meters to ensure accurate connections between mesh elements. The program automatically generated a waterline for each model, which is crucial for analyzing the buoy's interaction with the water's surface. For the different shapes of the buoys, the number of mesh elements varied: the circular design had 22,786 elements, the square design had 28,608 elements, and the triangular design had 21,137 elements. This difference in element quantity reflects how each shape interacts differently with the meshing process.

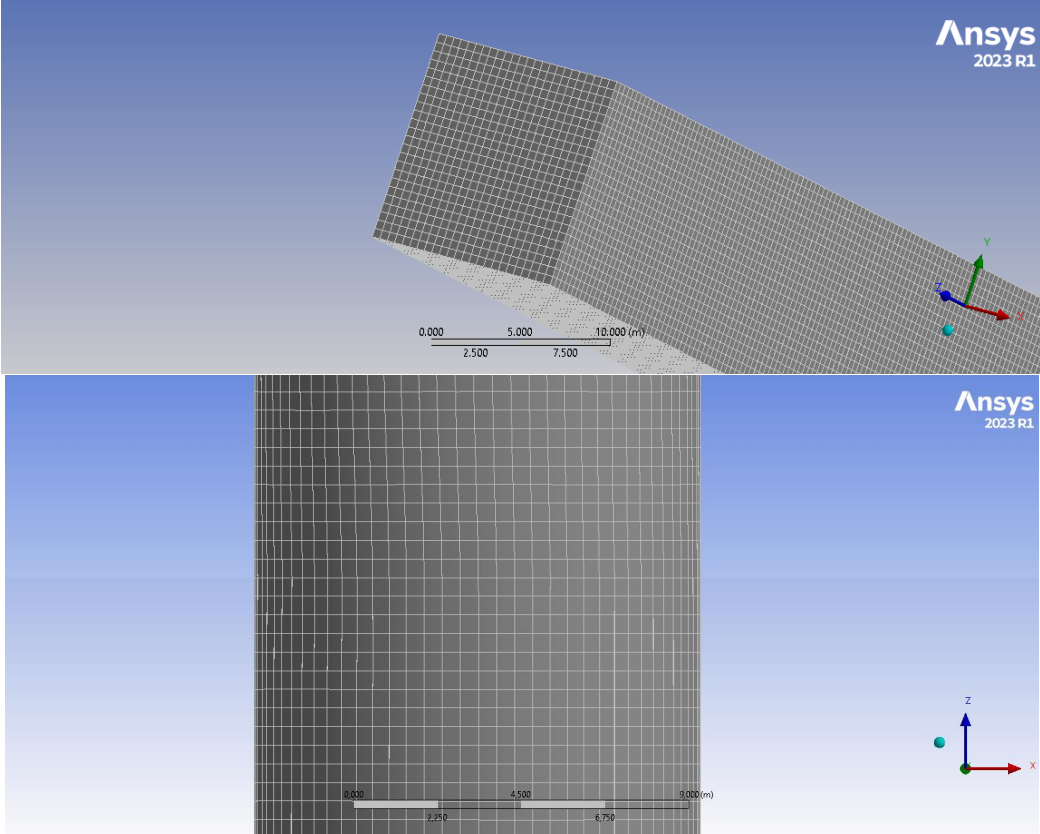


Figure 32. Mesh

5.3.4 Hydrodynamic Response

For response analysis on all three design configurations, a regular wave using stokes 2nd wave theory was used with a wave amplitude of 2.08m, wave period of 7.18 s, wave direction of 139.22-degree, wind speed of 8.36m/s and wind direction is same as wave direction. These environmental conditions are the mean operating conditions that were generated using NORA – 3 databases for meteorological conditions. Simulations run for 500 seconds with a time step of 1 second. Time domain response for structural response was generated for each degree of freedom.

Blue arrowhead and green arrowhead are showing the wave and wind direction respectively in Ansys Aqwa,

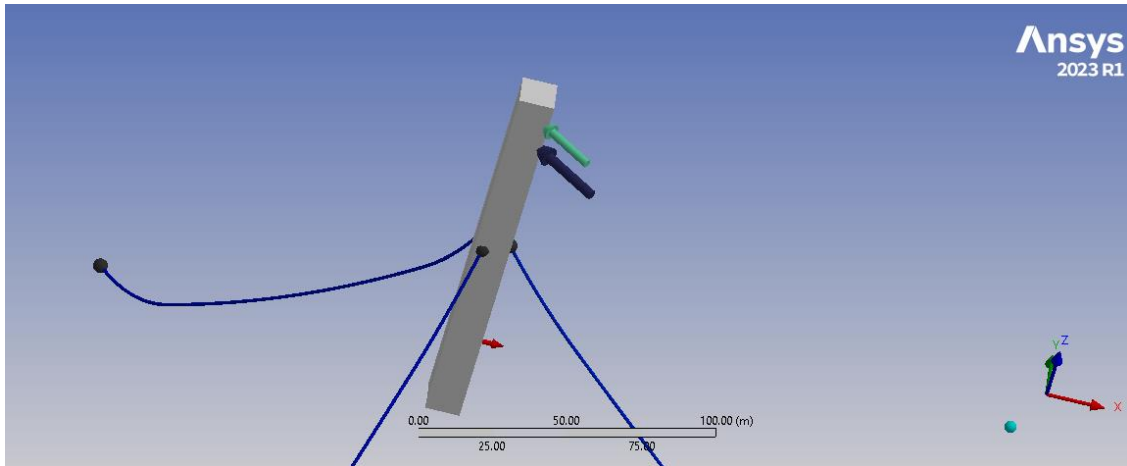


Figure 33. wind and wave direction in Ansys Aqwa

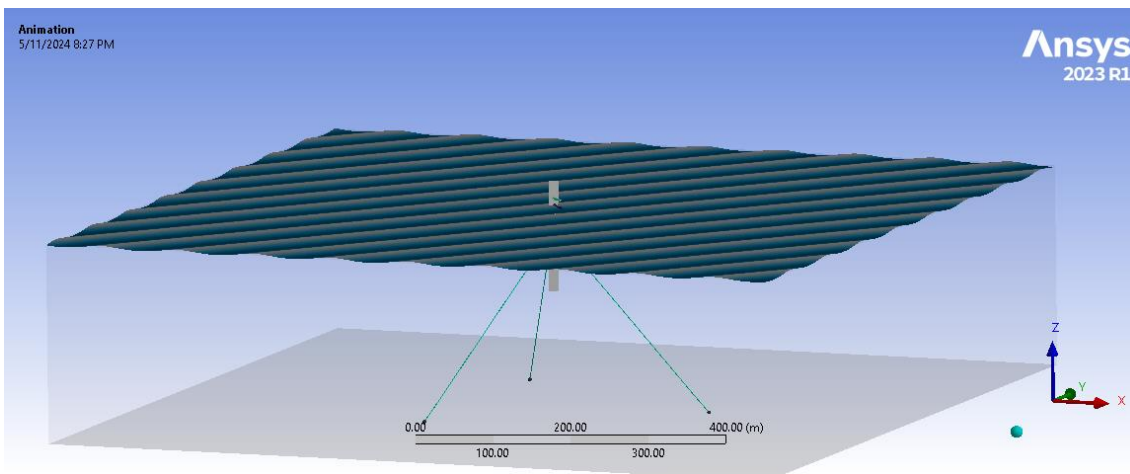


Figure 34. Wave modelling

5.3.5 Results & Analysis

5.3.5.1 Heave

Heave (up and down oscillations along z -axis) results were achieved relative to the center of gravity of the structure which is -93m for all the design configurations through time domain response for each configuration, In heave movement graphs of three different Spar buoy designs through time-domain graphs, distinct behaviors among the circular, square, and triangular configurations can be observed.

- The circular design displayed an impressive ability to stabilize quickly after an initial sharp heave that peaked at around -86.986 m. Following this peak, the oscillations reduced steadily and reached a stable equilibrium around -91 m, which is very close to its initial position of center of gravity, demonstrating effective damping characteristics. This rapid stabilization suggests that the circular design might be particularly suited for operations that require minimal movement, in heave direction.
- On the other hand, the square and triangular designs showed greater oscillations throughout the simulation period. The square design started with a peak similar to the circular but maintained larger and more sustained oscillations between -60 m and -90 m, indicating less damping and more continuous movement. The triangular design experienced the most dramatic initial movement, jumping to nearly -500 m. this depict the sinking / unstable behavior of triangular design configuration,

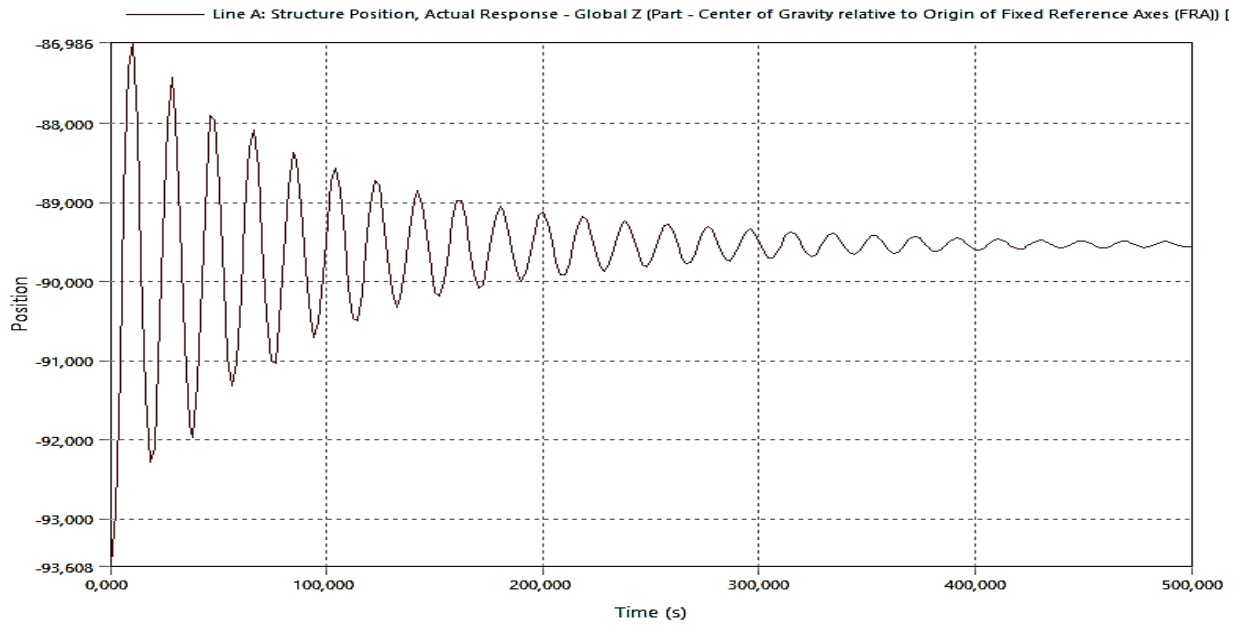


Figure 35. Heave motion in circular design configuration.

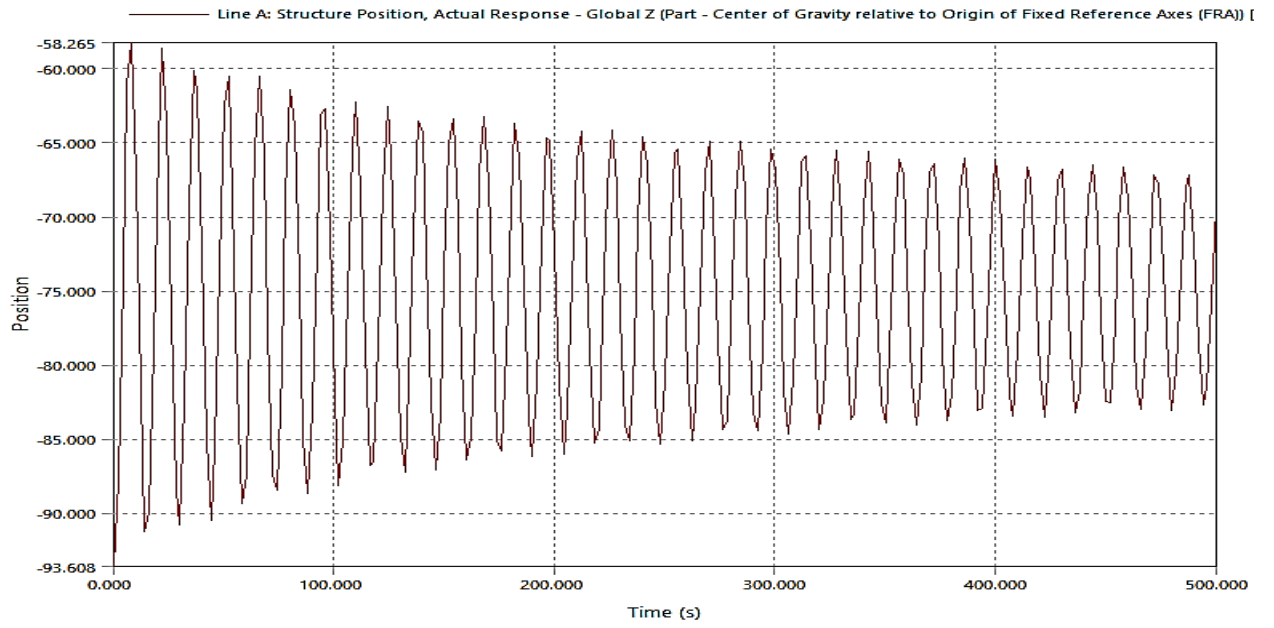


Figure 36. Heave motion in square design configuration.

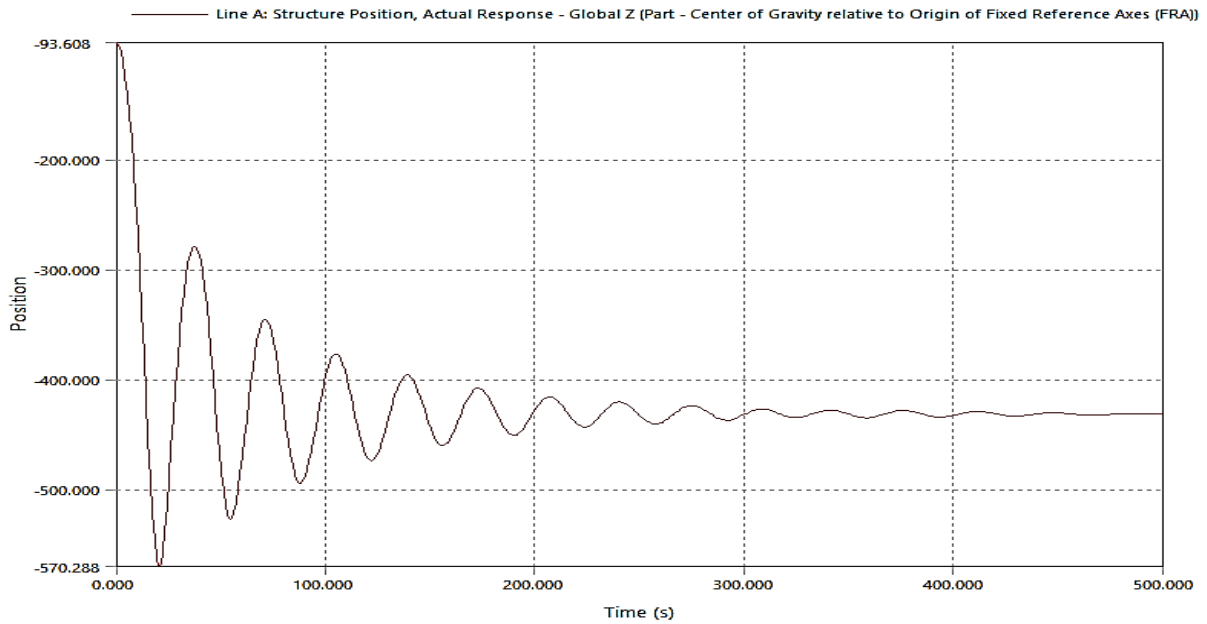


Figure 37. Heave motion in triangular design configuration.

5.3.5.2 Sway

Analyzing the sway movements (translational motion along Y – axis) from the time-domain graphs for three Spar buoy designs. The graphs provided show how the sway position changes over a period of 500 seconds, allowing us to compare the dynamic responses of each design configuration.

- The circular design exhibits a pronounced initial sway movement reaching a peak of about 0.2151m and then a substantial drop to approximately -0.1535m. Following this, the sway oscillations gradually decrease in amplitude and stabilize with minor fluctuations around initial position as the time progresses. This behavior indicates that the circular design manages to absorb and dampen the sway motion effectively, returning to a near-neutral position after the initial disturbances, which suggests a design well-suited to maintaining stability after sudden shifts.
- In contrast, the square design starts with smaller sway peaks compared to the circular design, with maximum excursions around 0.3955m and dipping to lows near -0.6456m. Notably, the oscillations decrease less significantly over time, maintaining a broader range of movement throughout the simulation period.
- The triangular design shows a different pattern, with an initial sway peak slightly above 0.504m, which is much smaller than those of the other designs. The graph displays a steady decrease in sway position, moving to a low point around -1.715m. This indicates a continuous drift rather than oscillatory sway, suggesting that once displaced, the triangular design gradually stabilizes but might take longer to return to its original position. This pattern could imply a design that, while stable under constant conditions, might struggle to quickly recover from large directional changes.

In summary, each buoy design exhibits distinct characteristics in handling sway motions: the circular design quickly dampens initial disturbances, the square maintains higher responsiveness throughout, and the triangular shows gradual stabilization.

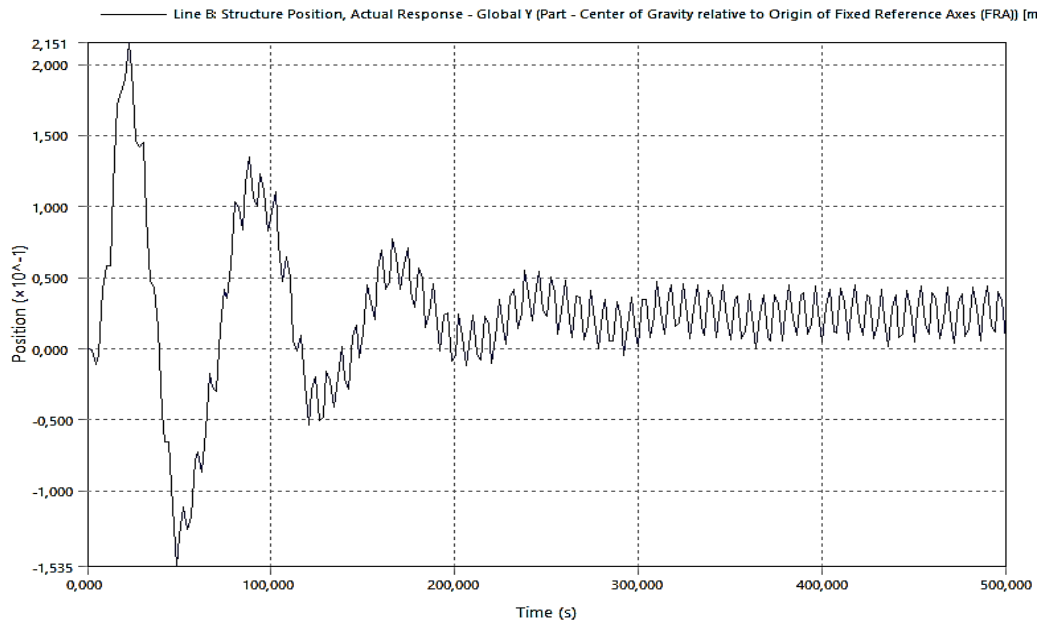


Figure 38. Sway motion in circular design configuration.

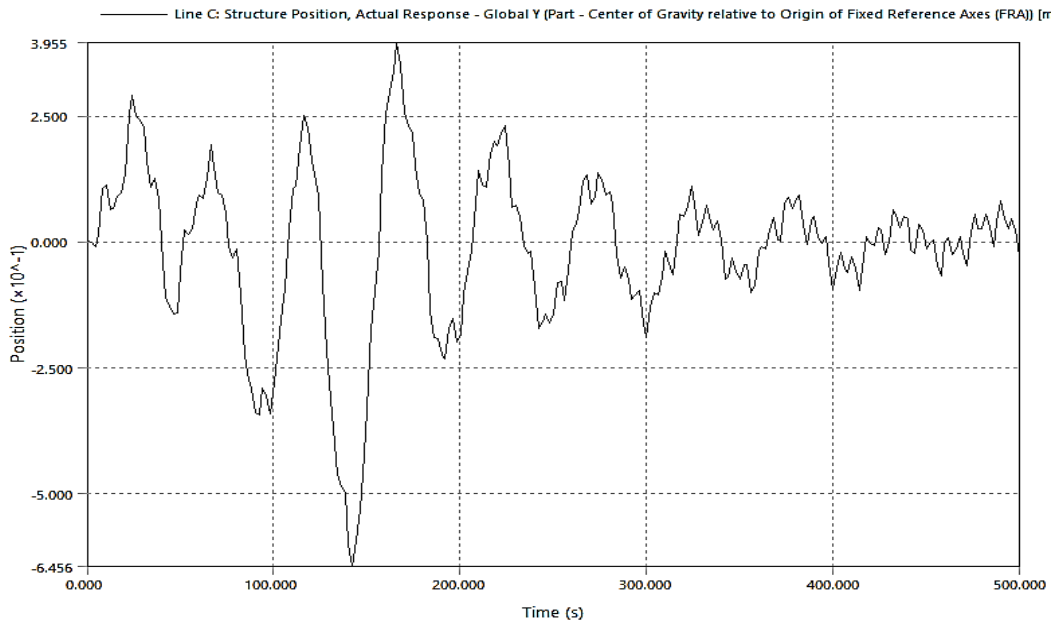


Figure 39. Sway motion in square design configuration.

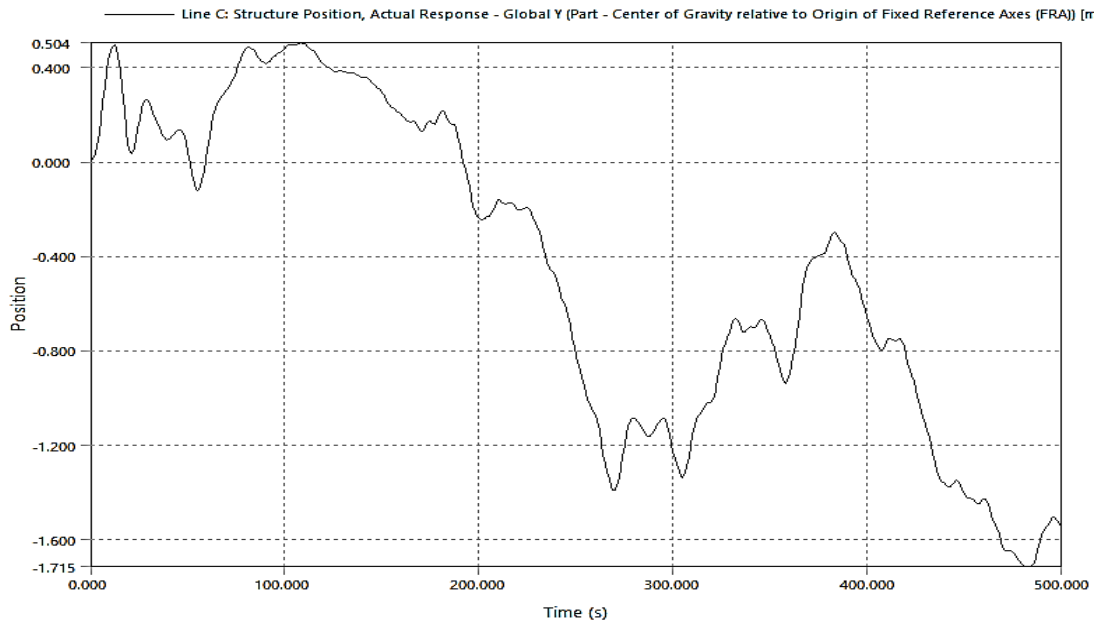


Figure 40. Sway motion in triangular design configuration.

5.3.5.3 Pitch

Through pitch movement graphs generated by Ansys Aqwa for each design configuration, we can observe each design's behavior through rotational movements along the Y-axis under simulated wave and wind conditions. These pitch graphs demonstrate the rotational stability and responsiveness of each design to the environmental forces acting upon them.

- For the circular design, the graph shows initial spike with a maximum peak of approximately 0.82 degrees and structure rotating the other way and reaching about -1.06 degrees. Following these initial fluctuations, the amplitude of the pitch oscillations gradually decreases, stabilizing around zero degrees as the time progresses which is the initial position of the structure. This behavior indicates effective damping where the design manages to stabilize back to neutral position relatively quickly after being disturbed, suggesting a resilient structure that can return to stability swiftly.
- The square design begins with extreme initial pitch movement, with the highest peak just above 1.05 degrees and the lowest dip around -1.75 degrees. Throughout the simulation, this design maintains moderate oscillations, which do not decrease significantly in amplitude. This constant range of motion indicates a less effective damping system compared to the circular design configuration. This suggests that the square design is the most sensitive to external forces, experiencing substantial rotational movement in pitch DOF.

- The triangular design exhibits the pitch with peaks going up to about 0.592 degrees and troughs down to -0.590 degrees. The pitch behavior demonstrates rotational movement along the Y – axis that decrease only slightly in amplitude throughout the simulation.

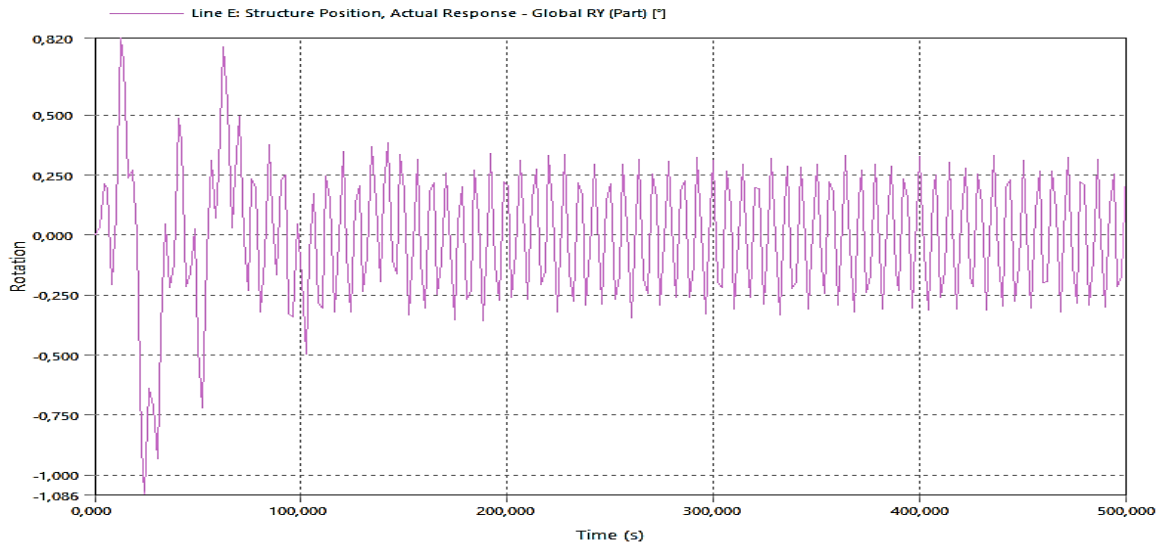


Figure 41. Pitch motion in circular design configuration.

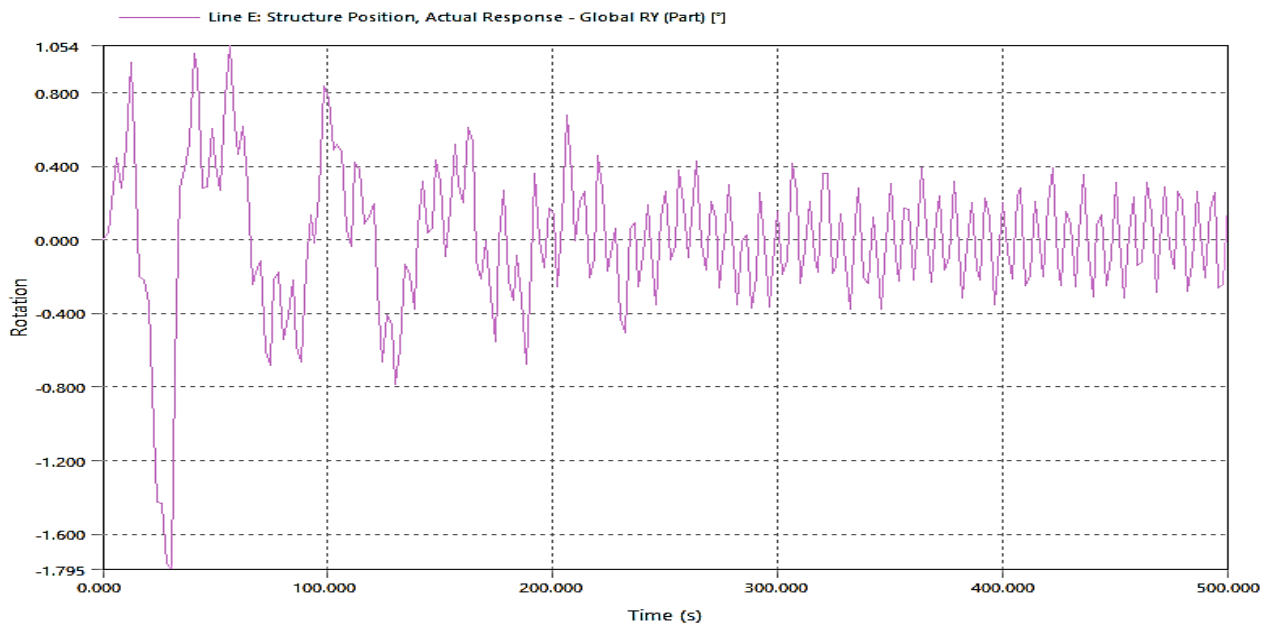


Figure 42. Pitch motion in square design configuration.

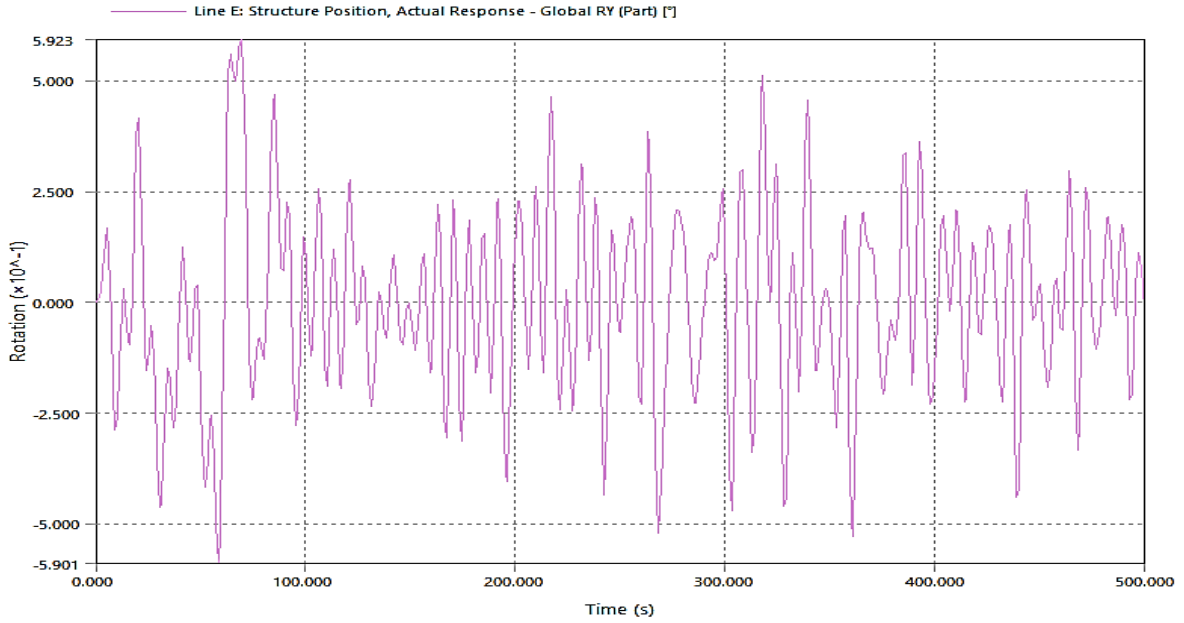


Figure 43. Pitch motion triangular design configuration.

5.3.6 Optimal Geometric Shape

After detailed analysis of heave, sway, and pitch movements for circular, square, and triangular Spar buoy designs, the circular design comes out as the best choice for designing the spar buoy platform for floating offshore wind turbines. It effectively stabilizes quickly after disturbances, which is crucial for maintaining operational integrity and efficiency on offshore platforms show more movement in each degree of freedom, which could affect the stability needed for offshore wind turbines. Therefore, the circular design, with its superior damping capabilities and stable performance, is the most suitable for supporting the operational demands of offshore wind energy systems.

5.4 Pressure and Motions

To find out the amplitude and location of highest and lowest structure motion and interpolated pressure, a simulation of circular spar buoy was run using values of mean operating conditions at Utsira Nord which are mentioned in Table.7, 8 and 9.

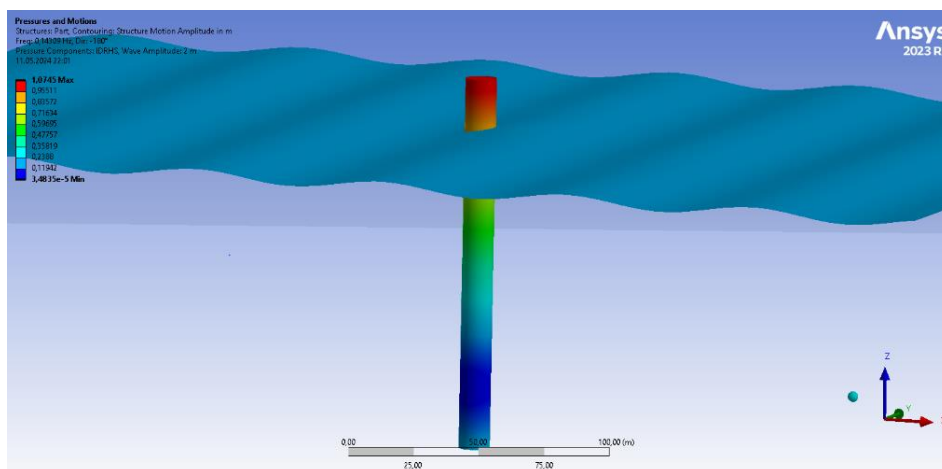


Figure 44. Structural motion during mean operating conditions.

It can be seen from the figure above that structure is stable enough and has a highest movement amplitude of 1.0745m. The location where the highest movement is taking place is the topmost part of the structure which is outside of the ocean and open to wind forces.

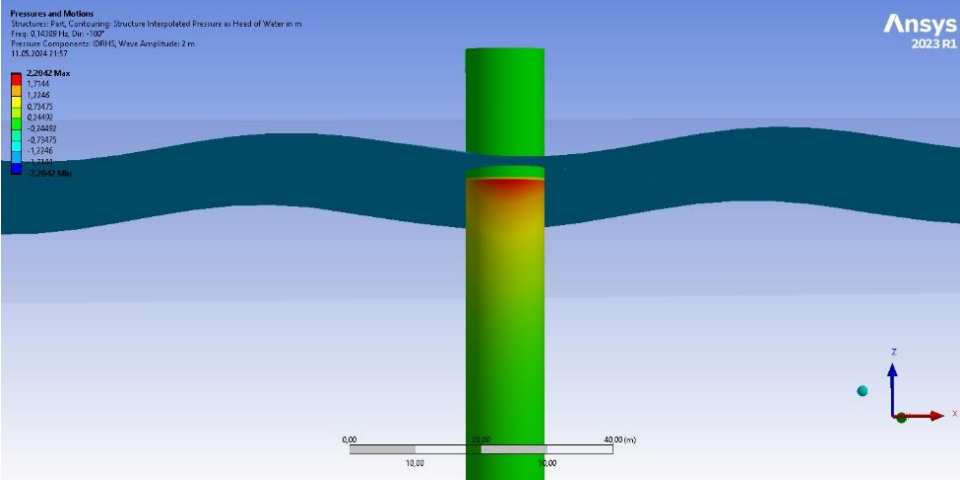


Figure 45. structure interpolated pressure during mean operating conditions.

From figure above the location and highest value of the structure interpolated pressure due to waves can be seen. Waves are exerting maximum pressure on the water line of the structure where wave – structure interaction is taking place.

CHAPTER 6

6 Full Scale Study of Optimal Spar Buoy Design

In this chapter, I will delve into a detailed study of a full-scale Spar buoy platform coupled with a 5 MW NREL wind turbine. Having selected the circular design configuration based on its superior stability and damping capabilities, this chapter focuses on the application of this design in real-world conditions. The study is grounded in extensive numerical simulations conducted with the data from past seven years (2015 to 2021), specifically at Utsira Nord. This location was chosen to gather realistic data on the operational conditions in the Arctic region.

The simulations have been carried out under both mean operating conditions, which represent normal environmental scenarios, and extreme conditions, which account for peak environmental values that the structure might face. This approach allows for a comprehensive understanding of how the chosen circular Spar buoy design performs under a range of conditions that are typical and extreme of the challenging Arctic environment. The insights from this study are crucial for confirming the suitability of the circular design for supporting offshore wind turbines, particularly in regions prone to extreme weather conditions. This chapter aims to provide a detailed analysis of the Spar buoy platform's behavior when exposed to the dynamic and potentially harsh conditions of the Arctic Sea.

6.1 Selection of Wind Turbine

The selection of the NREL 5 MW wind turbine for this analysis was made after several discussions with my thesis supervisor, emphasizing its suitability for offshore wind production. The NREL 5 MW wind turbine is specifically designed by the National Renewable Energy Laboratory (NREL) for offshore environments, making it an ideal choice for this study. This turbine is widely recognized for its efficiency and reliability in generating large amounts of power, which aligns perfectly with the goal of maximizing energy production from offshore wind farms.

6.1.1 Turbine Properties

For the numerical simulations in this study, I gathered specific turbine properties from the NREL technical report of *Definition of a 5-MW Reference Wind Turbine for Offshore System Development* by J. Jonkman, S. Butterfield, W. Musial, and G. Scott. This comprehensive report provides extensive information on various aspects of the turbine, including its structure, aerodynamics, and blade properties. From this detailed technical report, I selectively gathered only the data essential for my simulations. [55]

Rating	5 MW
Rotor orientation, configuration	Upwind, 3 blades
Rotor diameter	126 m
Hub diameter	3 m
Hub height	90 m
Rotor mass	110000 kg
Nacelle mass	240000 kg
Hub mass	56780 kg
Total mass of Nacelle, Rotor and Hub	406780 kg

Global Center of Gravity of Nacelle, Rotor and Hub	90 m
Second Moment of Inertia Ixx, Iyy	1700000000 kgm ²
Second Moment of Inertia Izz	4500000 kgm ²

Table 11. Nacelle, Hub and Rotor properties combined.

Dia bottom	7.5 m
Dia top	3.87 m
Height	87.6 m
Tower mass	347460 kg
Center of Gravity	38.234 m
Second moment of inertia Ixx, Iyy	223415259.8625 kgm ²
Second moment of inertia Izz	2443078.125 kgm ²

Table 12. Tower properties

6.2 Spar Buoy Hull Calculations

A realistic approach after extensive literature review was used for calculation of Spar hull draft and freeboard. Draft is called as the part of spar buoy which is submerged inside the water or in simple words it is the part which is under the water line in ocean. Freeboard is the part of spar hull which is outside of water and is used to mount the wind turbine over it. Several mathematical formulas were used to determine the design parameters of the Spar buoy platform. A single excel file containing three different sheets for formulations related to Spar hull design, Ballast calculations, Mass – buoyancy calculations and mooring system was created and will be presented in the appendix section of this thesis. However, some important formulas used in the excel file will be mentioned along with each section containing design properties in this chapter.

Diameter outer	12 m
Wall thickness	0.036 m
Diameter inner	11.964 m
Area outer	113.0973355 m ²
Area inner	112.4197694 m ²
Total length of spar hull	130 m
Draft	123 m
Freeboard	7 m
Freeboard Diameter bottom	12 m
Freeboard Diameter upper	7.5 m
Water displaced Volume	13910.97227 m ³
Mass of water displaced	14258746.58 kg
Center of buoyancy in Z – axis	-61.5 m
Seawater density	1025 kg/m ³
Material density (steel)	7850 kg/m ³
Spar hull mass	5496727 kg
Spar hull center of gravity in Z – axis	-58 m
Second moment of Inertia Ixx, Iyy	7790398023.31022 kgm ²
Second moment of Inertia Izz	98348329.95 kgm ²

Table 13. Spar Buoy hull design properties

6.2.1 Important Formulas

All the formulas mentioned below are based on the nomenclature and properties mentioned above in the Table 11, 12 and 13.

$$Area_{outer} = \frac{\pi}{4} \times D_o^2$$

$$Area_{inner} = \frac{\pi}{4} \times D_i^2$$

According to Archimedes, whenever a body is submerged partially or fully inside the water it displaces some volume of the water which is equal to the volume of the part of the body submerged inside the water.

$$Volume\ of\ displaced\ water = Area_{outer} \times Length\ of\ the\ draft$$

To calculate the mass of displaced water,

$$Mass\ of\ Water_{displaced} = Volume\ of\ displaced\ water \times Density_{seawater}$$

To calculate the mass of spar hull,

$$Mass_{spar\ hull} = Density_{steel} \times Volume_{spar\ hull}$$

$$Volume_{spar\ hull} = \pi \times \left((Radius_{outer}^2) - (Radius_{inner}^2) \right) \times Height_{spar\ hull}$$

For calculation of mass moment of Inertia of a circular cylinder,

$$I_{xx\ or\ I_{yy}} = \frac{1}{12} \times mass \times (3 \times radius_{inner}^2 + height^2)$$

$$I_{zz} = \frac{1}{2} \times mass \times radius_{inner}^2$$

6.3 Ballast Calculations

Ballast for FOWTs is essentially a weight used to stabilize the turbines. These turbines are placed in deep waters, where traditional foundations can't be used. The ballast helps to keep the structure upright and secure while the turbines interact with external environmental forces. This weight is typically made from materials like steel or concrete, and it is located at the base of the floating structure to lower its center of gravity and enhance stability. The ballast can be fixed, variable or either combination of both fixed and variable depending on the application. Variable ballast comes usually in terms of water that can be adjusted easily but for this study, after having discussions with my supervisor, only fixed ballast application has been used. It has several benefits as fixed ballast usually comes in the form of very denser materials and very less volume inside the spar hull is required to put it in. The lesser the volume fixed ballast will take in the base of spar hull, the lower the center of gravity it will have which will ultimately help us to make the turbine stable and have greater metacentric height.

Metacentric height is the difference between Global center of gravity and Global center of buoyancy. Ideally for spar hull stability point of view center of gravity should be lower in depth than center of buoyancy and a metacentric height greater than 5 is always recommended.

To keep the spar hull afloat at a desired height of draft (123 m), whole FOWT including tower, nacelle, rotor, hub, fixed ballast and spar hull should have enough mass to counterbalance the mass of displaced water. Enough buoyancy will only be achieved when mass of whole wind turbine becomes equal to mass

of displaced water. So, in order to estimate the mass of fixed ballast, let's have a look at the mass of displaced water which has been calculated already.

$$Mass_{Displaced\ water} = 14258746.58\text{ kg}$$

$$Mass_{FOWT\ without\ ballast} = Mass_{Spar\ hull} + Mass_{Tower} + Mass_{Nacelle} + Mass_{Hub} + Mass_{Rotor}$$

$$Mass_{FOWT\ without\ ballast} = 6250967\text{ kg}$$

To calculate the mass of fixed ballast,

$$Mass_{Fixed\ ballast} = Mass_{Displaced\ water} - Mass_{FOWT\ without\ ballast}$$

$$Mass_{Fixed\ ballast} = 8007779.577\text{ kg}$$

6.3.1 Material

To calculate the volume required inside the spar hull at the base location, material of fixed ballast needs to be defined. After having discussion with the supervisor **MegnaDense** mineral from a known Ballast material supplier, **LKAB** was chosen as the fixed ballast material due to its higher density and availability in the region. MagnaDense is manufactured from the natural mineral **Magnetite** [56], The **LKAB** mines are located in Kiruna and Malmberget in the northern part of Sweden which is very close to our chosen site location for the deployment of this FOWT. **LKAB** is quite famous for providing this material for the supporting application of fixed ballast to floating offshore structures already.

$$Density_{Magnetite} = 5000\text{ kg/m}^3$$

$$Volume_{fixed\ ballast} = \frac{Mass_{fixed\ ballast}}{Density_{fixed\ ballast}}$$

$$Volume_{fixed\ ballast} = 1601.56\text{ m}^3$$

$$Height_{fixed\ ballast} = \frac{Volume_{fixed\ ballast}}{\pi \times radius_{spar\ hull\ (inner)}^2}$$

$$Height_{fixed\ ballast} = 9.44\text{ m}$$

Mass	8007779.577 kg
Height	9.44 m
Center of gravity in Z – axis	-118.28 m
Second moment of Inertia Ixx, Iyy	131105083.6 kgm ²
Second moment of Inertia Izz	143276489.4 kgm ²

Table 14. Fixed ballast properties

Total mass of FOWT	14258746.58 kg
Total mass of displaced water	14258746.58 kg
Global Center of Gravity	-85.28627269 m
Global Center of buoyancy	-61.5 m
Metacentric height	23.78627269 m

Table 15. Properties for stability

Hence, total mass of displaced water is balanced by the total mass of whole FOWT including spar hull, fixed ballast, tower, nacelle, rotor and hub and metacentric height is greater than 5 as well. This justifies that our FOWT will be stable at a desired draft submerged height of 123 m.

6.4 CAD Modelling

CAD model was designed using Ansys design modeler which is a built in CAD design software inside Ansys package. Ansys Aqwa only supports the surface bodies for numerical simulations related to hydrodynamic analysis. Due to this restriction in Ansys Aqwa, CAD model of Spar Buoy platform and NREL 5 MW wind turbine’s Tower only was created. However, all the masses of each and every part of the whole FOWT were defined and assigned at their specific center of gravity locations in the numerical setup of FOWT. Design parameters mentioned in Table 11, 12 and 13 were used for creation of CAD model to import into numerical simulation for hydrodynamic analysis in Ansys Aqwa.

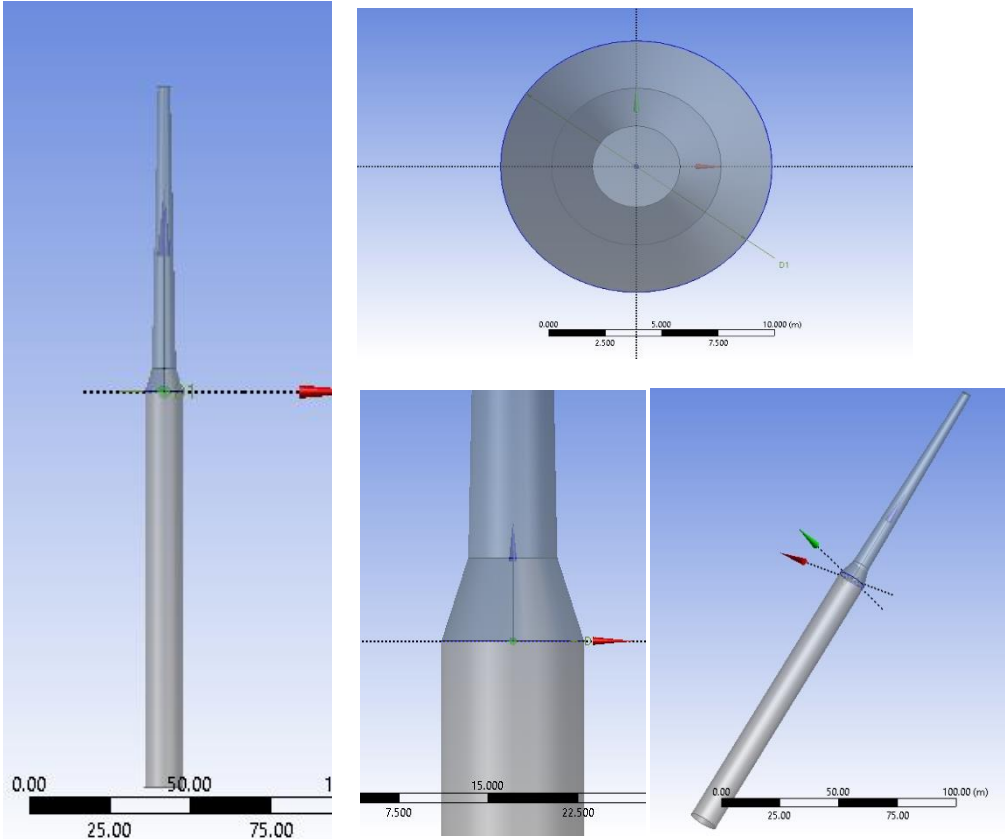


Figure 46. CAD model

6.5 Mooring System

It has been described in the earlier sections of this thesis that mooring system is necessary in order to keep the FOWT working at their best without being affected by the external operating conditions. Mooring lines help the FOWT to stand still at its mean position with having larger amplitudes of motions in any of the degree of freedom. In this study three half taut mooring lines with having 120-degree angle between each other, have been used in the numerical simulations due to several advantages such as reduced motion and improved stability. In taut leg mooring system, mooring lines are attached between the hull structure and sea floor at a 45-degree angle, and it remains always in very small amount of tension to restrict the structure’s movement even during the normal operating conditions. Due to this reason no part of mooring line rest on the sea floor. As this advantage restricts the movement of wind turbine but this makes it very important to calculate the right length and material of the mooring lines.

Taut leg mooring systems are more suitable than catenary systems in deeper waters due to their smaller area and shorter required mooring lines but in this type of mooring system anchors need to hold the vertical loads. So the choice of anchors and material of mooring lines become fairly important.

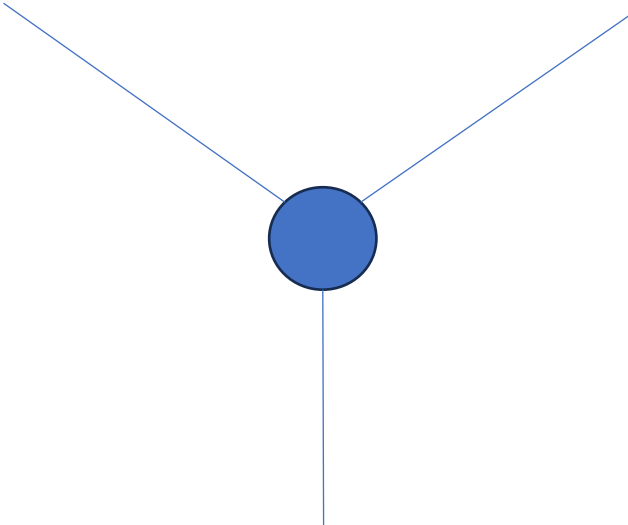


Figure 47. Mooring line

6.5.1 Materials

The mooring lines for this study were designed as a combination of chain – polyester configuration because of the advantages mentioned in the section of mooring system in the literature review. Polyester is considered as the best synthetic fiber line among all available options in the market due to its unique strength while being stretched and chains are widely used and accepted due to their better integration with the fairleads and anchor connection points. That is why in the top and bottom parts of my mooring lines, chains have been used for better connection integration with connection points. Chains and polyester mooring lines were selected from the product catalogue of a company called as **InterMoor**. It has been decided after having discussion with my thesis super visor that R3S Stud chain will be used for calculation of mooring line properties.

6.5.2 Mooring Line Properties

Mooring properties were calculated in the excel file available in the appendix section of this thesis. Some of the properties are mentioned in the table below,

No of mooring lines	3
Water depth	-259.93 m
fair lead depth (draft height where mooring lines are attached with the hull structure)	-49.2 m
Angle to vertical axis	45 degree
Mooring depth	-210.73 m
Length	298.017224 m
Radius	210.73 m

Table 16. Mooring system properties

Chain top	50 m
Chain bottom	50 m
Nominal Diameter	0.11938 m
Equivalent Diameter	0.23876 m
Equivalent Area	0.044772673 m ²
Dry mass	315 kg
Breaking load	13600000 N
Axial stiffness (EA)	1030000000 N

Table 17. Chain properties

Polyester length	198.017224 m
Nominal Diameter	0.21336 m
Equivalent Diameter	0.16002 m
Equivalent Area	0.02011122 m ²
Dry mass	44 kg
Breaking load	13200000 N
Axial stiffness (EA)	158000000 N

Table 18. Polyester properties

6.5.3 Mooring Lines Connection Points

Mooring lines are connected to structure connection points which are called as fairleads and fairleads are usually being made at 40 – 50 % of the draft length of spar hull. On the other mooring lines are being connected to the sea floor via anchor points. The location of all three fairleads and anchor points are mentioned in the tables below.

Location (degree)	x (m)	y (m)	z (m)
0	6	0	-49.2
120	-3	5.196152423	-49.2
240	-3	-5.196152423	-49.2

Table 19. Fairleads connection points location

Location (degree)	x (m)	y (m)	z (m)
0	216.73	0	-259.93
120	-105.365	182.4975333	-259.93
240	-105.365	-182.4975333	-259.93

Table 20. Anchor points location

6.6 Numerical Setup

6.6.1 Defination of Point Masses

After importing the CAD model to Ansys Aqwa, first of all point masses of spar hull, fixed ballast, nacelle (Nacelle, Rotor & Hub) and tower were assigned to the geometry at their specific center of gravities. Moment of inertia for each part was also described in the first step.

Details	
Name	Point Mass fix ballast
Visibility	Visible
Activity	Not Suppressed
Point Mass Properties	
Mass Definition	Manual Definition
<input type="checkbox"/> X	0.0 m
<input type="checkbox"/> Y	0.0 m
<input type="checkbox"/> Z	-118.28 m
<input type="checkbox"/> Mass	8007779.577 kg
Inertia Properties	
Define Inertia Values By	Direct Input of Inertia
Kxx	4.04625930177959 m
Kyy	4.04625930177959 m
Kzz	4.2299127642907 m
<input type="checkbox"/> bxx	131105083.6 kg.m ²
<input type="checkbox"/> byy	0.0 kg.m ²
<input type="checkbox"/> bzz	0.0 kg.m ²
<input type="checkbox"/> lxx	131105083.6 kg.m ²

Details	
Name	Point Mass hull
Visibility	Visible
Activity	Not Suppressed
Point Mass Properties	
Mass Definition	Manual Definition
<input type="checkbox"/> X	0.0 m
<input type="checkbox"/> Y	0.0 m
<input type="checkbox"/> Z	-58 m
<input type="checkbox"/> Mass	5496727 kg
Inertia Properties	
Define Inertia Values By	Direct Input of Inertia
Kxx	37.6458099045251 m
Kyy	37.6458099045251 m
Kzz	4.22991276497677 m
<input type="checkbox"/> bxx	7790000000 kg.m ²
<input type="checkbox"/> byy	0.0 kg.m ²
<input type="checkbox"/> bzz	0.0 kg.m ²
<input type="checkbox"/> lxx	7790000000 kg.m ²

Name	Point Mass Tower
Visibility	Visible
Activity	Not Suppressed
Point Mass Properties	
Mass Definition	Manual Definition
<input type="checkbox"/> X	0.0 m
<input type="checkbox"/> Y	0.0 m
<input type="checkbox"/> Z	38.234 m
<input type="checkbox"/> Mass	347460 kg
Inertia Properties	
Define Inertia Values By	Direct Input of Inertia
Kxx	25.3337816960084 m
Kyy	25.3337816960084 m
Kzz	2.65165042944955 m
<input type="checkbox"/> bxx	223000000 kg.m ²
<input type="checkbox"/> byy	0.0 kg.m ²
<input type="checkbox"/> bzz	0.0 kg.m ²
<input type="checkbox"/> lxx	223000000 kg.m ²

Details	
Name	Point Mass Nacelle
Visibility	Visible
Activity	Not Suppressed
Point Mass Properties	
Mass Definition	Manual Definition
<input type="checkbox"/> X	0.0 m
<input type="checkbox"/> Y	0.0 m
<input type="checkbox"/> Z	87 m
<input type="checkbox"/> Mass	406780 kg
Inertia Properties	
Define Inertia Values By	Direct Input of Inertia
Kxx	64.6464475747174 m
Kyy	64.6464475747174 m
Kzz	3.32603228806602 m
<input type="checkbox"/> bxx	1700000000 kg.m ²
<input type="checkbox"/> byy	0.0 kg.m ²
<input type="checkbox"/> bzz	0.0 kg.m ²
<input type="checkbox"/> lxx	1700000000 kg.m ²

Figure 48. Definition of point masses in ansys aqua

6.6.2 Modelling of Mooring Lines

Mooring lines with a combination of chain – polyester were designed and modelled in the Ansys Aqua using mooring system properties and fairleads & anchor points locations mentioned in the table 16,17,18,19 and 20.

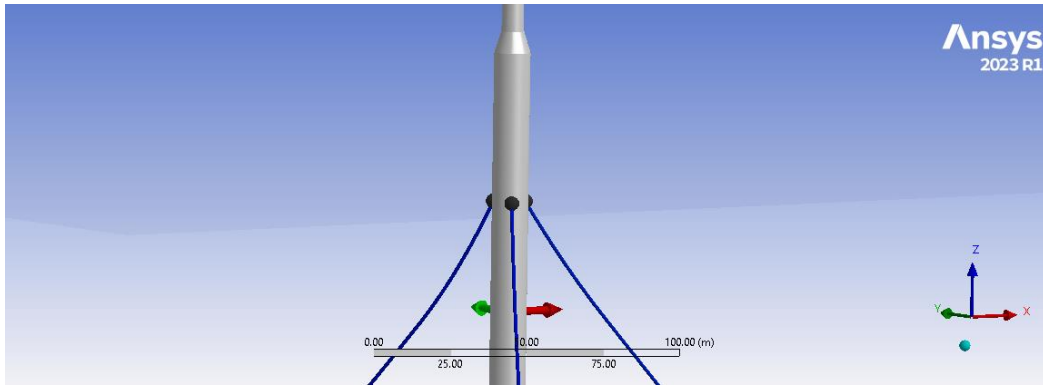


Figure 49. Fairleads

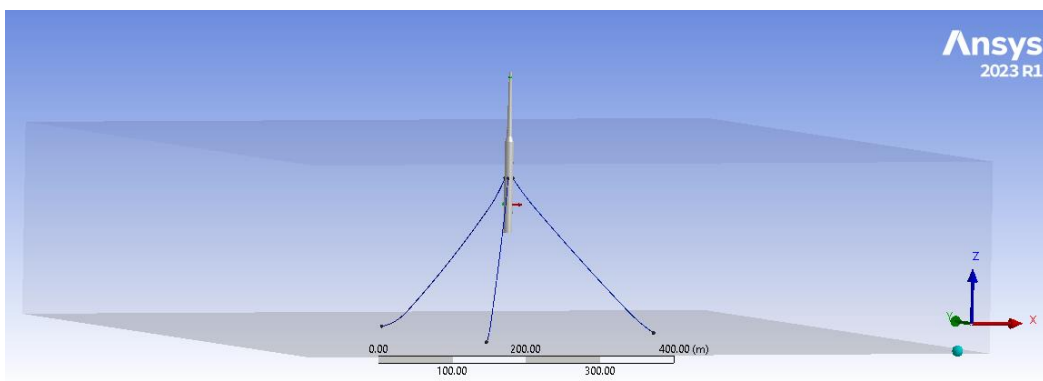


Figure 50. Mooring lines side view

6.6.3 Mesh

Meshing plays a vital role in simulating the model and approximating the results for a real time scenario. It works on the basic principle of splitting the whole model into small sized elements, these small elements represent a volume depending on size of mesh given. Ansys then uses mathematical algorithms and equations based on location and size of each element and computes results. These results when compiled represent the virtual behavior of body under defined loads. In the simulation setup for the Spar buoy designs, I used a mesh size of 0.5 meters along with a connection tolerance of 0.05 meters to ensure accurate connections between mesh elements. The program automatically generated a waterline for each model, which is crucial for analyzing the buoy's interaction with the water's surface. After successful meshing, 26668 nodes and 26668 elements were created.

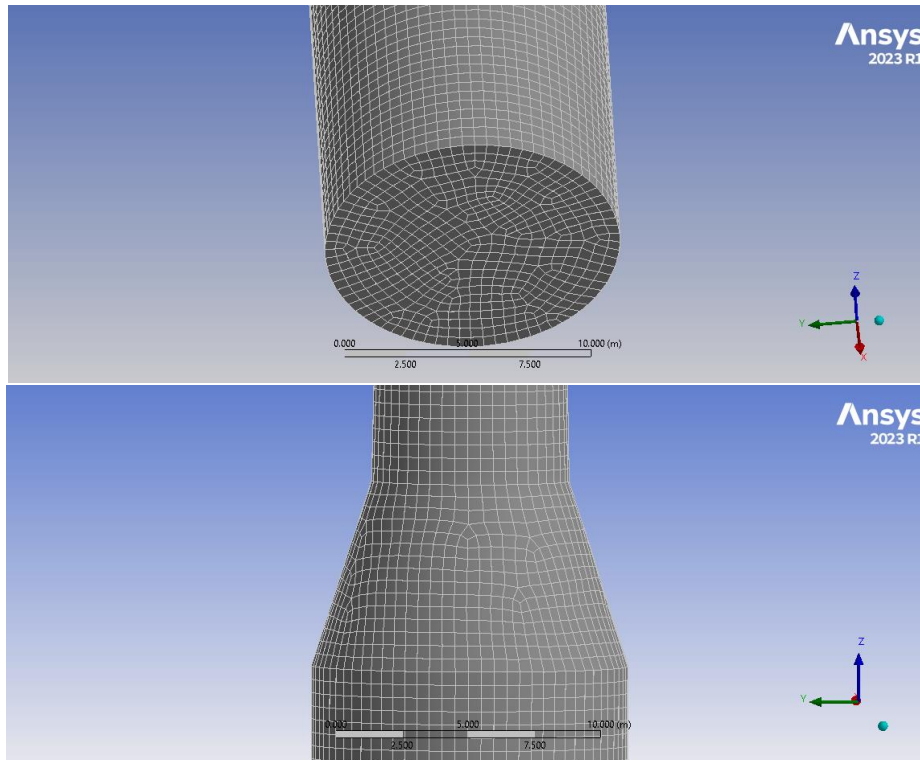


Figure 51. Mesh

6.7 Operating Conditions

To investigate the hydrodynamic response and behavior of designed FOWT, application of operating conditions at selected site has significant importance. It has been decided after having discussions with my thesis supervisor that hydrodynamic response for this FOWT will be evaluated during mean operating conditions which represent the routine environmental conditions and extreme operating conditions which represent the worst possible environmental conditions available at Utsira Nord during past seven years (2015 – 2021). To assign the wind turbine with such mean and extreme operating conditions, a python script was run to get the hourly data from the NORA – 3 databases. More details about extraction of operating conditions at Utsira Nord during 2015 – 2021 from NORA – 3 databases are available in the chapter of Design of Experiments of this thesis. A statistical analysis was conducted to average the mean conditions and extraction of extreme conditions. For prediction of extreme conditions, highest ever significant height, highest possible wind speed, mean wave and wind direction and wave periods / wave frequency was observed during that scenario. This situation is called as survival mode of the FOWT. The value of wave frequency / wave period at which highest ever significant height was occurred can be extracted from the CSV file generated through the python script and specific wave frequency / period can be observed. It is important to understand that longest wave period or shortest

wave frequency and highest ever significant wave height didn't occur at a same time. To find out the value for wave period / frequency at which wave with highest ever significant height was occurred during 2015 – 2021 to model the extreme operating conditions for the response evaluation of FOWT. This wave frequency / period can be called as effective wave frequency / period.

However, Numerical simulation was run with the input of range of all possible wave frequencies and then hydrodynamic response at desired mean and extreme operating conditions can be evaluated.

Significant wave height	2.079067841 m
Wave period	7.182680855 s
Wave frequency	0.139223783 Hz
Wind speed	8.369807404 m/s
Wind and wave direction	139.2186272 degrees

Table 21. Mean operating conditions

Significant wave height	14.74 m
Effective Wave period	13.26 s
Effective Wave frequency	0.075414781Hz
Wind speed	29 m/s
Wind and wave direction	139.2186272 degrees

Table 22. Extreme operating conditions

Details	
[-] Details of Wave Frequencies	
Name	Wave Frequencies
Intervals Based Upon	Frequency
[-] Incident Wave Frequency/Period Definition	
Range	Manual Definition
Definition Type	Range
Lowest Frequency Definition	Manual Definition
Lowest Frequency	0.04596 Hz
Longest Period	21.76 s
Highest Frequency Definition	Manual Definition
Highest Frequency	0.3096 Hz
Shortest Period	3.23 s
Number of Intermediate Values	18
Interval Frequency	0.01388 Hz

Figure 52. Range of wave frequencies / periods for numerical simulation in Ansys Aqwa

6.8 Hydrodynamic Solution

Two major simulations were conducted to predict the hydrodynamic response of FOWT in mean and extreme conditions. To model a realistic approach, an irregular wave with slow drift was modelled using Jonswap (Hs) wave spectrum type. Simulation was run from shortest ever wave period (highest wave frequency) till longest ever wave period (lowest wave frequency) during 2015 – 2021 at Utsira Nord for 500 seconds with a time step of 1 second. Time domain response was gained as an output for the evaluation of response of FOWT under mean and extreme operating conditions. Through this time

domain response, movement of FOWT with designed spar buoy platform can be observed in six degrees of freedom (three translational and three rotational). Movement in translational degrees of freedom (Heave, Surge and Sway) was gained in the units of meters and for movement in rotational degrees of freedom (Yaw, Roll and Pitch) was gained in the units of degrees.

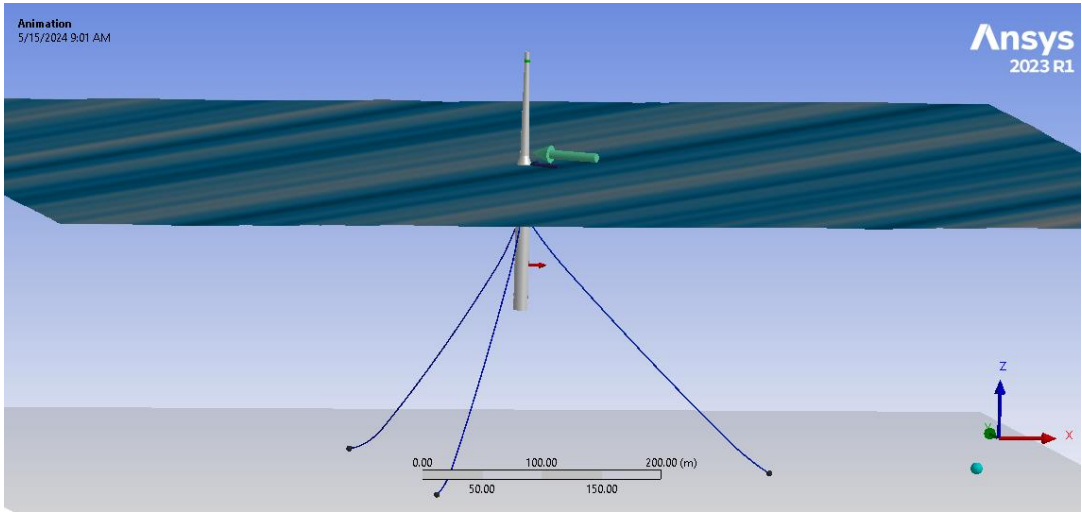


Figure 53. Wave modelling

6.8.1 Solution During Mean and Extreme Operating Conditions

Values for mean and extreme operating conditions were put as an input using table. 21 & 22 for evaluation of the response of FOWT in such conditions.

Details		Details	
Activity	Not Suppressed	Name	Irregular Wave 1
Wave Range Defined By	Period	Visibility	Visible
<input checked="" type="checkbox"/> Wave Spectrum Details		Activity	Not Suppressed
Wave Type	JONSWAP (Hs)	Wave Range Defined By	Period
<input type="checkbox"/> Direction of Spectrum	139.22°	<input checked="" type="checkbox"/> Wave Spectrum Details	
Wave Spreading	None (Long-Crested Waves)	Wave Type	JONSWAP (Hs)
Spectrum Presentation Method	1D Graph	<input type="checkbox"/> Direction of Spectrum	139.22°
Seed Definition	Program Controlled	Wave Spreading	None (Long-Crested Waves)
Number of Spectral Lines Definition	Program Controlled	Spectrum Presentation Method	1D Graph
Omit Calculation of Drift Forces	No	Seed Definition	Program Controlled
Start and Finish Period Definition	Manual Definition	Number of Spectral Lines Definition	Program Controlled
<input type="checkbox"/> Start Period	10 s	Omit Calculation of Drift Forces	No
<input type="checkbox"/> Finish Period	3.23 s	Start and Finish Period Definition	Manual Definition
<input type="checkbox"/> Significant Wave Height	2.079067841 m	<input type="checkbox"/> Start Period	21.76 s
<input type="checkbox"/> Gamma	2	<input type="checkbox"/> Finish Period	3.23 s
<input type="checkbox"/> Peak Period	7.18 s	<input type="checkbox"/> Significant Wave Height	14.76 m
Export CSV File	Select CSV File...	<input type="checkbox"/> Gamma	2
		<input type="checkbox"/> Peak Period	13.26 s

Figure 54. Irregular wave model with Jonswap (Hs) for mean and extreme operating conditions.

6.8.1.1 Heave

6.8.1.1.1 During Mean Operative Conditions

Time domain response for heave motion was generated in Ansys Aqwa. The graph illustrates the heave response of designed FOWT over a 500-second simulation period, measured relative to its center of gravity at approximately -85.35 meters. The graph shows a repetitive oscillatory pattern in Z – axis which represents the heave motion of the FOWT under simulated normal environmental conditions at Utsira Nord. These conditions included irregular waves modelled with JONSWAP waves spectrum with a significant wave height of 2.08 meters and both wind and wave directions at 139.22 degrees, with a wind speed of 8.36 meters per second.

The peaks and troughs in the graph represent the maximum and minimum heave positions of the FOWT structure, which fluctuate around the center of gravity. The time domain response of this FOWT shows that the structure moved only about 3 meters along z – axis in direction downwards. Also, Structure is coming to its initial position and reducing the peak motion amplitudes after regular intervals which is showing the good damping ability of the structure. The regular pattern suggests a stable response to the wave conditions, indicating that the FOWT is reacting predictably to the simulated marine environment.

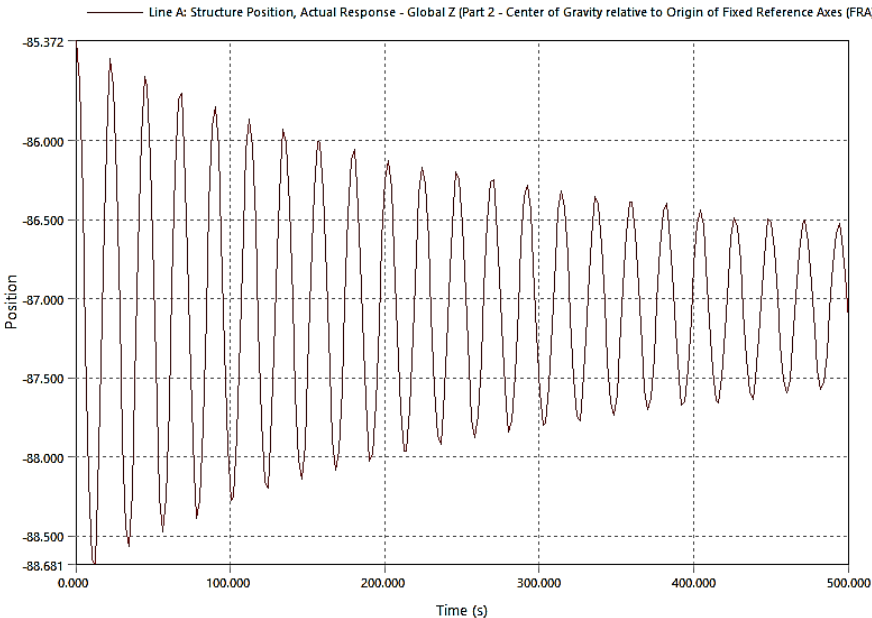


Figure 55. Heave time domain response during mean operating conditions.

6.8.1.1.2 During Extreme Operating Conditions

While during extreme operating conditions, the graph illustrates the heave response of designed FOWT over a 500-second simulation period, measured relative to its center of gravity at approximately -85.35 meters. The graph shows a repetitive oscillatory pattern but with a greater amplitude specially along Z – axis downwards which represents the considerable heave motion of the FOWT under simulated extreme environmental conditions at Utsira Nord. These conditions included irregular waves modelled with JONSWAP waves spectrum with a significant wave height of 14.76 meters with a peak wave period of 13.26 s and both wind and wave directions at 139.22 degrees, with a wind speed of 21 meters per second.

The peaks and troughs in the graph represent the maximum and minimum heave positions of the FOWT structure, which fluctuate relative to the center of gravity. The time domain response of this FOWT shows that the structure moved only about 4 meters along z – axis in direction downwards. Also,

Structure is coming to its initial position and reducing the peak motion amplitudes as the time progresses which is showing the good damping ability of the structure. The regular pattern suggests a stable vertical response to the wave conditions, indicating that the FOWT is reacting predictably to the simulated marine environment. Overall, the FOWT's heave response to the simulated extreme conditions suggests a relatively resilient performance and wind turbine can survive easily in this degree of freedom.

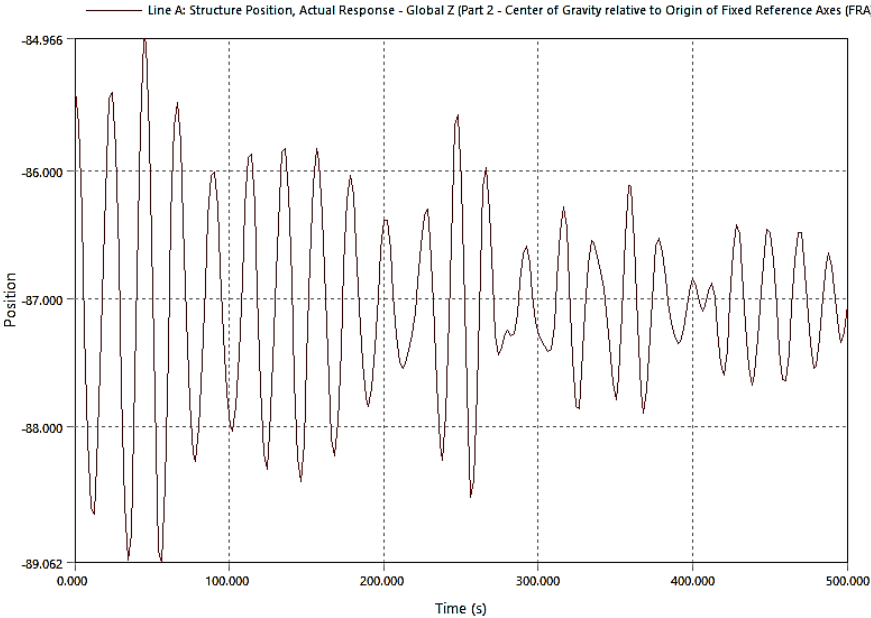


Figure 56. Heave time domain response during extreme operating conditions.

6.8.1.2 Surge

6.8.1.3 During Mean Operating Conditions

Aqwa generated a time domain response for surge movement which is translational movement in x - axis. The graph shows that the structure fluctuates in a sinusoidal pattern, indicating a periodic movement back and forth along the x – axis. This motion is typical for responses to wave and wind forces at Utsira Nord, where the peak amplitude of the waves is given as 2.08 meters. The graph's vertical axis, showing that the structure moved a maximum of 7.5 m in surge because the external forces are acting in direction almost parallel to the longitudinal axis.

The response shows two complete cycles within the 500-second period, with each cycle lasting about 250 seconds. The peak positions occurred near 125 seconds and 375 seconds. This pattern suggests that the FOWT is responding predictably to the combined effects of wind and waves.

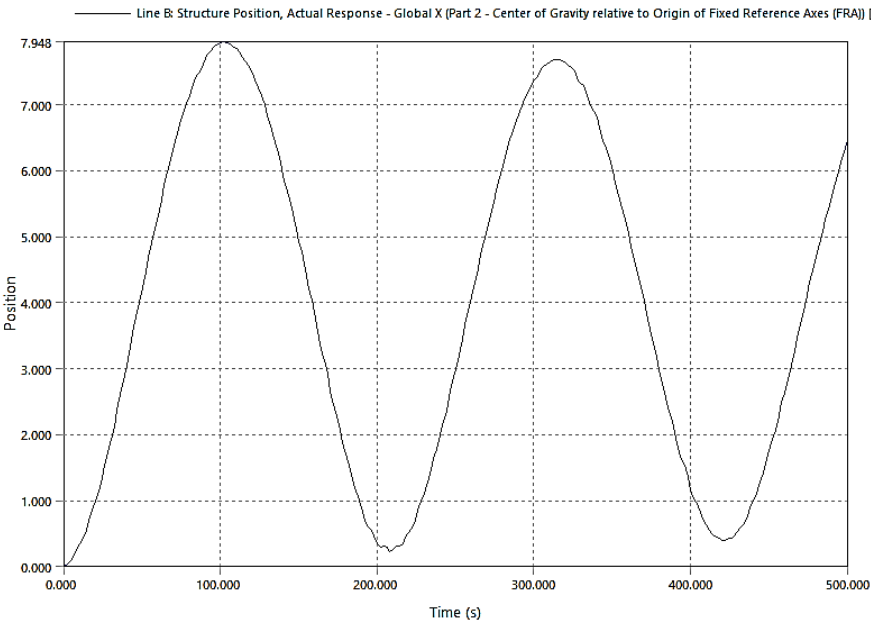


Figure 57. Surge time domain response during mean operating conditions.

6.8.1.3.1 During Extreme Operating Conditions

The graph shows that the FOWT’s position fluctuates significantly between approximately 1.25 meters and peak of 7.5 meters. The movement is little similar to response in mean operating conditions but with a series of large, irregular oscillations, reflecting the dynamic and powerful impact of extreme wind and wave conditions. The peak movement amplitudes in surge direction are greater because the direction of external forces such as wind and waves are quite parallel to the longitudinal axis. These conditions include extremely high wave amplitude of 14.76 meters and strong wind speeds of 21 m/s, both aligned in the same direction. Thus, these extreme conditions combined force the structure to move in greater amplitude in surge degree of freedom.

The pattern in the graph represents that the FOWT is initially struggling to stabilize against the force of the extreme waves and winds but gradually finds a somewhat more stable oscillatory pattern as time progresses. This can be seen from the slightly reduced amplitude of movements towards the latter part of the time domain response graph, although the movements remain greater in amplitudes.

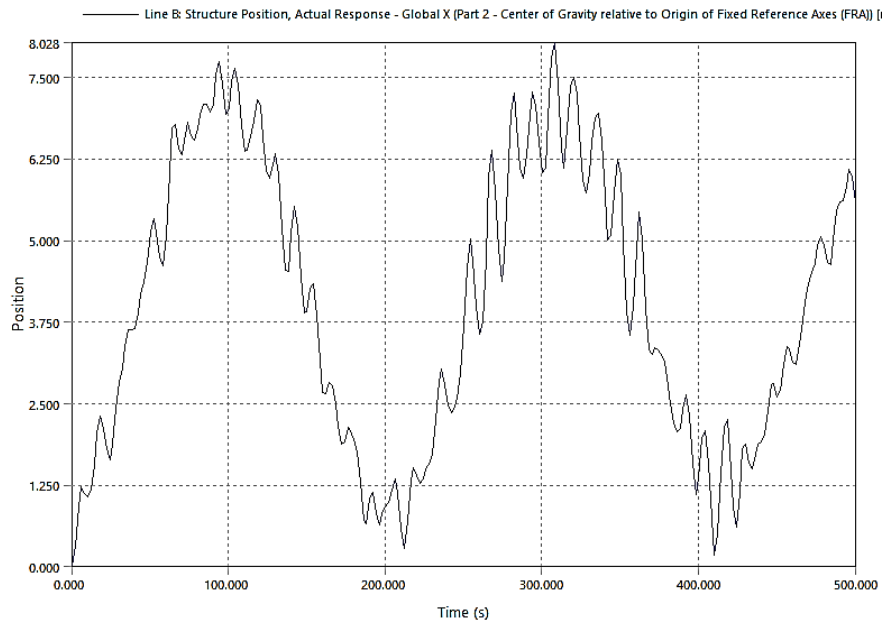


Figure 58. Surge time domain response in extreme operating conditions.

6.8.1.4 Sway

6.8.1.4.1 During Mean Operating Conditions

The graph provided showcases the sway movement of designed FOWT over a 500-second simulation period under normal operational conditions at an offshore site. Sway refers to the lateral movement of the FOWT structure along the y - axis. The time domain response displays a movement that starts near zero, fluctuates through various peaks and troughs, and finally ends with a sharp decline, ranging from about 1.18658e-4meters to nearly -3.52506e-4meters.

The movement pattern suggests a series of increasing movement that peak around 500 seconds into the simulation. This kind of behavior typically represents how the structure reacts to lateral forces caused by the combination of wave and wind conditions. This observed sway behavior indicates the FOWT's dynamic stability in responding to these environmental forces. The return towards a more negative position in the latter part of the graph might suggest a response to a particularly strong or long-lasting wave force but the structure might come back to its initial position after some additional time period because the amplitude of the motion is very small.

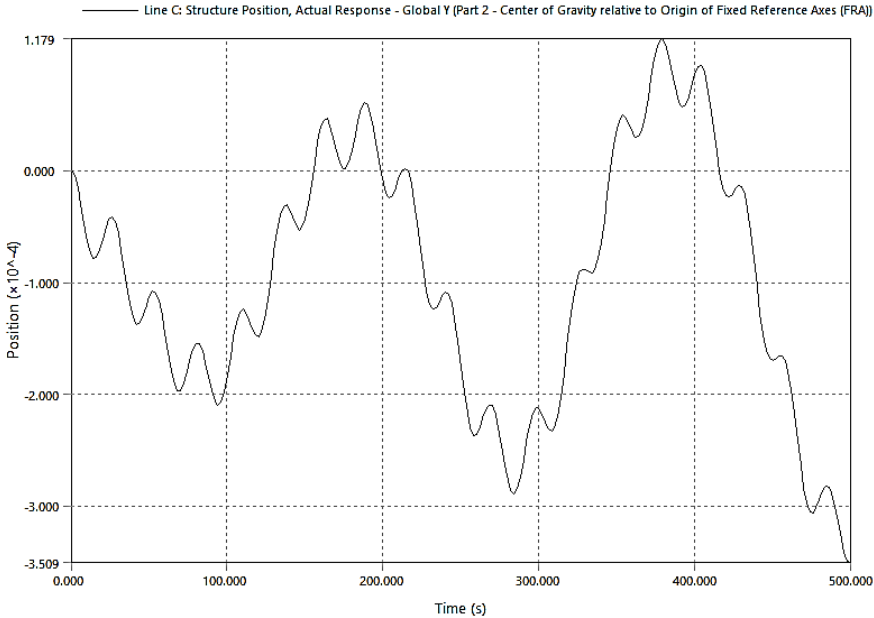


Figure 59. Sway time domain response during mean operating conditions

6.8.1.4.2 During Extreme Operating Conditions

The graph provided represents the sway movement of designed FOWT over a 500-second simulation period under extreme operational conditions at an offshore site. Sway refers to the lateral movement of the FOWT structure along the y – axis. While during extreme conditions turbine showcases a regular and controlled response in the earlier stages of the simulation but showed a sudden irregular behavior in the later stages of time period. The graph indicates that the structure moved from -4.31273e-3 to 2.17001e-3 mm in the peak wave periods. This tells us that wind turbine went through extreme external forces in the lateral direction as the time progressed. However, movement amplitude was still very small and it can be seen in the animation of the simulation that turbine can easily survive the extreme operating conditions occurred at Utsira Nord.

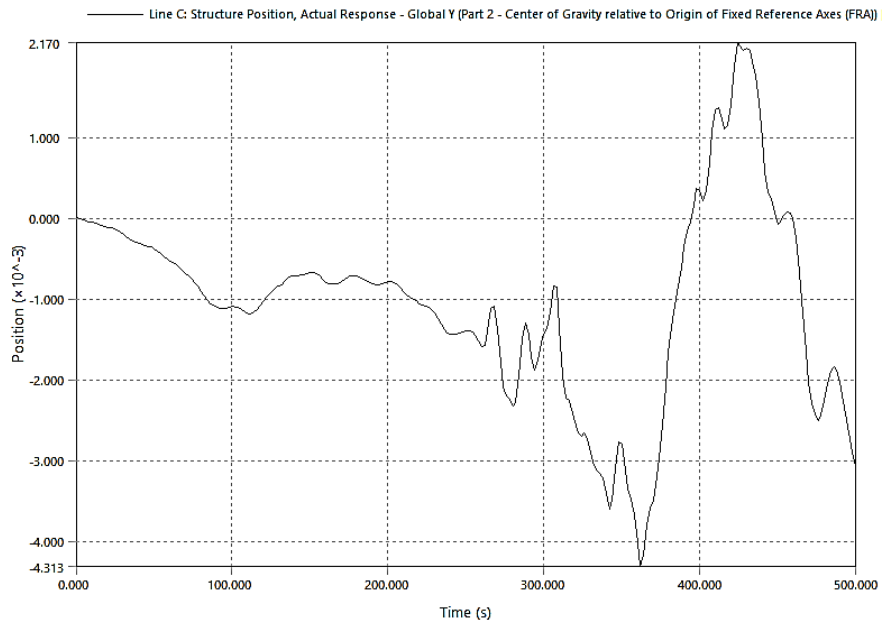


Figure 60. Sway time domain response during extreme operating conditions

6.8.1.5 Roll

6.8.1.5.1 During Mean Operating Conditions

Time domain response during mean operating conditions shows dynamic response of FOWT in rotational movement around global x – axis during a 500-second simulation in degrees. The pattern shown in the ansys’s generated graph is a regular and repetitive rotational movement, indicating a consistent response to the simulated environmental conditions. The roll values fluctuate between approximately 1.1964e-5degrees and -2.88184e-4degrees.

This continuous response suggests that the FOWT is stable enough and ability to rotate towards the initial condition after regular intervals of time. The roll motion is very less, which indicates that the turbine and the spar structure has good damping capability to resist enough movement during mean conditions and stay operative.

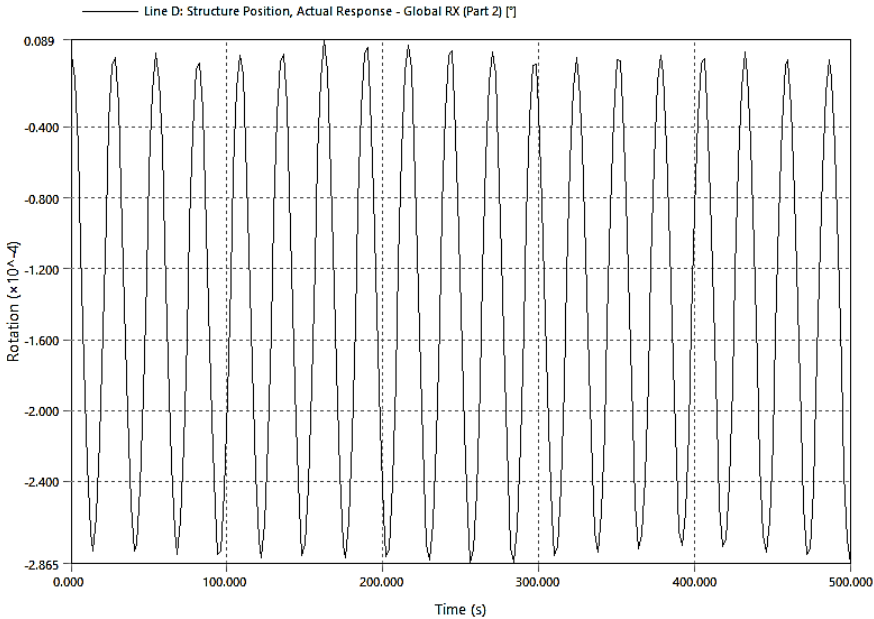


Figure 61. Roll time domain response during mean conditions.

6.8.1.5.2 During Extreme Operating Conditions

Time domain response during extreme operating conditions shows dynamic response of FOWT in rotational movement around global x – axis during a 500-second simulation in degrees. The pattern shown in the ansys’s generated graph is a regular and repetitive but increasing rotational movement with time. The roll values fluctuate between approximately 2.94208e-3degrees and -3.37766e-3degrees.

This response shows that the turbine didn’t rotate much till first 250 seconds but started rotating rapidly in a regular manner but still the amplitude of the rotation was not very large.. This continuous response suggests that the FOWT is under the influence of strong wave and wind interaction during the later stages of time period. However, the amplitude in such extreme conditions is not that big and predictable which suggests that FOWT is stable enough and able to rotate towards the initial condition after regular intervals of time. The roll motion is relatively less, which indicates that the turbine and the spar structure has good damping capability to resist enough movement during extreme conditions and stay operative.

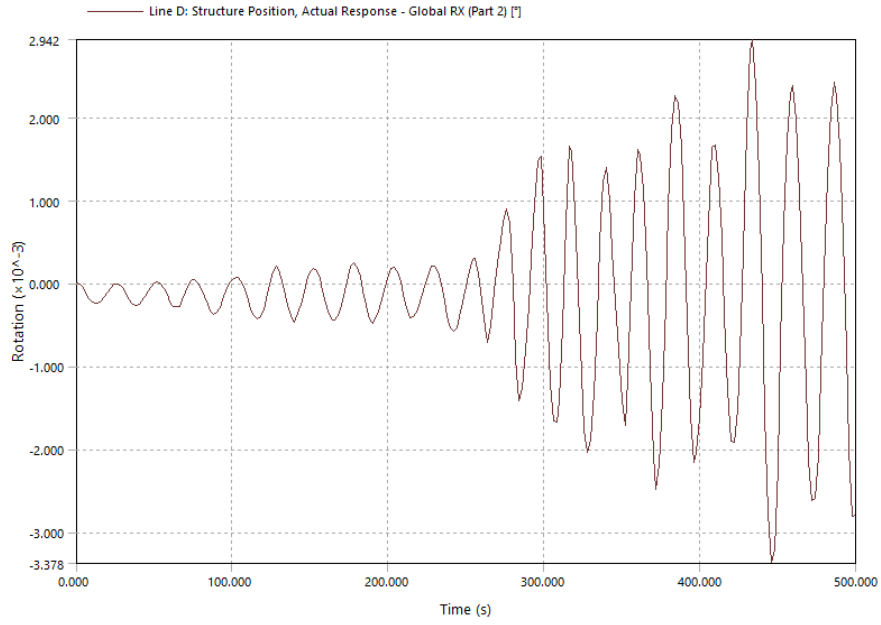


Figure 62. Roll time domain response during extreme operating conditions.

6.8.1.6 Pitch

6.8.1.6.1 During Mean Operating Conditions

Unlike other graph patterns, pitch movement during mean operating conditions shows an irregular and rapidly changing behavior of the wind turbine. Pitch actually is the rotational movement around the lateral axis which is global – y axis in this case. The reason behind these rapid fluctuations are the combined external forces being applied through waves and wind in 139.22 degrees direction, the direction of the wind is forcing the FOWT to rotate more rapidly around y – axis during this irregular wave modelled by JONSWAP (Hs) which represent the realistic wave model in the oceans.

However, the response of the structure in pitch movement is quite irregular but not very big in amplitude, which shows the dynamic stability of the wind turbine and mooring system. A maximum peak of -0.20504degrees was observed during the whole time period which stayed at the peak for a very short time period and tend to rotate back to initial position. And the whole pattern shows that the structure is staying closer to it’s mean (initial) position for the whole time period and wind turbine can operate freely. Mooring lines are working well to damp the pitch movement during mean operating conditions.

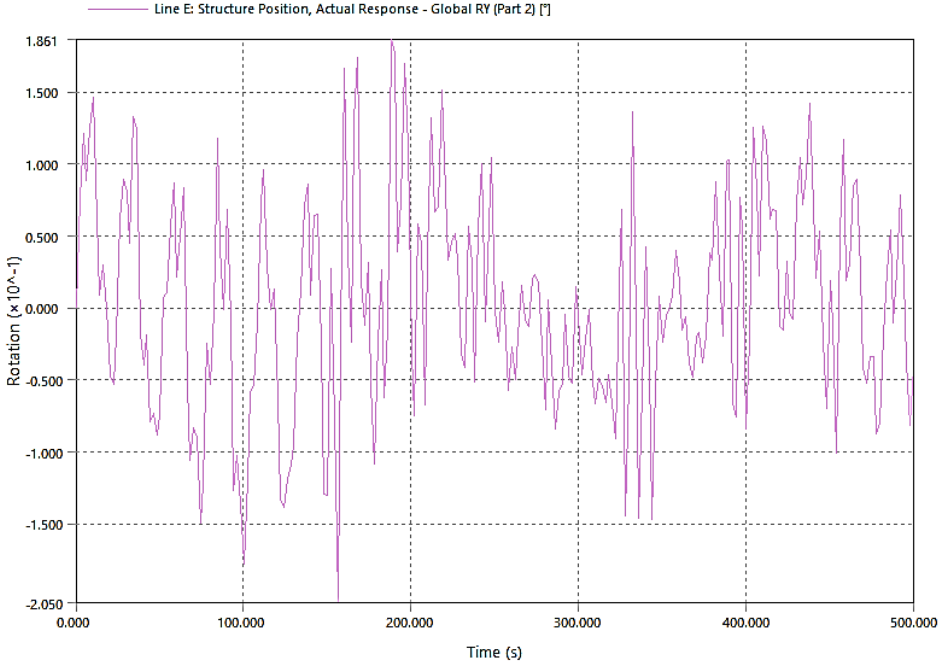


Figure 63. Pitch time domain response during mean operating conditions.

6.8.1.6.2 During Extreme Operating Conditions

Pitch movement during extreme operating conditions gives greater response as in extreme operating conditions shows an irregular and rapidly changing behavior of the wind turbine. This shows that increase in the significant wave height, wind speed and changing in the peak wave period influenced much in the behavior of wind turbine’s rotation around the lateral axis which is global – y axis in this case. The reason behind these rapid fluctuations are the combined external forces being applied through waves and wind in 139.22 degrees direction, the direction of the wind is actually forcing the FOWT to rotate more rapidly around y – axis during this irregular wave modelled by JONSWAP (Hs) which represent the realistic wave model in the oceans.

However, the response of the structure in pitch movement is quite irregular but not very big in amplitude, which shows the dynamic stability of the wind turbine and mooring system. A maximum peak of 2.999 degrees was observed during the whole time period which stayed at the peak for a very short time period

and tend to rotate back to initial position. And the whole pattern shows that the structure is staying closer to its mean (initial) position for the whole time period and wind turbine can operate freely. Mooring lines are working well to damp the pitch movement during mean operating conditions.

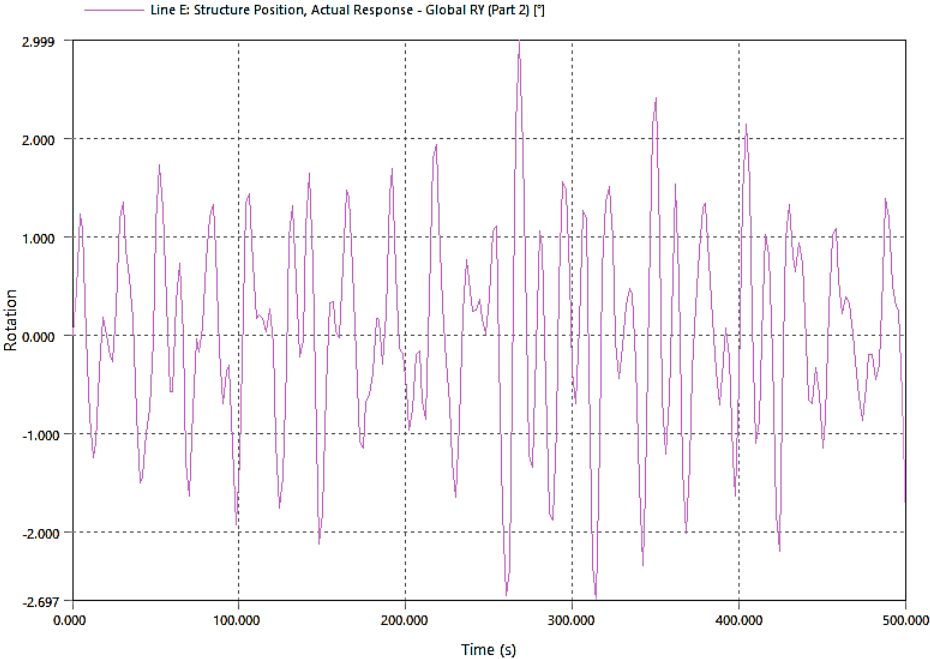


Figure 64. Pitch time domain response during extreme operating conditions

6.8.1.7 Yaw

6.8.1.7.1 During Mean Operating Conditions

Time domain response of rotational movement in degrees around vertical axis (z – axis) shows quite regular manner. The initial trough went to a amplitude of $-4.72938e-4$ degrees which represent the wave loads in 139.22 degree direction. This wave forced the structure to rotate negatively (left – side rotation if seen from the top) right at the start of the time period but after that structure and mooring system’s damping ability forced the structure to tend back to initial position when the significant wave height was not present at that particular period of time. When the structure was rotating towards initial position another excited wave with a significant wave height of 2.08 m interacted with the structure and wind turbine rotated positiviey (right – side direction) with a greater amplitude of the rotational movement. This happened because of the structure stored inertia while rotating towards initial position around global z – axis. A maximum peak of $5.06058e-4$ degrees was observed during the whole time period. However, the yaw motion is still controlled enough for the turbine to stay in the operative condition during mean operating conditions.

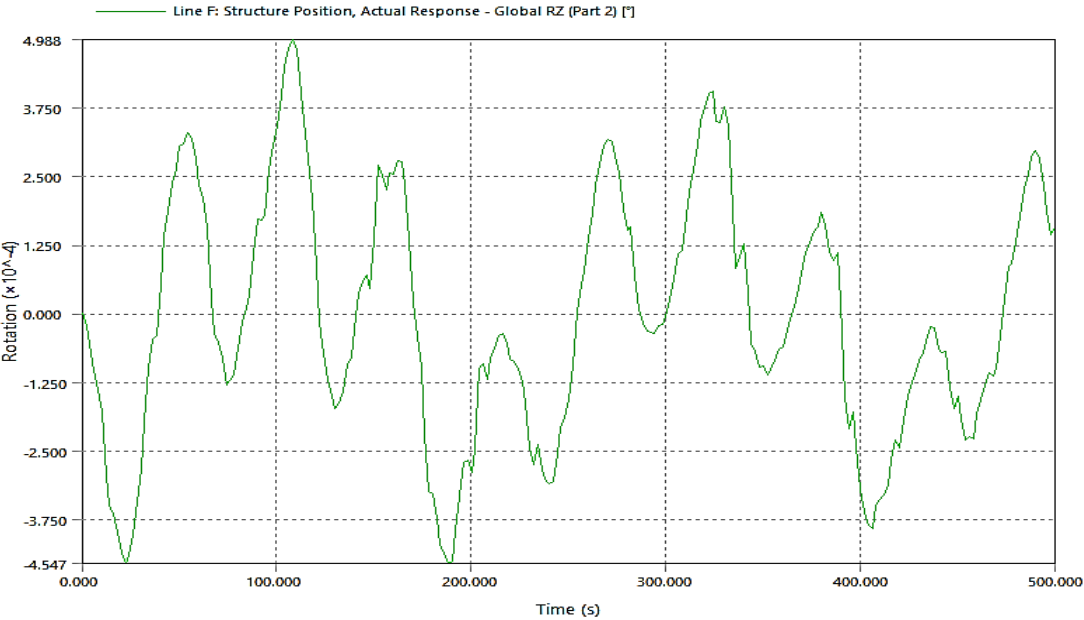


Figure 65. Yaw time domain response during mean operating conditions

6.8.1.7.2 During Extreme Operating Conditions

The yaw rotation remained very controlled, and turbine stayed at almost in its initial position but rose quickly and sharply as the simulation goes on, especially after 300 seconds, causing the turbine to experience slightly larger rotational movements around global z – axis. These significant variations, which are noticeable in the irregular rapid peaks, probably result from reactions to variation of wind and wave speeds which were numerically modelled as irregular wave spectrum with JONSWAP model. This irregular wave during its peak period forced the structure to rotate negatively (left – side rotation if seen from the top) firstly but after that structure and mooring system’s damping ability forced the structure to tend back to initial position when the significant wave height was not present at that particular period of time. When the structure was rotating towards initial position another excited wave with a significant wave height of 14.76 m interacted with the structure and wind turbine rotated positiviey (right – side direction) with a slightly greater amplitude of the rotational movement. This happened because of the

structure stored inertia while rotating towards initial position around global z – axis. A maximum peak of -0.03862 degrees was observed during the whole time period.

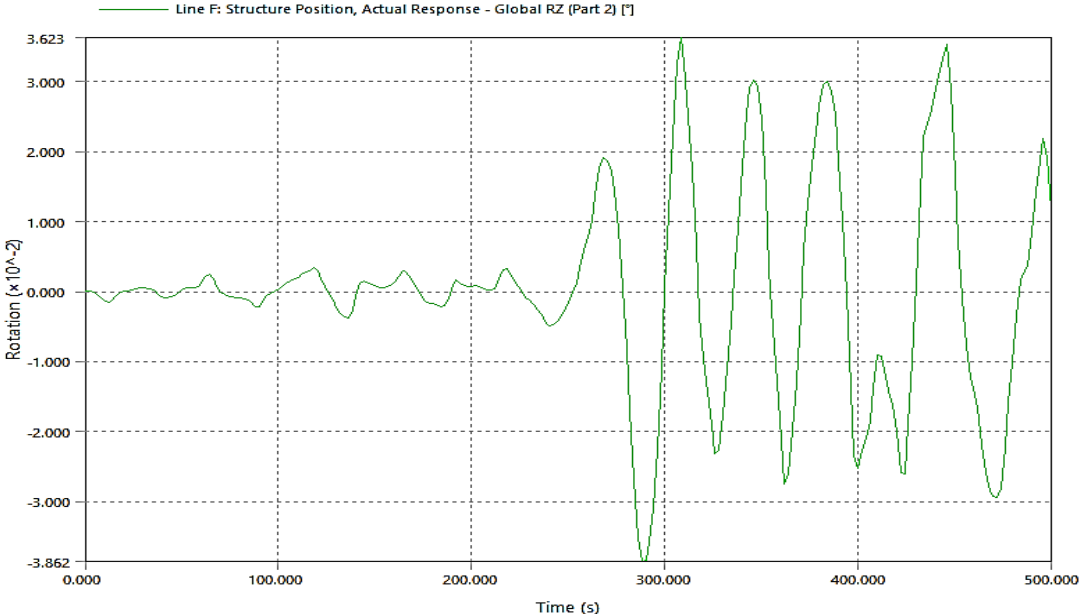


Figure 66. Yaw time domain response during extreme operating conditions

6.8.1.8 Frequency Domain Response

The inertia force and diffraction force acting on the main body of the spar hull are computed in the frequency domain analysis using linear diffraction theory in potential flow. Frequency domain analysis in this study was conducted to evaluate the natural frequencies in each degree of freedom. When Natural frequency of the structure becomes equal or similar to the wave frequency in the ocean a phenomenon of Resonance occurs. During Resonance the structure moves very irregularly and higher amplitudes which risks the ability of the whole wind turbine and mooring system to survive in such conditions.

I evaluated all DOF but considered only three DOF (Heave, Surge and Yaw) to mention in this study because these DOF exhibited larger amplitudes of motions. Another reason for this consideration is frequency-based response was quite similar for all the DOF as the lowest wave frequency was evaluated to be the apparent resonant frequency for five DOF other than Yaw only.

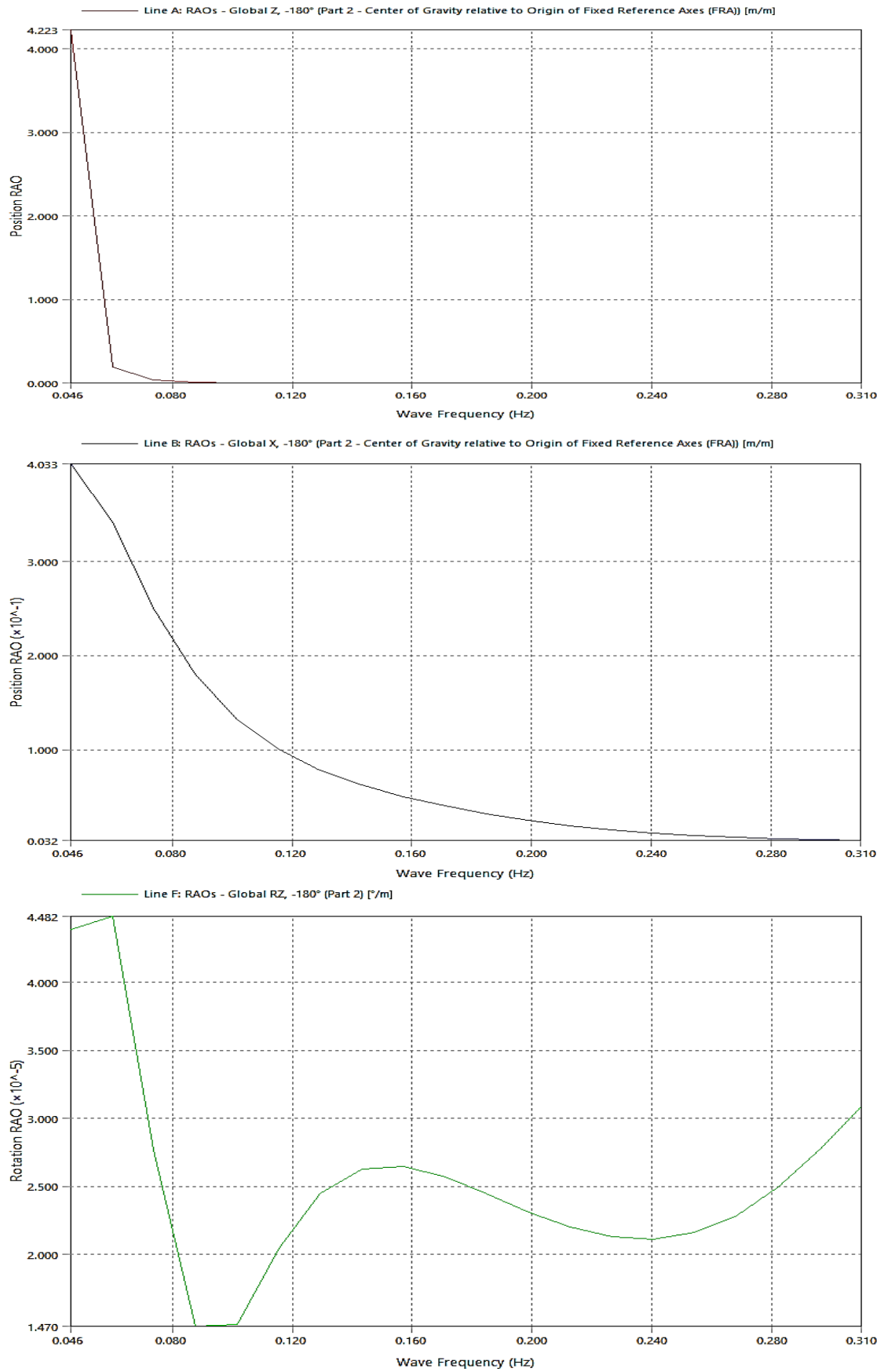


Figure 67. Frequency domain response for heave, surge and yaw RAO

The above graphs represent frequency response of heave, surge, and yaw response amplitude operators (RAO). Heave and Surge RAO decreases with the increase of wave frequency. Differing from heave and surge RAO, Yaw RAO increase first and then decrease with the growth of wave frequency. Resonant frequencies for each DOF can be seen from the above given graphs. For heave & surge RAO, the resonance frequency is about 0.046 degree/s, while 0.05983 degree/s for yaw RAO, clearly showing the coupling effects of heave and surge motions. When our structures operate at these wave frequencies which are natural frequencies of each RAO, structure's response to wave-induced forces is maximally amplified. Hence, it could be concluded from the frequency response that the natural frequency of our designed FOWT is quite low. So, it is always recommended to avoid deploying this FOWT to ocean where wave frequencies are quite like these natural frequencies.

6.8.1.9 Time Domain Response on Resonant Frequencies

It became interested to evaluate the FOWT response to the resonant natural wave frequencies. So, I modelled the operating conditions according to resonant natural frequencies calculated in previous section just to have a look at the dynamic response of designed FOWT.

Simulation was run for 500 s with each time of 1 s and peak motion amplitudes in each DOF are mentioned in the table below,

Degree of Freedom	Peak motion amplitudes in both positive and negative directions
Heave (relative to COG)	-79.86233 to -96.05903 m
Surge (relative to initial position 0)	11.04815 to -0.16417 m
Sway (relative to initial position 0)	0.06006 to -0.04975 m
Roll (relative to initial position 0)	0.03566° to -0.02702° degrees
Pitch (relative to initial position 0)	3.74629° to -3.75072° degrees
Yaw (relative to initial position 0)	44.53693° to -27.0619°degrees

Table 23. Time domain response of FOWT in all DOF during extreme resonant frequency during first 500 s

6.8.1.10 Tension forces in Mooring lines during extreme resonant Operating Conditions

Tension forces in the designed mooring lines can be checked in ansys aqwa. If the tension forces are less than the critical tension values of mooring lines, then the mooring system is considered as safe. Otherwise, to make the mooring system survive in the worst ever extreme resonant wave frequencies mooring system needs to be redesigned. Let’s have a look at time domain response of all three mooring lines in extreme resonant wave frequencies and extreme operating conditions.

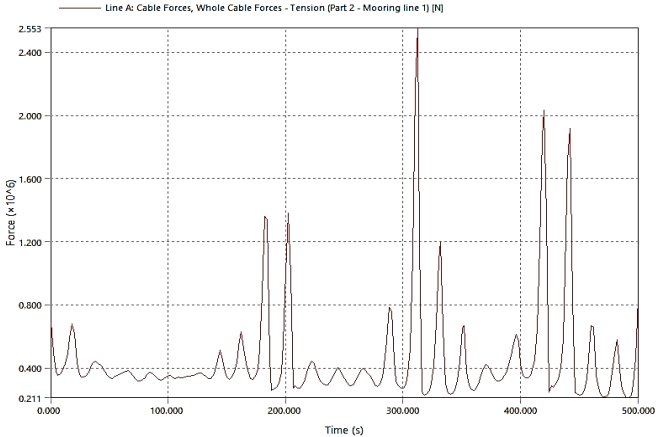


Figure 68. Tension force along time domain response on Mooring line 1.

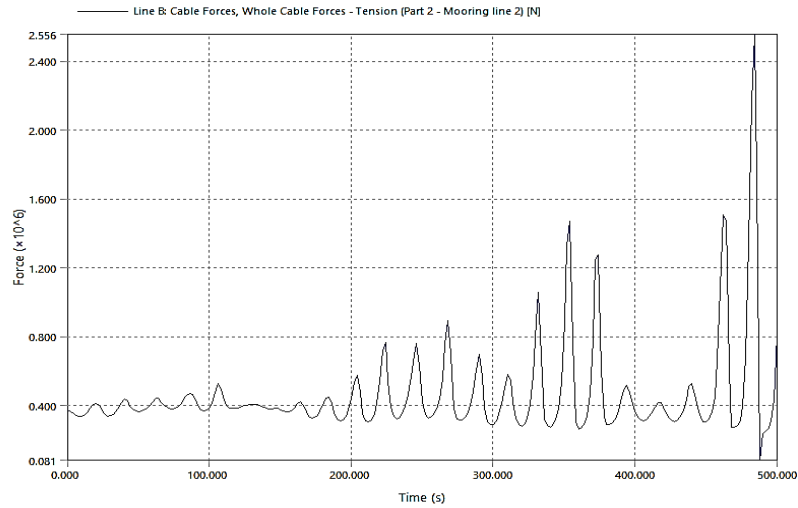


Figure 69. Tension force along time domain response on Mooring line 2.

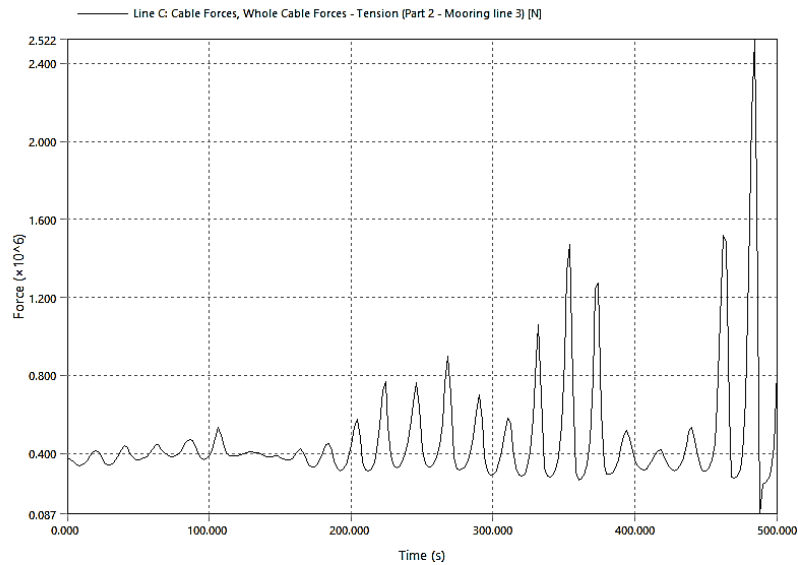


Figure 70. Tension force along time domain response on Mooring line 3.

It can be analyzed from the above graphs that the mooring line 2 bear the largest tension forces during the extreme environmental conditions of resonance phenomenon which is 2556319.5 N. This largest tension force in mooring line 2 is still less than the critical tension value of both chain and polyester mooring line. Maximum breaking loads of both of these mooring line combination materials are given in table 17 & 18. Maximum breaking loads for designed chain and polyester mooring lines are 13600000 N and 13200000 N respectively. So, it can be concluded that the design mooring system is safe to operate even at the resonant frequencies.

6.8.2 Pressure and motions

6.8.2.1.1 During mean Operating Conditions

It can be seen from the figures below that during the hydrodynamic diffraction when structure didn't conclude the effects of mooring lines in the simulation, FOWT moved about 1.489 m and the location where this movement occurred was the topmost part of the wind turbine tower.

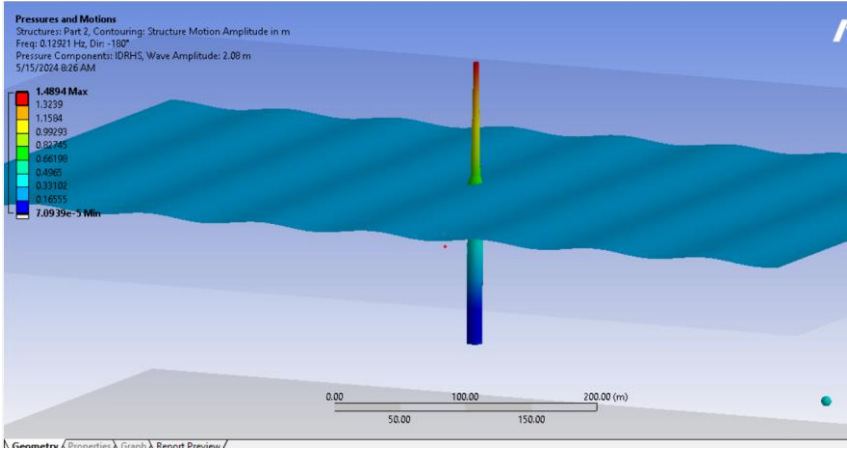


Figure 71. Structure motion amplitude in hydrodynamic diffraction during mean operating conditions.

Also, during mean operating conditions maximum structure interpolated pressure occurred at height of 2.2755 m and the location was freeboard part where wave – structure interaction took place.

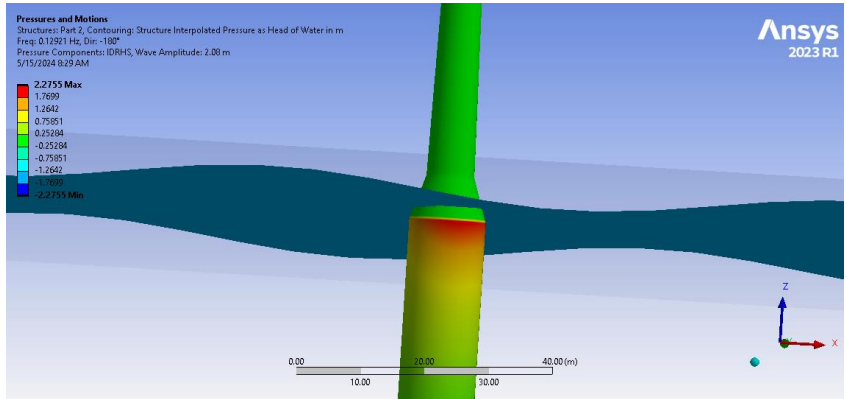


Figure 72. Structure interpolated pressure during extreme operating conditions.

6.8.2.1.2 During Extreme Operating Conditions

It can be seen from the figures below that during the hydrodynamic diffraction when structure didn't conclude the effects of mooring lines in the simulation, FOWT moved about 24.18 m and the location where this movement occurred was the topmost part of the wind turbine tower.

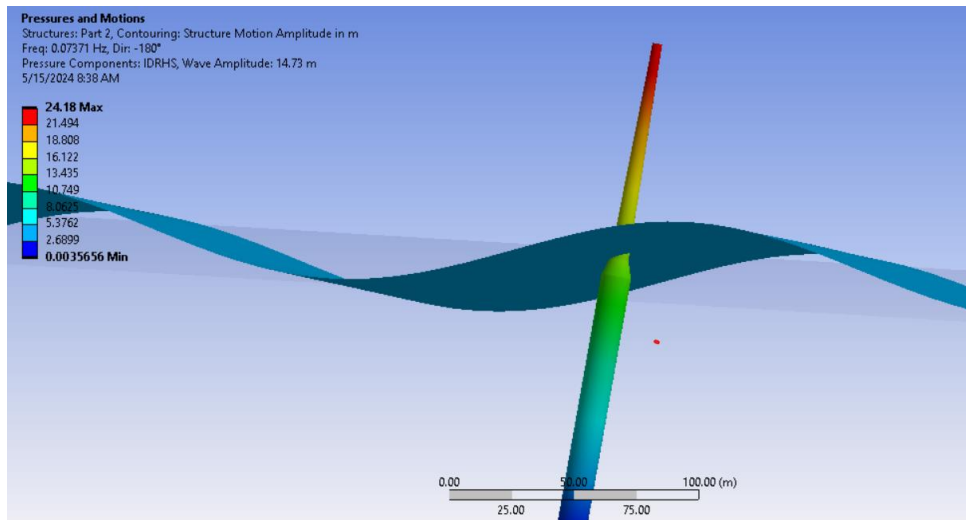


Figure 73. Structure motion amplitude in hydrodynamic diffraction during extreme operating conditions.

Also, during mean operating conditions maximum structure interpolated pressure occurred at height of 15.044 m and the location was freeboard part where wave – structure interaction took place.

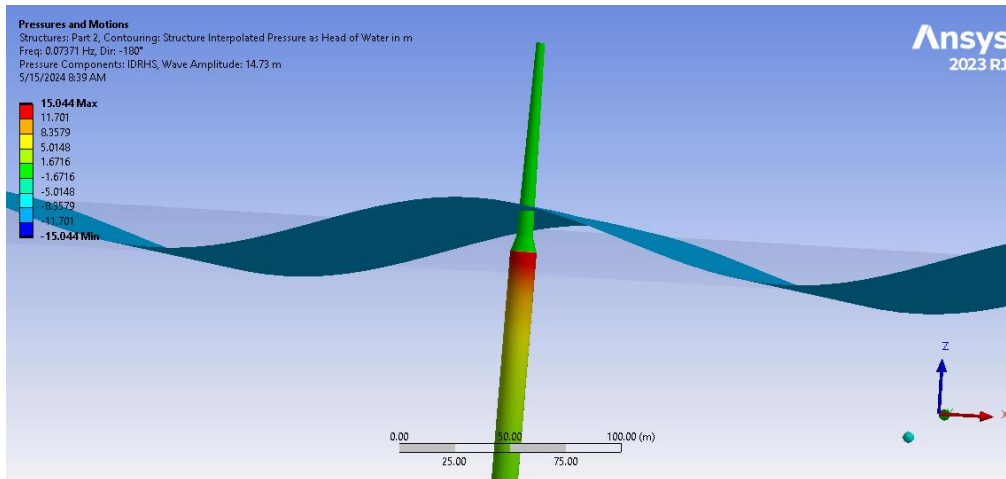


Figure 74. Structure interpolated pressure during extreme operating conditions.

Chapter 7

7 Conclusions and Future Work

7.1 Conclusions

The main aim of this thesis was to model a Floating Offshore Wind Turbine with Spar buoy floating platform in numerical prestressed hydrodynamic analysis. A commercially used software – Ansys Aqwa was chosen to model the numerical simulation and evaluation of dynamic response of designed FOWT in Arctic region's environmental operating conditions. For this reason, an NVE's identified location for floating offshore wind farm was chosen systematically and meteorological data for past seven years (2015 – 2021) was extracted through NORA – 3 database using a python script. A realistic buoyant spar platform was 3D modelled using surface tools and simulated in various operating scenarios to analyze and evaluate its dynamic response in six degrees of freedoms.

- First of all, an optimal design configuration (circular) was chosen out of three different design configurations based on their time domain response analysis. All three design configurations were simulated using same design parameters, boundary, and operating conditions. Circular design configuration gave lesser motion amplitudes overall in all degrees of freedom, especially in Heave direction where other two design configurations showed a very severe response and tend to move in very larger amplitudes.
- Two major simulations were conducted to analyze the FOWT dynamic response in mean and extreme operating conditions.
 - During mean operating conditions FOWT remained in stable and operative condition overall as none of the movement in any DOF was greater in amplitude throughout the simulation time period of 500 seconds. However, Surge time domain response exhibited a relatively greater amplitude in along the x – axis. The main reason behind this massive movement was coupling between the direction of external forces and longitudinal axis of Surge. All other translational and rotational movement didn't exhibit any significant movement overall which supports the stance that FOWT can be deployed in operate during normal routine environmental conditions at Utsira Nord which is a location selected for this thesis study.
 - During Extreme operating conditions Heave, Surge and Pitch movements responded with relatively higher amplitudes where structure travelled a distance of almost 4 meters in downwards direction in z – axis & came back to its initial position and structure travelled a distance of more than 8 meters in positive x – axis which is quite significant and better damping or design optimization is needed to reduce the translational motion in these two degrees of freedom.
 - FOWT rotated around 2.99 degrees around lateral axis at time period of almost 260 seconds in time domain response which the peak amplitude in pitch movement, but it can be seen from the graph that the structure remained at peak amplitude for a very short period of time (almost 2 seconds) and returned back to its initial position.

- However, structure moved back to its initial position after regular intervals of time throughout the simulation period which supports the resistivity and motion damping capability of my designed structure. A little design optimization is needed to even resist the motion in translation degrees of freedom.
- Whole numerical study during extreme operating conditions suggests that structure will remain in its initial position and can survive the extreme weather condition without being tip over or being destroyed. However, keep staying in operative condition during these extreme conditions is a question that can be answered through the studies of power rating capacity of wind turbines which was out of scope of this response evaluation study.
- For full scale study of FOWT, mooring systems and fixed ballast were designed and calculated that supported the stability of designed FOWT very well. Resonant wave frequency operating conditions were applied to run the simulations and it was checked that wind turbine responded well in such extreme conditions as well as it didn't tip over neither the mooring system was broken. All the resulted values were under control, and this supports the survivability of our structure.
- Natural frequencies in each DOF were also evaluated. For all DOFs other than yaw, natural frequency was the lowest wave frequency in our extracted meteorological data which was 0.046 degrees per second. This represents a very long wave period of 21.76 seconds which is not a very common phenomenon in any part of the world unless until significant wave heights occur with greater amplitudes. For yaw, 0.05983 degrees was evaluated as the natural frequency.
 - To avoid the resonance phenomenon, it is compulsory to design the system in such a way that natural frequency of the system does not match with the wave frequency.
- A simulation was also conducted to evaluate the FOWT response in extreme resonant frequencies and results in time domain response suggest that FOWT can still survive and will not be destroyed during a simulation time period of 500 seconds. However, the amplitude of the movement in all DOF was very large and can be found in the table no. 22. It can be concluded that turbine cannot operate during such extreme resonant conditions.
- A time domain response was also conducted to check if all three mooring lines will survive during extreme resonant conditions. Through the achieved results, it can be concluded that all mooring lines will survive during such conditions as top tensions in all mooring lines are less than the critical tension values of both chain and polyester mooring line.

Despite the comprehensive analysis, the study had limitations such as geometrical limitations leading to mass distribution difference, time constraints to dive deeper, and approximations in operating conditions in ANSYS AQWA. The findings are significant for study of dynamic response of floating offshore wind turbines in arctic region since the data obtained through all simulations can contribute to comparing numerical results with experimental studies in the future. Finally, the insights derived in this study underscore the importance of hydrodynamics analysis in ANSYS AQWA in revolutionizing floating offshore structures, leading to efficient and more reliable structures.

7.2 Future Work

In this thesis main aim was to conduct the hydrodynamic response analysis of floating offshore wind turbine (FOWT). To get the broader understanding of practical application of this FOWT it can be coupled with other types of research methodologies that support other aspects of practical application of floating offshore structures. A few suggestions are as follows:

- In this study, constant wind velocity was applied on the whole structure outside of water and no realistic parabolic wind force modelling was done as wave modelling was the main focus for generating the operating conditions in Ansys Aqwa for hydrodynamic response. This study can be coupled with extensive CFD modelling where realistic wind pressures can be evaluated and applied through defining the right drag coefficients for better understanding of how the whole system will behave during more realistic operating conditions.
- However, in this study point masses were defined and applied for nacelle, rotor and hub but no CAD modelling was done to create a realistic prototype which can be exported to CFD first to evaluate the wind forces, right estimation of center of masses and mass moment of inertias. So, in the future, a more detailed CAD model can be exported to numerical simulations to predict the accurate behavior of FOWT in operating conditions.
- In the future, this numerical model can be coupled with static structural Ansys suit to conduct detailed structural analysis, where several structural parameters could be evaluated such as fatigue, deformation, forces, and stresses. A detailed study for the selection of design optimization with selection of right materials can be conducted in the future as well.
- Mooring system is one of the major things to consider while designing or modelling the FOWT in any operating conditions and it cost a lot of money to design, fabricate and assemble the mooring lines to the structure with the sea floor. In the future a detailed study on the mooring lines can be conducted using this numerical model to reduce the complexity and total cost of mooring system.
- To predict the FOWT response in the extreme operating conditions in Arctic region, Ice loads can be modelled with other operating conditions as well. This can give us realistic overview that how sea ice and atmospheric ice can change the response and behavior of FOWT under different loading conditions.

References

1. McGowan, J.G. and S.R. Conners, *Windpower: A turn of the century review*. Annual Review of Energy and the Environment, 2000. **25**: p. 147-197.
2. *EU goals 1*.
3. *EU goals 2*.
4. de Souza Mendonça, A.K., T.G. Braga, and A.C. Bornia, *Airborne Wind Energy Systems: Current state and challenges to reach the market*. 2020.
5. Corbetta, G., et al., *Wind energy scenarios for 2030*. European Wind Energy Association, 2015.
6. *RenewableEnergyWorld 2019*; .
7. Aspelund, A., et al., *Conditions for growth in the Norwegian offshore wind industry. International market developments, Norwegian firm characteristics and strategies, and policies for industry development*. 2019.
8. Tande, J.O.G., *EERA DeepWind'2019 Conference 16–18 January 2019*. SINTEF Rapport, 2019.
9. SOARES, C.G., J. BHATTACHARJEE, and D. KARMAKAR *OVERVIEW AND PROSPECTS FOR DEVELOPMENT OF WAVE AND OFFSHORE WIND ENERGY*. An International Journal of Naval Architecture and Ocean Engineering for Research and Development, 2014. **65**: p. 23.
10. Hau, E., *Wind Turbines*. 2013: Springer Berlin, Heidelberg. 879.
11. Assessment, A., *Offshore Wind Market and Economic Analysis-Annual Market Assessment*. Document Number: DE-EE0005360, US Department of Energy, 2013.
12. Castro-Santos, L. and V. Diaz-Casas, *Floating Offshore Wind Farms*. 2016, Springer International Publishing : Imprint: Springer: Cham.
13. Manwell, J.F., J.G. McGowan, and A.L. Rogers, *Wind energy explained : theory, design and application*. 2nd ed. 2009, Chichester, U.K.: Wiley. xii, 689 p.
14. Thiagarajan, K. and H. Dagher, *A review of floating platform concepts for offshore wind energy generation*. Journal of offshore mechanics and Arctic engineering, 2014. **136**(2): p. 020903.
15. Tande, J.O.G., et al., *Floating offshore turbines*. Wiley Interdisciplinary Reviews: Energy and Environment, 2015. **4**(3): p. 213-228.
16. Burton, T., et al., *Wind energy handbook*. 2011: John Wiley & Sons.
17. Atcheson, M., et al., *Floating offshore wind energy*. by Joao Cruz and Mairead Atcheson. Springer International Publishing. Chap. Looking back. doi, 2016. **10**(1007): p. 978-3.
18. Musial, W., S. Butterfield, and A. Boone. *Feasibility of floating platform systems for wind turbines*. in *42nd AIAA aerospace sciences meeting and exhibit*. 2004.
19. Harris, R.E., L. Johanning, and J. Wolfram, *Mooring systems for wave energy converters: A review of design issues and choices*. Marec2004, 2004: p. 180-189.
20. Wang, H.Y., et al., *Conceptual design and hydrodynamic performance of a floating offshore wind turbine cell-spar-buoy support structure*. Applied Mechanics and Materials, 2014. **472**: p. 291-295.
21. Guoqin, L., Z. Huiqin, and L. Jiachun, *Effects of incident wind/wave directions on dynamic response of a SPAR-type floating offshore wind turbine system*. 2019.
22. Bozzo, A., *Dynamic Analysis of Floating Offshore Wind Turbines Under Extreme Operational Conditions*. 2023, ProQuest Dissertations Publishing.
23. Subbulakshmi, A., et al., *Recent advances in experimental and numerical methods for dynamic analysis of floating offshore wind turbines—An integrated review*. Renewable and Sustainable Energy Reviews, 2022. **164**: p. 112525.
24. Curfs, C., *Dynamic behaviour of floating wind turbines-A comparison of open water and level ice conditions*. 2015.
25. (NVE), N.W.r.a.E.D., *NVE - Rapport 47-12 Havvind – strategisk konsekvensutredning*.
26. Hølleland, S., et al., *Optimal allocation of 30GW offshore wind power in the Norwegian Economic Zone*. Wind Energy Science Discussions, 2024. **2024**: p. 1-26.

27. Srinivas, A., et al., *Impact of limited degree of freedom drag coefficients on a floating offshore wind turbine simulation*. Journal of Marine Science and Engineering, 2023. **11**(1): p. 139.
28. Tiyip, E. and J. Amdahl, *Short simulation approach for floating offshore wind turbine design load case*.
29. Messmer, T., et al. *A six degree-of-freedom set-up for wind tunnel testing of floating wind turbines*. in *Journal of Physics: Conference Series*. 2022. IOP Publishing.
30. Shalabe, A., et al., *Experimental investigation on the dynamic characteristics of a spar-type offshore wind turbine under irregular waves*. Journal of Al-Azhar University Engineering Sector, 2023. **18**(69): p. 830-849.
31. Ewelina ciba, P.d., *Simulation of the Dynamics of Spar-type Floating Offshore Wind Turbine in the ANSYS Aqwa Environment Extended by the Coefficients of Viscosity Forces Determined on the Basis of RANSE-CFD Analysis*.
32. Castro-Santos, L. and V. Diaz-Casas, *Floating offshore wind farms*. 2016: Springer.
33. Andrew Ho and I. Pineda., *Wind energy scenarios for 2030*. 2015, European Wind Energy Association
34. Samson Afewerki, A.A., Øyvind Bjørgum, Jens Hanson, Asbjørn Karlsen, Assiya Kenzhegaliyeva, Håkon Endresen Normann, Markus Steen, Erik Andreas Sæther, *CONDITIONS FOR GROWTH IN THE NORWEGIAN OFFSHORE WIND INDUSTRY*. 2019.
35. L Battisti, et al., *Sea ice and icing risk for offshore wind turbines*, in *Owemes*. 2006: Italy.
36. Virk, F.A.M., *Review of Icing Effects on Wind Turbine in Cold Regions*.
37. Virk, M., S., M. Homola, C., and P. Nicklasson, J. , *Effect of Rime Ice Accretion on Aerodynamic Characteristics of Wind Turbine Blade Profiles*. Wind engineering, 2010. **34**: p. 207-218.
38. Peter, D. *Numerical simulation of ice accretion on wind turbines*. in *IWAIS 2009*. 2009.
39. Duncan, T., et al. *Understanding icing losses and risk of ice throw at operating wind farms*. in *Winterwind 2008*. 2008. Norrköping, Sweden.
40. L Hu, et al., *Wind turbine ice distribution and load response under icing conditions*. Renewable Energy, 2017. **113**: p. 608-619.
41. Antonie Lacroix and J.F. Manwell, *Wind Energy: Cold Weather Issues*. 2000, University of Massachusetts Renewable energy research laboratory.
42. Barati-Boldaji, R. and M. Komareji, *Techniques of identifying icing and de-icing of wind turbines*. Signal Processing and Renewable Energy, 2017. **1**(4): p. 27-35.
43. Helge Gravesen, et al., *Ice loading on Danish wind turbines: Part 2. Analyses of dynamic model test results*. Cold regions science & technology, 2005. **41**(1): p. 25-47.
44. Hayo Hendrikse and T.S. Nord., *Dynamic response of an offshore structure interacting with an ice floe failing in crushing*. Marine Structures, 2019. **65**: p. 271-290.
45. Hayo Hendrikse and A.V. Metrikine., *Interpretation and prediction of ice induced vibrations based on contact area variation*. International Journal of Solids & Structures, 2015. **75-76**: p. 336-348.
46. Hayo Hendrikse and M. Seidel., *Analytical assessment of sea ice-induced frequency lock-in for offshore wind turbine monopiles*. Marine Structures, 2018. **60**.
47. Li Zhou, et al., *Numerical simulation of moored structure station keeping in level ice*. Cold regions science & technology, 2012. **71**: p. 54-66.
48. Tavner, P.J., *Offshore Wind Turbines-Reliability, Availability & Maintenance*. 2012: Institution of Engineering and Technology (IET).
49. Brons-Illing, C., *Analysis of operation and maintenance strategies for floating offshore wind farms*. 2015, University of Stavanger, Norway.
50. Hassan, G.G., *A guide to UK offshore wind operations and maintenance*. 2013: Scottish Enterprise.
51. Guo, X., et al., *Integrated Dynamics Response Analysis for IEA 10-MW Spar Floating Offshore Wind Turbine*. Journal of Marine Science and Engineering, 2022. **10**(4): p. 542.
52. Karyotakis, A. and R. Bucknall, *Planned intervention as a maintenance and repair strategy for offshore wind turbines*. Journal of marine engineering & technology, 2010. **9**(1): p. 27-35.

53. Santos, F., Â.P. Teixeira, and C.G. Soares, *Modelling and simulation of the operation and maintenance of offshore wind turbines*. Proceedings of the Institution of Mechanical Engineers, Part O: Journal of Risk and Reliability, 2015. **229**(5): p. 385-393.
54. Energy, R.N.M.o.P.a., *Announcement of competition for project areas in Utsira Nord for offshore renewable energy production*.
55. Jonkman, J., et al., *Definition of a 5-MW reference wind turbine for offshore system development*. 2009, National Renewable Energy Lab.(NREL), Golden, CO (United States).
56. minerals, L., *Megnadense*

Appendix

Python Script for NORA – 3

```
import netCDF4 as nc
import numpy as np
import pandas as pd
import datetime as dt

# Define the function to extract data and save DataFrame to CSV
def extract_and_save_data(opendap_url, Enter_lat, Enter_lon):
    # Open the dataset
    dataset = nc.Dataset(opendap_url)

    # Extract latitude, longitude, and time variables
    latitude_variable = dataset.variables['latitude'][:]
    longitude_variable = dataset.variables['longitude'][:]
    time_variable = dataset.variables['time'][:]

    # Calculate differences
    lat_diff = np.abs(latitude_variable - Enter_lat)
    lon_diff = np.abs(longitude_variable - Enter_lon)

    # Find indices of minimum differences
    lat_index, lon_index = np.unravel_index((lat_diff + lon_diff).argmin(), lat_diff.shape)

    # Create lists to store data
    data = {
        'Date': [],
        'Time': [],
        'Nearest Latitude': [],
        'Nearest Longitude': [],
        'Index of Nearest Latitude': [],
        'Index of Nearest Longitude': [],
        'Total significant wave height (m)': [],
        'Total mean period (s)': [],
        'Total peak period (s)': [],
        'Total mean wave direction (deg)': [],
        'Wind speed (m/s)': [],
        'Wind direction (deg)': [],
        'Water depth (m)': []
    }
```

```

# Loop through time steps
for time in range(8760):
    # Extract the time for the timestep
    timestep = time_variable[time]
    # Convert time to a human-readable format
    date_time = dt.datetime(1970, 1, 1) + dt.timedelta(seconds=int(timestep))

    hs = dataset.variables['hs']
    hs_value = f"{hs[lat_index, lon_index, time]:.2f}"

    tmp = dataset.variables['tmp']
    tmp_value = f"{tmp[lat_index, lon_index, time]:.2f}"

    tp = dataset.variables['tp']
    tp_value = f"{tp[lat_index, lon_index, time]:.2f}"

    thq = dataset.variables['thq']
    thq_value = f"{thq[lat_index, lon_index, time]:.2f}"

    ff = dataset.variables['ff']
    ff_value = f"{ff[lat_index, lon_index, time]:.2f}"

    dd = dataset.variables['dd']
    dd_value = f"{dd[lat_index, lon_index, time]:.2f}"

    model_depth = dataset.variables['model_depth']
    model_depth_value = f"{model_depth[lat_index, lon_index]:.2f}"

# Append data to lists
data['Date'].append(date_time.date())
data['Time'].append(date_time.time())
data['Nearest Latitude'].append(round(latitude_variable[lat_index, lon_index], 2))
data['Nearest Longitude'].append(round(longitude_variable[lat_index, lon_index], 2))
data['Index of Nearest Latitude'].append(lat_index)
data['Index of Nearest Longitude'].append(lon_index)
data['Total significant wave height (m)'].append(hs_value)
data['Total mean period (s)'].append(tmp_value)
data['Total peak period (s)'].append(tp_value)

```

```

data["Total mean wave direction (deg)"].append(thq_value)
data["Wind speed (m/s)"].append(ff_value)
data["Wind direction (deg)"].append(dd_value)
data["Water depth (m)"].append(model_depth_value)

# Create DataFrame
df = pd.DataFrame(data)

# Extract year from the OPENDAP URL
year_start_index = opendap_url.find('_v4_') + 4
year_end_index = opendap_url.find('_tiled')
year = opendap_url[year_start_index:year_end_index]

# Construct file name using latitude, longitude, and year
file_name = f"Wave_Data_{Enter_lat}_{Enter_lon}_{year}.csv"

# Save the DataFrame to a CSV file
df.to_csv(file_name, index=False)

print(f"DataFrame for year {year} saved to {file_name}")

# Define the initial OPENDAP URL and coordinates
Enter_lat = 59.2
Enter_lon = 4.5

# Loop through years from 2019 to 2022
for year in range(2015, 2022):
    # Update the year in the OPENDAP URL
    opendap_url =
f"https://thredds.met.no/thredds/dodsC/nora3_subset_wave/wave_tser_agg/wave_v4_{year}
_tiled.ncml"

# Call the function to extract data and save DataFrame to CSV
extract_and_save_data(opendap_url, Enter_lat, Enter_lon)

```


Approximate weight of details (kg)

	Common Stud	Common Studless	Enlarged Link	End Link	RF Connector	Joining Shackles	Joining Shackles	Anchor Shackles	Anchor Shackles
Diameter	Link	Link				Type D	Type D LTM	Type D	Type D LTM
mm	kg	kg	kg	kg	kg	kg	kg	kg	kg
76	39	36	50	60	65	100	110	140	155
78	43	39	55	65	70	105	115	150	165
81	48	44	60	70	79	120	130	170	185
84	53	49	70	80	88	135	145	195	210
87	58	54	75	85	95	150	165	220	240
90	65	60	80	95	104	165	185	245	265
92	70	64	90	100	106	175	191	255	280
95	77	70	100	110	123	200	220	290	315
97	82	75	100	120	131	210	230	305	330
100	90	82	110	130	144	230	250	335	365
102	95	87	120	140	151	245	265	350	380
107	110	100	140	160	163	285	310	410	445
111	123	112	160	175	175	305	335	445	485
114	133	121	175	195	180	325	360	475	520
117	144	131	185	210	200	345	385	505	555
122	163	149	210	235	245	380	420	550	600
127	184	168	235	260	280	420	465	600	660
132	207	189	260	305	320	480	530	675	740
137	231	211	285	330	350	550	605	750	825
142	257	235	325	375	390	650	710	900	985
147	285	260	395	410	450	720	790	1055	1145
152	315	288	410	460	515	845	885	1200	1300
157	347	317	455	510	585	932	975	1550	1655
162	382	349	500	560	660	1025	1070	1700	1820
167	418	382	540	630	725	1125	1175	1970	2100
172	457	417	590	680	800	1225	1285	2300	2440
177	498	455	640	730		1340	1400	2700	2855

Excel file

	A	B	C	D	E	F	G	H	I	J	K	L	M	N	O	P	Q		
1																			
2		Spar size							Properties										
3		Do		12 m					Seawater density		1025 kg/m ³								
4		Area, o		113.097336 m ²					Magnetite density		5000 kg/m ³								
5		Length		130 m															
6		Freeboard		7 m															
7		Draft		123 m					Mass Summary										
8		Porosity		0.997					Part	Mass, kg	CoG	Moment, kg.m							
9		Di (equiv)		11.964 m					Hull	5496727	-58	-318810166							
10		Area, i		112.419769					Fixed Ballast	8007780	-118.3	-947160168							
11		Displacement(water by submerged)		13910.9723 m ³					NLE+Rotor	406780	90	36610200							
12				14258746.6 kg					Tower	347460	38.23	13284785.6							
13		CoB		-61.5 m					Total	14258747		-1216075349							
14																			
15		Fixed Ballast																	
16		Magnetite		9.44 m					Global CoG		-85.2863 m								
17		Mass		8007779.58 kg					COB		-61.5 m								
18		CoG		-118.28 m					Metacentric Height		23.78627 m								
19		lx, lyy		131105083.6 kg/*2					Balance of Mass										
20		lzz		143276489.4 kg/*2					Displaced ocean water mass	14258747	kg								
21									Total Mass	14258747	kg								
22									Difference	0	kg								
23									This difference should be equal to zero in order to achieve equilibrium. We can do it by changing height of variable ballast										
24									Balance of Mass										
25									Displaced ocean water mass	14258747									
26									Total Mass	14258747									
27									Difference	0									
28																			
29		Hull Mass																	

	A	B	C	D	E	F	G	H	I	J	K	L	M
28										Total Mass	14258747		
29										Difference	0		
30													
31													
32													
33													
34													
35													
36													
37													
38													
39													
40													
41													
42													
43													
44													
45													
46													
47													
48													
49													
50													
51													
52													
53													
54													
55													
56													
57													

	A	B	C	D	E	F	G	H	I	J	K	L	M	N	O
1															
2															
3															
4															
5															
6															
7															
8															
9															
10															
11															
12															
13															
14															
15															
16															
17															
18															
19															
20															
21															
22															
23															
24															
25															
26															
27															
28															
29															

Numerical setup in Ansys Aqwa

